ONE-STEP PREPARATION AND INVESTIGATION OF HIGH STRENGTH TEXTILE REINFORCED HYDROGEL COMPOSITES

Ümit KOÇ

T.C.
BURSA ULUDAĞ UNIVERSITY
GRADUATE SCHOOL OF NATURAL AND APPLIED SCIENCES

**ONE-STEP PREPARATION AND INVESTIGATION OF HIGH STRENGTH
TEXTILE REINFORCED HYDROGEL COMPOSITES**

ÜMİT KOÇ
0000-0002-9061-3040

Assoc. Prof. Dr. Yakup AYKUT
(Supervisor)

Prof. Dr. Recep EREN
(Second Supervisor)
Bursa Uludağ University

PhD THESIS
DEPARTMENT OF TEXTILE ENGINEERING

BURSA – 2020

THESIS APPROVAL

This thesis titled "ONE-STEP PREPARATION AND INVESTIGATION OF HIGH STRENGTH TEXTILE REINFORCED HYDROGEL COMPOSITES" and prepared by Ümit KOÇ has been accepted as a **PhD THESIS** in Bursa Uludağ University Graduate School of Natural and Applied Sciences, Department of Textile Engineering following a unanimous vote of the jury below.

Supervisor   : (Assoc. Prof. Dr. Yakup AYKUT)
Second Supervisor   : (Prof. Dr. Recep EREN, Bursa Uludağ University)

      Head   :   Assoc. Prof. Dr. Yakup AYKUT   Signature
                   0000-0002-5263-1985
                   Bursa Uludağ University,
                   Faculty of Engineering,
                   Department of Textile Engineering

      Member: Prof. Dr. Hasan Basri KOÇER   Signature
                   0000-0003-2612-6712
                   Bursa Technical University,
                   Faculty of Engineering and Natural Sciences,
                   Department of Polymer Materials Engineering

      Member: Assoc. Prof. Dr. Hakan AYDIN   Signature
                   0000-0001-7364-6281
                   Bursa Uludağ University,
                   Faculty of Engineering,
                   Department of Mechanical Engineering

      Member: Assist. Prof. Halil İbrahim AKYILDIZ   Signature
                   0000-0002-8727-5829
                   Bursa Uludağ University,
                   Faculty of Engineering,
                   Department of Textile Engineering

      Member: Assist. Prof. Cihan KABOĞLU   Signature
                   0000-0002-6249-0565
                   Bursa Technical University,
                   Faculty of Engineering and Natural Sciences,
                   Department of Metallurgical and Materials Engineering

I approve the above result

Prof. Dr. Hüseyin Aksel EREN
Institute Director

I declare that this thesis has been written in accordance with the following thesis writing rules of the U.U Graduate School of Natural and Applied Sciences;

- All the information and documents in the thesis are based on academic rules,

- audio, visual and written information and results are in accordance with scientific code of ethics,

- in the case that the works of others are used, I have provided attribution in accordance with the scientific norms,

- I have included all attributed sources as references,

- I have not tampered with the data used,

- and that I do not present any part of this thesis as another thesis work at this university or any other university.

25./12./2020

Ümit KOÇ

ÖZET

Doktora Tezi

YÜKSEK MUKAVEMETLİ TEKSTİL TAKVİYELİ HİDROJEL KOMPOZİTLERİN TEK AŞAMALI HAZIRLANMASI VE ARAŞTIRILMASI

Ümit KOÇ

Bursa Uludağ Üniversitesi
Fen Bilimleri Enstitüsü
Tekstil Mühendisliği Anabilim Dalı

Danışman: Doç. Dr. Yakup AYKUT
İkinci Danışman: Prof. Dr. Recep EREN (Bursa Uludağ Üniversitesi)

Hidrojeller, ilaç salınımında, tarımsal alanda, biyomedikal alanda, gıda korumasında ve doku uygulamalarında etkin ve yaygın olarak kullanılan polimerik jellerdir. Hidrojellerin yumuşak ve esnek özellikte olması disiplinler arası yaklaşımın ilerlemesini önemli ölçüde sağlamaktadır. Fakat hidrojeller uygulanan mekanik kuvvetler altında düşük dirence sahiptir. Bu durum hidrojellerin kullanımı sırasında kırılmalara neden olmaktadır. Bu bağlamda, tekstil takviyeli hidrojel kompozitler hidrojellerin mekanik problemlerini çözmek için disiplinler arası bir yaklaşım sunmaktadır.

Bu çalışmanın amacı mekanik özellikleri iyileştirilmiş dokuma kumaş takviyeli hidrojel kompozit yapıların incelenmesidir. Bu bağlamda, hidrojel iplik formunda olan polivinil alkol (PVA), uygulanan mekanik kuvvete karşı direncini artırmak için mukavemetli pamuk, keten, yün, viskon ipliklerle güçlendirildi. Bu nedenle, kumaş takviyeli hidrojel kompozitlerin üretimi için PVA/Pamuk, PVA/Keten, PVA/Yün, PVA/Viskon karışımlı dokuma kumaşlar hazırlandı. Hibrit dokuma kumaşlar, farklı oranlarda glutaraldehit ve boraks çözeltileri ile muamele edildi. Hibrit dokuma kumaşta bulunan PVA iplikleri çapraz bağlı jel yapılara dönüşürken, pamuk, keten, yün ve viskon iplikler, takviye elemanı olarak dokuma kumaşlarda kalmıştır. İplik ve kumaşla güçlendirilmiş hidrojel kompozitlerinin karakterizasyonları Fourier-transform kızılötesi spektroskopi (FT-IR), termogravimetrik analiz (TGA), X-ışını kırınımı (XRD), taramalı elektron mikroskobu (SEM) ile gerçekleştirildi. Hidrojel kompozitlerdeki çapraz bağlayıcı oranına ve su içeriklerine bağlı olarak numunelerin şişme dereceleri ve mekanik özellikleri incelendi. Tüm sonuçlar göz önüne alındığında, doğal lif takviyeli dokuma kumaşlar hidrojel kompozitlerin mekanik özelliklerini önemli ölçüde artırmıştır. Bu tezde sunulan yayımlanmış her makalenin bulguları, gelecekteki çalışmalar için birtakım önemli çıkarımlara sahiptir.

Anahtar Kelimeler: Hidrojel kompozit, çapraz bağlanma, polivinil alkol, pamuk, keten, yün, boraks, glutaraldehit, hibrit iplik

2020, xi + 102 sayfa.

ABSTRACT

PhD Thesis

ONE-STEP PREPARATION AND INVESTIGATION OF HIGH STRENGTH TEXTILE REINFORCED HYDROGEL COMPOSITES

Ümit KOÇ

Bursa Uludağ University
Graduate School of Natural and Applied Sciences
Department of Textile Engineering

Supervisor: Assoc. Prof. Dr. Yakup AYKUT
Second Supervisor: Prof. Dr. Recep EREN (Bursa Uludağ University)

Hydrogels are one of the most widely used polymeric gels and have been extensively used for drug delivery, agricultural and biomedical fields, food preservation, and tissue applications. Hydrophilic, soft, and flexible properties of hydrogels provide a significant opportunity to advance the understanding of interdisciplinary approach. However, hydrogels have low resistance under the applied mechanical forces. This situation results in hydrogels to break during usage. In this regard, textile reinforced hydrogel composite presents an interdisciplinary approach to solve mechanical problems of hydrogels.

The aim of this thesis is to investigate development of woven fabric reinforced hydrogel composite structure with enhanced mechanical properties. In this respect, polyvinyl alcohol (PVA) in yarn form was reinforced with another durable cotton, flax, wool and viscose yarns to produce a hydrogel composite structure with improved resistance to the applied mechanical forces. For this purpose, PVA/Cotton (Co), PVA/Flax (F), PVA/Wool (W), PVA/Viscose (VI) blended woven fabrics were manufactured for the forming fabric reinforced hydrogel composites. The hybrid woven fabrics were treated with different concentrations of glutaraldehyde and borax solutions. PVA yarns in the hybrid woven fabric turned into crosslinked gel structures, whereas cotton, flax, wool and viscose yarns remained in the woven fabrics as a reinforcing element. The characterizations of yarn and fabric reinforced hydrogel composites have been carried out by Fourier-transform infrared spectroscopy (FT-IR), thermogravimetric analysis (TGA), X-ray diffraction (XRD), and scanning electron microscope (SEM). The swelling degree and mechanical properties of the samples were investigated with respect to the crosslinker ratio and water contents in the hydrogel composites. Considering all results, natural fiber woven fabric reinforcement significantly increased the mechanical properties of hydrogel composites. The findings of each article presented in this thesis have a number of significant implications for future researchs.

Key words: Hydrogel composite, crosslinking, polyvinyl alcohol, cotton, flax, wool, borax, glutaraldehyde, hybrid yarn

2020, xi + 102 pages.

ACKNOWLEGDEMENT

Ümit KOÇ
…/…/…….

CONTENTS

v

SYMBOLS and ABBREVIATIONS

Symbols	Definition
°C	Celcius
cm	Centimeter
mg	milligram
mm/min	millimetres per minute
N	Newton
Ph	Power of Hydrogen
wt. %	Weight percent
w/v %	Weight /Volume percent

Abbreviation	Definition
BAP	Scientific Research Project Unit
Co	Cotton
CoHE	The Council of Higher Education
CF	Continue Filament
DSC	Differential Scanning Calorimetry
GA	Glutaraldehyde
FT-IR	Fourier-transform Infrared Spectroscopy
F	Flax
HCI	Hydrochloric Acid
Ne	Number of hangs (840 yards) in one pound of yarn
Nm	Number of 1000m (meter) units in a kg (kilogram) of yarn
PVA	Polyvinyl Alcohol
r	The correlation coefficient
SEM	Scanning Electron Microscope
SPSS	Statistical Package for Social Sciences
TGA	Thermogravimetric Analysis
OE	Open End
W	Wool
XRD	X-ray Diffraction

FIGURES

viii

TABLES

1. INTRODUCTION

Hydrogels, that have an important place in biomaterials in the last 50 years, are being improved day by day in biomedical engineering applications like contact lenses, drug delivery systems and tissue engineering with high water content besides their flexible and soft properties (Caló and Khutoryanskiy 2015, Chirani 2015). Despite these advantageous properties, hydrogels have low mechanical properties due to swelling of polymer structures in water (Zhao 2014). To enhance mechanical properties of hydrogels, hydrogel matrix is reinforced by short fibers ,woven fabrics and nonwoven sheet. This structure is also known as fiber/fabric reinforced hydrogel composite (Agrawal et al.2013, Lee et al.2016). In this regard, textile components such as fiber, yarn, two-dimensional (2D) and three-dimensional (3D) fabrics and nonwovens used as a reinforcing materials in hydrogel composite structures not only provide excellent tensile properties but also exhibit high toughness (Agrawal et al.2013, Huang et al.2017).

There is a growing interest in the use of fiber/fabric reinforced polyvinyl alcohol (PVA) based hydrogel composites for biomedical applications or research studies (Agrawal et al.2013) since PVA demonstrates quite good properties such as biocompatibility, high swelling, non-toxic properties. Due to its low mechanical strength without reinforcement, PVA-based hydrogels possess limited applications. PVA has been blended with chitin nanofibers, cellulose, silk, and cellulose whiskers to overcome this problem. Desirable properties of PVA-based hydrogels are obtained by using these additional components. Another important factor enhancing the mechanical performance of PVA based hydrogel is the crosslinking methods. PVA hydrogel formation can be obtained by chemical crosslinking or physical crosslinking method (Liu et al.2009). Chemical crosslinking methods include radical polymerization, enzyme treatment, high energy irradiation, and complementary groups' chemical reaction such as borax, glutaraldehyde, and tannic acid (Hennink and van Nostrum 2012, Spoljaric et al.2014, Pandit et al.2019). Addition of the crosslinking agent also increases the mechanical features of PVA/polymer blends (Hassan and Peppas 2000, Chiellini et al.2003). Physical crosslinking methods contain hydrogen bonds, ionic interactions, hydrophobic interactions, and crystallization (Hennink and van Nostrum 2012).

The specific aim of this thesis was to assess the extent to which parameters were enhancing the mechanical properties of textile reinforced hydrogel composite for use in hydrogel applications where mechanical strenght is of paramount importance. These parameters were; determination of optimum borax ratio (Koc et al.2020a), comparison of borax and glutaraldehyde crosslinking agents (Koc et al.2019a), type of convenient natural fibers (cotton, flax and wool) (Koc et al.2020b), and yarn construction (staple or continuous filament), mechanical investigation of hydrogel composite yarn (Koc et al.2019b). In this perspective, natural fibers (cotton/wool/flax) based fabrics and regenerated cellulose fiber (viscose open end/viscose continue filament/viscose ring) based fabrics used as the reinforcement materials, while gelation of PVA yarn in the fabric as the matrix material.

Firstly, PVA/Co woven fabric was produced by using PVA yarns in the weft direction and Co yarns in the warp direction. Yarn reinforced hydrogel composites were prepared by crosslinking of PVA with aqueous borax solution in the fabric structure. Optimum borax/water concentration was investigated depending on the swelling percentage. On the other hand, the mechanical performance of yarn reinforced hydrogel composites (1 wt.% borax/water treated) has been examined with respect to the water content in both warp and weft directions (Koc et al.2020a).

Secondly, hybrid yarns consisting of PVA and Co yarns to manufacture fabric for reinforcing hydrogel composites were produced. While PVA yarn and PVA/Co hybrid yarns were used as the warp in the woven fabric, cotton yarn was inserted as the weft yarn. After production of woven fabrics, each woven fabric sample was treated with previously prepared borax/water solutions and glutaraldehyde (GA)/water solutions (contains hydrochloric acid as the catalyst) to obtain cotton fabric reinforced hydrogel composite. Effect of the aqueous borax and GA solutions on chemical structure, thermal stability and crystalline microstructures were examined via ATR-FTIR, TGA and X-ray diffraction analysis by conducting the tests on the dried samples. Mechanical properties were also investigated using the dried samples. Effect of the water content in the composite hydrogel structures on the mechanical properties was investigated from both borax and GA samples by changing the cross linker ratio (Koc et al.2019a).

In the third step, the suitability of cotton, flax, and wool natural fiber yarns was discussed considering their effect to improve the mechanical properties. This approach presented a conclusive result for the best natural reinforcement materials (cotton, wool, linen) to strengthen hydrogel composites (Koc et al 2020b).

In the fourth step, the effect of yarn structure (continuous filament and staple viscose fiber) on the mechanical properties of fabric reinforced hydrogel composite was investigated. The relation between breaking force of regenerated cellulose (viscose ring, viscose OE, viscose CF) woven fabric reinforced hydrogel composites and borax-water concentration was analyzed by using statistical package for social sciences (SPSS) both in warp and weft directions.

Another research hydrogel composite yarn has been produced from PVA/Co hybrid yarn and then deepened into the previously prepared borax/water solution to obtain a proper hydrogel yarn structure. Visual, chemical, thermal and mechanical investigation of hydrogel yarns were examined in the study (Koc et al.2019b).

In conclusion, the findings in this PhD thesis made several contributions to the current literature. Firstly, research in the previous literature has been focused on coating fabrics with liquid hydrogel precursors, while in the context of this thesis, PVA fibers were used in yarn forms, and these fibers were added to the fabric structure during weaving process. Then, PVA fibers inside the fabric structure were treated with borax/water or glutaraldehyde/water solutions. In this way, a homogeneous composite hydrogel structure was produced. Secondly, preparation of fabric reinforced structure is considered as a novel in the area to produce mechanically enhanced hydrogels (Koc et al.2019a, Koc et al.2020a, Koc et al.2020b).

Outline of the thesis

1. Section 1 presents the motivation and aim of the thesis.

2. Section 2 describes the main concepts of hydrogels in the literature.

3. Section 3 provides the experimental work the thesis.

4. Section 4 explains the obtained results and discusses the results.

5. Section 5 is the concluding thesis.

2. THEORETICAL BASICS AND LITERATURE REVIEW

2.1. Hydrogel

At the end of 19th century, the term "hydrogel" was first mentioned by Bemmelen (1894) in the scientific study to explain the colloidal gel of salts, which is one of the inorganic compounds (Buwalda et al.2014, Thakur et al.2018). In the mid-20th century, PHEMA hydrogels were formed by chemical crosslinking with the EGDMA molecule of the HEMA monomer synthesized by Wichter and Lim (1969) (Basan et al. 2001, Hoffman 2012, Buwalda et al.2014, Maitra and Shukla 2014, Thakur et al.2018). In this regard, PHEMA hydrogels were the first synthetic hydrogels used for contact lenses due to their biocompatible properties (Idris 2013, Buwalda et al.2014, Thakur et al.2018, Ferreira et al. 2018). Figure 2.1 described this historical outlook of hydrogel research.
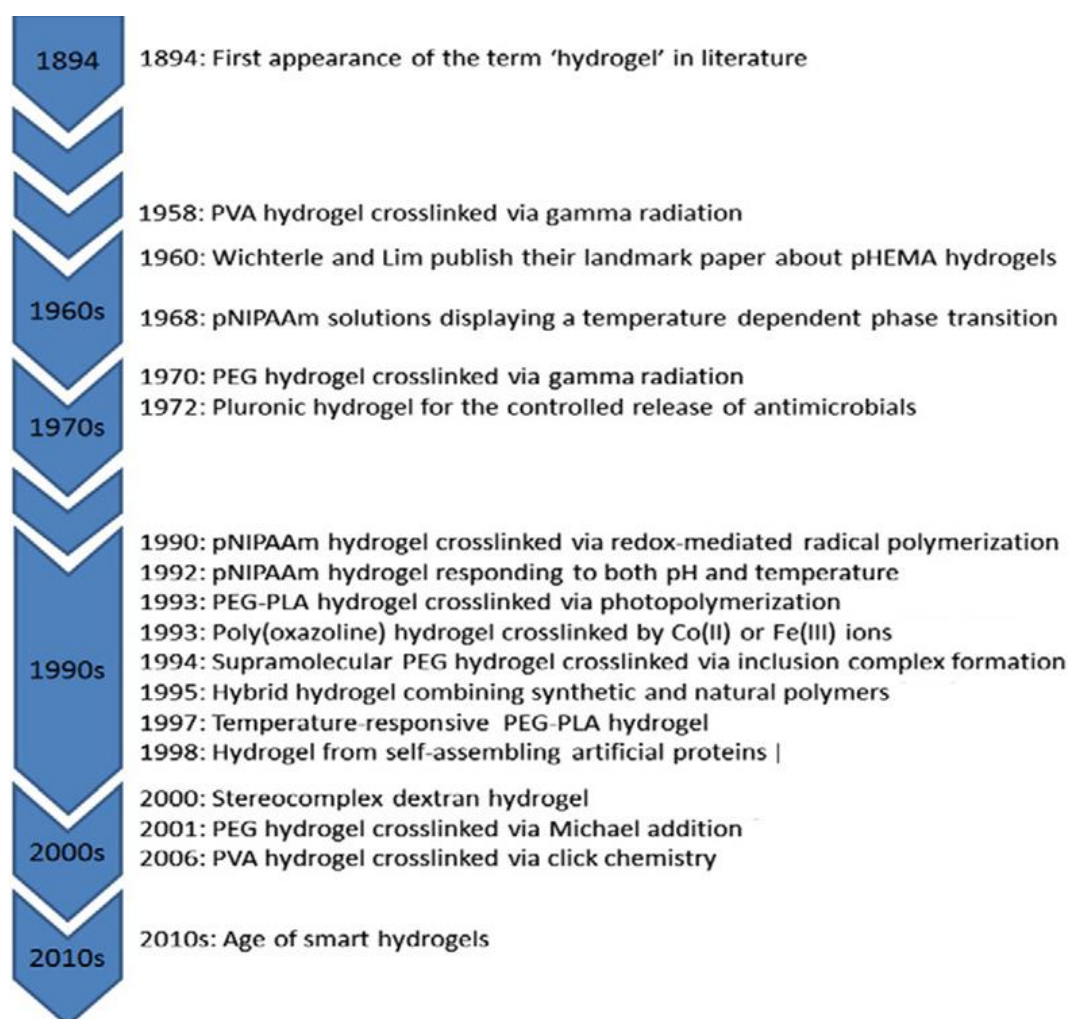
Figure 2.1. Timeline of the development of hydrogel (Buwalda et al.2014)

Nowadays, researchers describe hydrogels as three-dimensional (3D) hydrophilic polymer structures obtained by physical or chemical crosslinking process (Kabir et al.2018, Lin et al.2019, Zhang et al.2020). This three dimensional polymer can hold enormous amount of water in their 3D network structure that cannot be dissolved in water (Ahmed 2015, Zhang et al.2020). Therefore hydrogels demonstrate the ability to swell in water (Zhang et al. 2020, Koc et al. 2020a).

"Smart" or "Intelligent" types, also known as stimuli-responsive hydrogels, respond to changes in surroundings conditions, namely temperature, pH value, electricity, magnetism and light (Khan et al.2016, Eslahi et al.2016).

The physical stimuli include electricity, temperature, magnetism and light whereas chemical stimuli contain pH, ions etc. (Eslahi et al. 2016, Shi et al.2019, Gholamali 2019) (Table 2.1).

Table 2.1. Behavior of different types of smart hydrogels to external stimuli (Eslahi et al.2016)

Stimuli	Mechanism	Schematic representation	Materials
Temperature	Changes in hydrophilic-hydrophobic balance		NIPAAm, Pluronic, PEG copolymers
pH	Association/disassociation of pendant acidic/basic groups with hydrogen ions		Polyelectrolytes, PAAc, Chitosan, poly(N-vinylcaprolactam)
Light	Incorporation of photo-sensitive functional groups into the hydrogel networks		Azobenzenes, Poly(cinnamic acid), Triphenylmethane
Electric field	Generation of electrical polarization in polyelectrolytes		Chitosan/PAN, Hyaluronic acid/PVA, Alginate/PMAA
Mechanical stress	Induced conformational changes		Peptides, Acrylate-based block copolymers
Biomolecules	Dissolution–precipitation dynamics		Glucose-sensitive, DNA-responsive, Enzyme-sensitive hydrogels

The use of hydrogels is becoming widespread because of its advantageous features like swelling, softness, and biocompatibility (see 2.2 for details) (Caló and Khutoryanskiy 2015, Ahmed 2015, Thakur et al.2018). In this context, hydrogels are used as superabsorbent polymers in disposable diapers and hygienic materials (Peng et al.2016), wound dressings (Koehler et al. 2018), tissue engineering (Sheffield et al. 2018), contact lenses (Musgrave and Fang 2019), drug delivery systems (Aswathy et al.2020) and agricultural water retention materials (Liu et al. 2020). Figure 2.2 presents application of hydrogels in various areas.
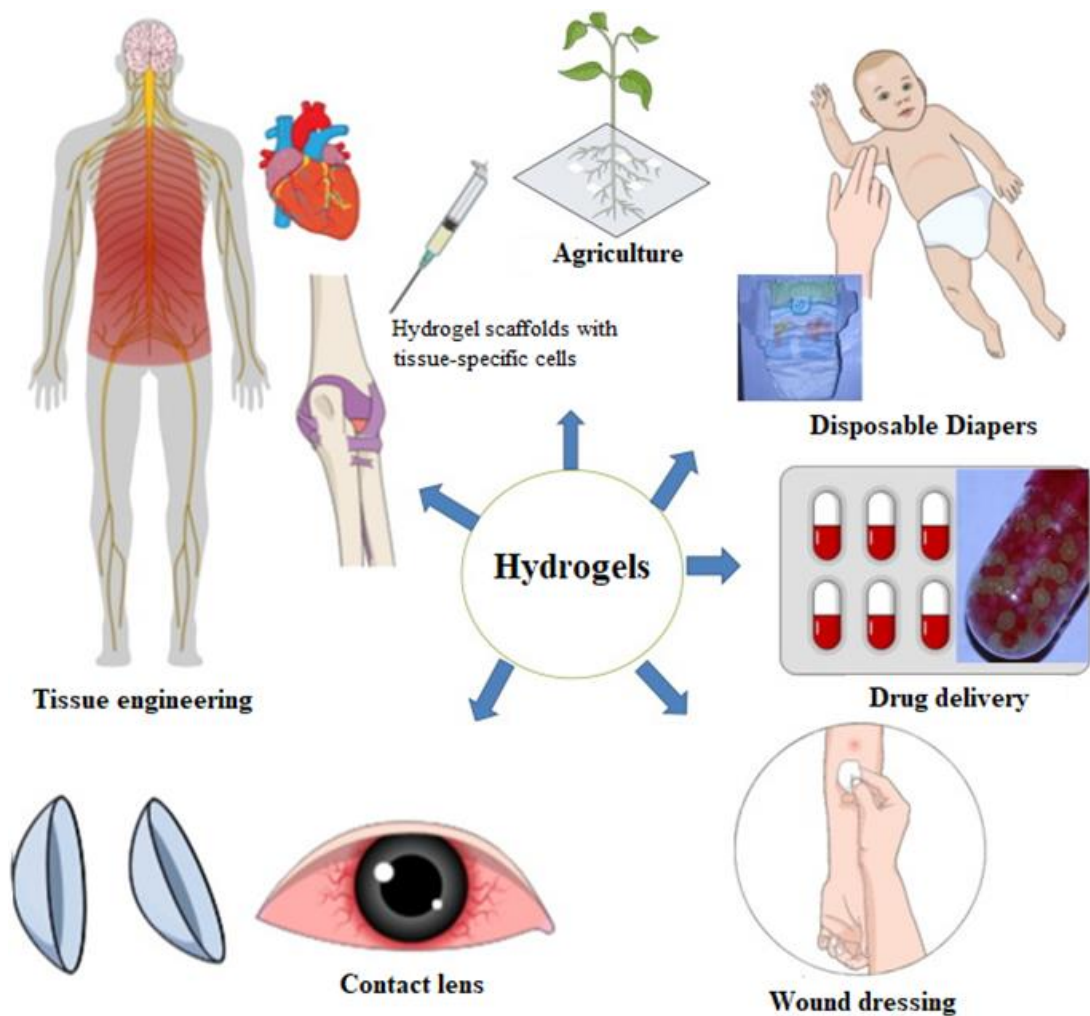
Figure 2.2. Applications of hydrogels in different fields (Varaprasad et al.2017)

2.2. Properties of Hydrogel Materials

2.2.1. Swelling

Swelling, which is one of the essential properties of hydrogels, happens in three stages as listed below and showed in Figure 2.3 (Buenger et al.2012, Vasile et al.2020):

I) Water molecules diffuse into hydrogel structure

II) The hydration process provides relaxation of polymeric chains

III) Dilation of crosslinking polymer structure.
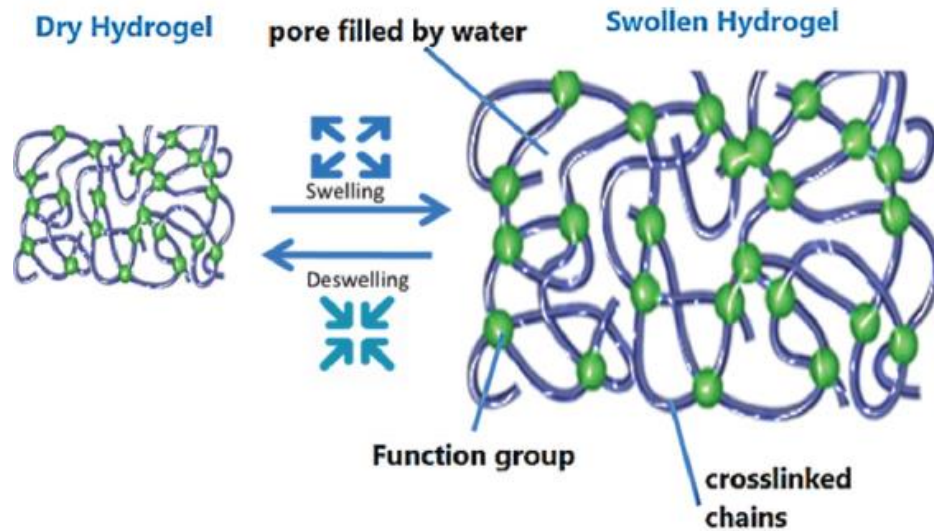
Figure 2.3. Schematic illustration of swelling or deswelling mechanism of hydrogels **(**Mohamed 2018)

Polymer concentration and density of crosslinking affect swelling rate. In this context, increasing of crosslinking density results in reducing of swelling ratio because it enhances the hydrogel structures becoming more frequent (Brahima 2016, Aswathy et al.2020). This situation prevents the mobility of polymer chains and therefore swelling ratio decreases (Amsden 1998, Brahima 2016). On the other hand, the characterization of hydrogels is determined by measuring the swelling ratio of hydrogels (Richbourg and Peppas 2020).

Swelling ratio is calculated using the following formula 2.2 (Yang et al.2012)

Swelling ratio % = ((wet weight –dry weight (mg))/ dry weight (mg)) x100   (2.2)

2.2.2. Mechanical properties

The low mechanical characteristics of hydrogels restrict their use in biomedical applications and other fields.

Most significant variables of hydrogels, such as swelling ratio, conditions for polymerization and density of cross-linking have a significant effect on mechanical properties of hydrogels. In general, extension and compression tests are conducted for the examination of the mechanical behavior of hydrogels. The compression test is better than the extension test because it does not depend on the material shape like strips or rings (Thakur et al.2018). Different approaches have been used to increase the mechanical properties of hydrogels, such as incorporation of polymers, addition of the various cross-linkers and using dissimilar cross-linking ratios (Peng et al.2016, Thakur et al.2018), the addition of fibers and fabrics as a reinforcement to make a composite hydrogel structure (Koc et al. 2019a), using plasticizers like xylitol, sorbitol, and glycerin (Hassan et al. 2018).

2.3. Classification of hydrogel materials

As specified in Figure 2.4, hydrogels can be classified in several ways. Hydrogels may be divided into two groups according to their origins, natural origin like chitosan, alginate, collagen or synthetic origin like poly(vinyl alcohol)(PVA). According to polymer composition, hydrogels are classified as; homopolymer hydrogels (refer to polymer networks obtained from a single type of monomer), copolymer hydrogels (are derived from two different monomer one of which is hydrophilic), hybrid hydrogels (are produced by mixing natural and synthetic polymers each other), composite hydrogels and interpenetrating polymeric hydrogels (are produced two natural and/or synthetic polymer which are independent crosslinked form) (Kishida and Ikada 2001, Mazzarotta 2017,

Thakur et al.2018). Depending on the sensitivity to stimuli; they are classified into three groups: physical stimulus, chemical stimulus, and biochemical stimulus. Based on the charge of polymer networks, hydrogels are grouped as non-ionic (neutral), ionic (cationic or anionic), zwitterion (move negative and positive charges similar the polymer chain) and amphoteric (including acidic and basic groups) hydrogels (Kishida and Ikada 2001, Ahmed 2015, Garg et al. 2016, Products et al.2017, Thakur et al. 2018). Another classification is done according to their crosslinking networks (Physical crosslinking and chemical crosslinking).

In physically cross-linked gels, polymer chains have physical interactivity without using any crosslinking agents such as borax, glutaraldehyde, etc. while in chemically crosslinked gels, covalent bonds occur between polymer chains (Ahmed 2015, Akhtar et al. 2016).
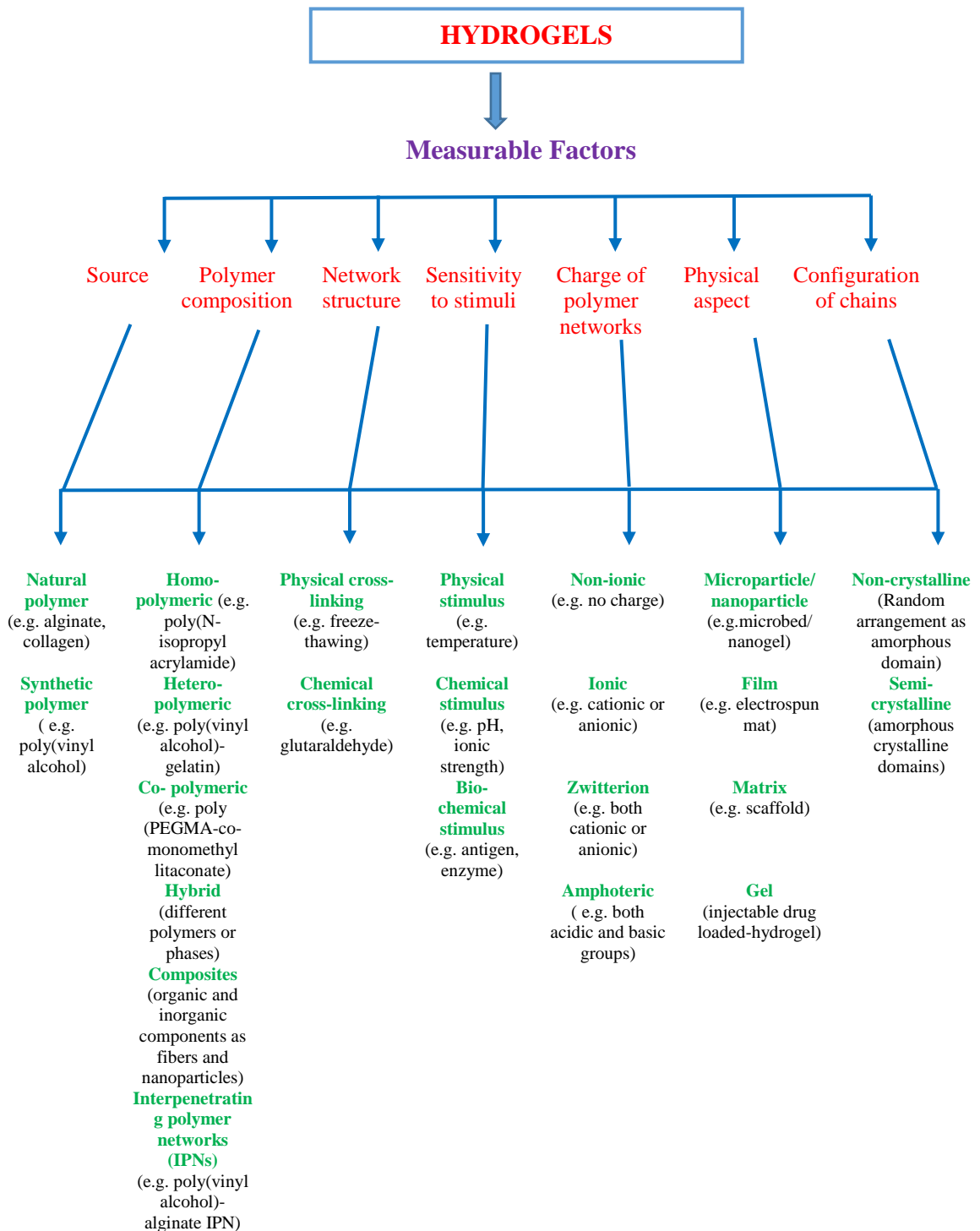
Figure 2.4. Classification of hydrogels according to different parameters (Vasile et al.2020)

2.4. Methods to Synthesize Hydrogels

Hydrogels can be prepared by various routes via chemical crosslinking or physical crosslinking methods (Hennink and van Nostrum 2012, Akhtar et al. 2016).

2.4.1. Physically cross-linked hydrogels (reversible)

To obtain physically crosslinked gels or self-assembled hydrogels, different methods have been used (Hennink and van Nostrum 2012, Akhtar et al. 2016). The methods are given as follows:

Crosslinking by hydrogen bonds

Complex formation occurs between Poly (acrylic acid) (PAA) and poly (methacryilic acid) (PMA) with poly (ethylene glycol) (PEG). These complexes bond by hydrogen bonds between the oxygen of the PEG and the carboxylic group of PMA. Hydrogen bonding happens between poly (methacryilic acid) and (PMA) poly (ethylene glycol) (PEG). Similarly, hydrogen bonding occurs in polymethacryilic acid and g- ethylene glycol. Protonation of carboxylic acid groups' result in the formation of hydrogen bonds. This indicates that pH is significantly important parameter for swelling of these gels (Hennink and van Nostrum 2012, Yokoyama and Yusa 2013, Akhtar et al. 2016).

Ionic interactions

Ionic interactions are derived from electrostatic interactions between two groups, which are cations and anions. When two opposite charges such as polyelectrolyte solution and multivalent ions are mixed, ionic crosslinking hydrogel structure is obtained. These opposite charges of ions result in electrostatic interaction. Therefore electrostatic interaction of molecules increases crosslinked polymeric composition. Multivalent ions are separated by specific chelators in the polymeric structure (Hospodiuk et al. 2017).

Hydrophobic interactions

To obtain physically (non-covalent) crosslinked hydrogels, another method is hydrophobic interaction occurring hydrogels. Hydrophilic or water soluble precursors include hydrophobic units or side chains, during the hydrophobic interaction in gel formation (Guo et al.2020).Temperature makes a significant contribution to hydrophobic interaction and changes the hydrogel structure's rheological properties via altering temperature (Hospodiuk et al.2017).

Crystallization

Crosslinking by crystallization can be achieved using crystallization in homopolymer systems and crosslinking by stereo complex formation(Hennink and van Nostrum 2012, Varaprasad et al.2017). PVA based hydrogels are an example of crystallization in homopolymer systems. This method includes repetitive cycles of freeze-thawing process. In this process, the microcrystal formation structure is obtained via freezing and thawing (Varaprasad et al.2017).

PLLA (the homopolymers of L-lactic acid) and PDLA (the homopolymers of D-lactic acid) are semi- crystalline substances (Hortós et al. 2019) . Blending of PLLA and PDLA is observed to melt 230° C. This association of PLLA and PDLA is attributed to the stereocomplex formation (Hennink and van Nostrum 2012, Akhtar et al. 2016).

2.4.2. Chemical cross-linking methods

Chemical crosslinking by radical polymerization

The conventional free radical polymerization reaction includes 3 stages;

➢ Initiation
➢ Propagation
➢ Deactivation via chain transfer or via termination (Mantha et al. 2019).

For manufacturing tubular hydrogel systems, PVA/PHEMA hydrogel tube system was obtained via radical polymerization of 2-hydroxyethyl methacrylate (HEMA). Potassium persulfate (KPS) in the presence of (N, N'- methylene bis (acrylamide) (BIS)) was used as initiator (Ma et al.2018). On the other hand, chemically cross-linked hydrogels could be fabricated via radical polymerization of dextran, albumin, poly (vinyl alcohol) (water-soluble polymers). Radical polymerization of this water soluble polymers were obtained by the derivation of polymerizable compounds (Hennink and van Nostrum 2012).

Crosslinking using enzyme

The transglutaminases (TGase) which are calcium (Ca^{2+}) dependent enzymes catalyze crosslink reactions (formation of covalent bond) between the lysine and glutamine in proteins (Figure 2.5) (Hennink and van Nostrum 2012, Martins et al. 2014, Duarte et al.2020). Generally, TGase has been used to prepare hydrogels via enzymatic crosslinking mechanism due to excellent crosslinking capability (Nezhad-Mokhtari et al. 2019).

Enzymatic crosslinking process

Covalently bonded

◉ : Transglutaminase (TGase)
Enzyme

Figure 2.5. Crosslinking mechanism of Transglutaminase enzyme (Source: Nezhad-Mokhtari et al.2019)

Chemical crosslinking via high energy irradiation

Unsaturated compound which contains carbon-carbon double bonds or triple bonds were polymerized by using gamma and electron beam irradiation. In this context, Polyvinyl alcohol (PVA) and poly(acrylic acid) polymers were crosslinked using high energy irradiation (Hennink and van Nostrum 2012).

Crosslinking via complementary groups' chemical reaction

The hydrophilic polymers are crosslinked by chemical reaction of complementary groups (Hennink & van Nostrum, 2012b).

This crosslinking mechanism are divided into three categories:

- **Crosslinking with aldehydes**

Polyvinyl alcohol (PVA), which includes hydroxyl groups, is soluble in water (Kadajji and Betageri, 2011). Glutaraldehyde (GA) as a crosslinking agent can be used in chemical crosslinking of PVA (Koc et al. 2019a, Mallakpour and Rashidimoghadam 2020).

- **Crosslinking using addition reactions**

Hydrophilic polymers can be transformed into hydrogels via the reaction between 1,6-hexamethylene diisocyanate and polysaccharides such as chitosan by addition reactions (Hennink and van Nostrum 2012, Gallego et al. 2013).

- **Crosslinking using condensation reactions**

Polymers such as polyesters and polyamides are synthesized by condensation reaction between carboxylic acid and amines. In this way, hydrogels are produced via a condensation reaction (Hennink and van Nostrum 2012).

2.4.3. Comparison of physical and chemical hydrogel formation methods

Table 2.2 indicates differences between physical and chemical hydrogels according to the hydrogel formation, bonds, preparation, degradation and mechanical properties.

Table 2.2. Comparison of physical and chemical hydrogels (Hennink and van Nostrum 2012, Parhi 2017, Mondal et al.2020)

Physical Hydrogel		Chemical Hydrogel
• Molecular entanglements • Non-covalent interactions (H-bonding) (Crystallization)	Hydrogel Formation	Cross-linking through covalent bonds
Non-covalent bonds (Physical interactions) (Reversible)	Bonds	Covalent bonds are strong (irreversible)
Without the use of cross-linking entities	Preparation	With the using cross-linking entities such as borax, glutaraldehyde
Less stable against degradation	Degradation	Very stable against degradation.
Poor mechanical properties due to the reversible physical interactions	Mechanical properties	High mechanical properties due to covalent bonds

2.5. PVA

2.5.1. Synthesis of PVA

Polyvinyl alcohol (PVA) is a semi crystalline, hydrophilic, nontoxic and biocompatible synthetic polymer (Ma and Xiong 2008, He et al. 2014, Zhang et al.2018). PVA contains a pendant hydroxyl group in its chemical structure and it is manufactured in two stages (Kumar and Han 2017) because vinyl alcohol is more unstable than its tautomer, acetaldehyde (Hassan and Peppas 2000, Satoh 2014). So, firstly PVA is produced by the polymerization of vinyl acetate to PVAc (polyvinyl acetate) and secondly hydrolysis of PVAc to PVA (Figure 2.6) (Hassan and Peppas 2000, Çavuşoğlu 2016, Kumar & Han, 2017).

Figure 2.6. Conventional PVA manufacturing process (Çavuşoğlu 2016)

Commercial PVA grades are categorized according to the degree of hydrolysis. One of the degree of hydrolysis of PVA grades is between 87% and 89% (partially hydrolyzed), other is from 98 to 99% (fully hydrolyzed). As shown in Figure 2.7, the degree of hydrolysis(DH) changes different parameters of PVA (Hassan and Peppas 2000, Çavuşoğlu 2016, Toxqui-López et al.2018, Nawaz and Hümmelgen 2019).

INCREASING DEGREE OF HYDROLYSIS	
DECREASES	**INCREASES**
Solubility	Tensile strength
Flexibility	Water resistance
Water sensitivity	Solvent resistance
Adhesion to hydrophobic surfaces	Adhesion to hydrophobic surfaces

Figure 2.7. Different properties of PVA based on degree of hydrolysis (Nawaz and Hümmelgen 2019)

2.5.2. Crosslinking of PVA

As was pointed out in the Methods to Synthesis Hydrogels (See 2.4), PVA can be crosslinked with crosslinking agent such as glutaraldehyde, borax by chemical crosslinking methods (Miyazaki et al.2010, Gadhave et al .2019). As shown in Figure 2.8, chemical reaction between PVA and glutaraldehyde (GA) occurs via the formation of acetal bridge (Dai and Barbari 1999, Rudra et al.2015, Çavuşoğlu 2016). According to Mansur et al. (2008), reducing of PVA/GA ratio enhanced significantly acetal bridge formation.
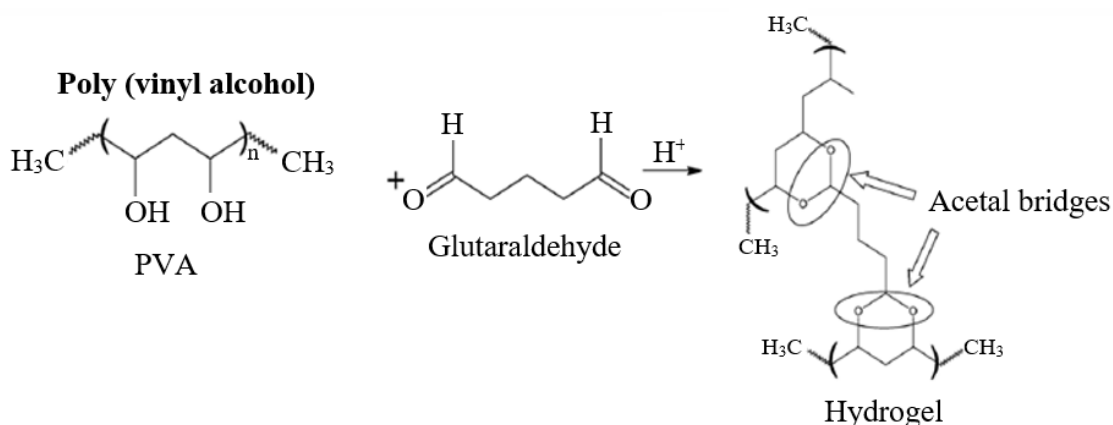
Figure 2.8. Chemical reaction between PVA with glutaraldehyde (Mansur et al.2008)

Cyclic compound occurs as a result of reaction between PVA and sodium tetraborate (Figure 2.9) (Çavuşoğlu 2016).
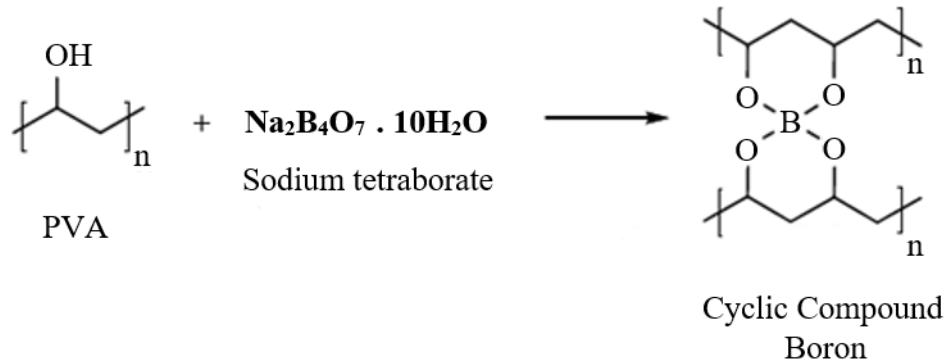
Figure 2.9. Crosslinking mechanism of PVA with sodium tetraborate (Çavuşoğlu 2016)

Another mechanism of hydrogel production includes physical crosslinking because of crystalline structure. Crosslinking agent is not essential for this method. Also PVA based hydrogels obtained by physical crosslinked techniques showed better mechanical performance than their counterparts due to the distribution of mechanical strenght throughout the crystallites of the 3D (three-dimensional) structure (Hassan and Peppas 2000).

To produce hydrogel by physical method, aqeous PVA solution was exposed to freezing-thawing cycles since freezing-thawing method enhanced hydrogel crystallinity. Several factors such as number of freezing/thawing cycles, concentration of polymer affect PVA hydrogel properties. These parameters improve crystallinity structure in the polymer matrix (Hassan and Peppas 2000, Ricciardi et al. 2004, Butylina et al.2016, Lee et al.2017).

2.6. Hydrogels with self-healing ability

One of the outstanding features of the biomaterials, such as bone and skin, is self-healing (Samadi et al.2018).

Self-healing hydrogels can be defined as follows: They have property to autonomously heal themselves after a damage and restore its structure. As shown in Figure 2.6, self-healing hydrogels can be categorized according to the chemical covalent or physical noncovalent reactions (Talebian et al.2019).
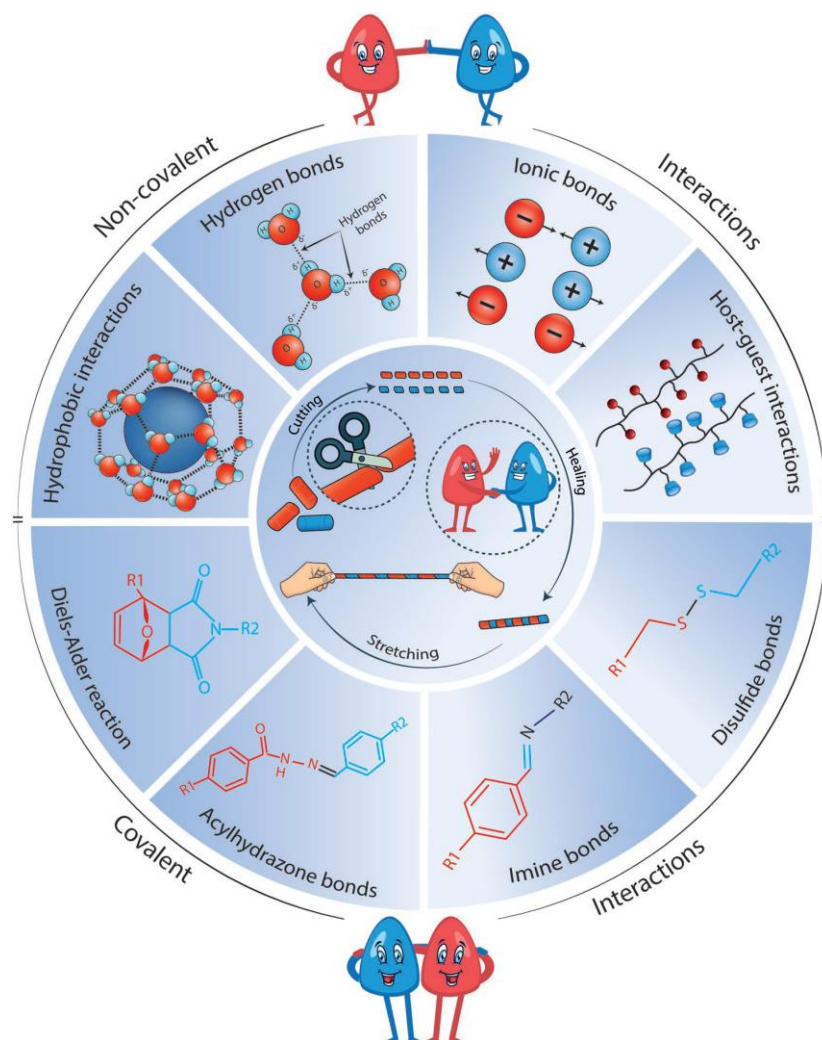
Figure 2.10. Self-healing mechanism of hydrogel based on physical and chemical methods (Talebian et al.2019)

Self-healable hydrogels produced by noncovalent reactions contain hydrophobic interactions, hydrogen bonds, ionic bonds, host-guest interactions whereas self-healable hydrogels formed by covalent reactions or crosslinks include Diels-Alder reaction, Acylhydrazone bonds, Imine bonds and disulfide bonds (Li et al.2017, Liu and Hsu 2018, Talebian et al.2019). Hydrogel blend produced from PVA, nanofibrillated cellulose (NFC) and borax led to self-healable behavior with enhanced mechanical performance.

Hydrogen bonding between PVA and NFC resulted in this situation (Spoljaric et al 2014, Taylor and in het Panhuis 2016, Talebian et al.2019).

2.7. Introduction to Composite materials

According to a definition provided by Saçak (2014), composite materials that include at least two or more different components, combines the optimal properties of various substances to obtain a new material. As shown in Figure 2.11, these components consist of reinforcement with fibers or particles (discontinuous phase), matrix (continuous phase) and interface. Reinforcement and matrix are essential components in the composite materials (Baghaei 2015). While the reinforcing fiber is responsible for the mechanical strength of the composite, the matrix component of the composite holds the reinforcing materials together (Saçak 2014). At the same time, the matrix protects the reinforcement from environmental conditions like moisture, heat and so on (Baghaei 2015). The most common definition of the "interface" in a composite structure is the area or line between reinforcement and matrix (Kim and Mai 1998, Ma et al.2010).
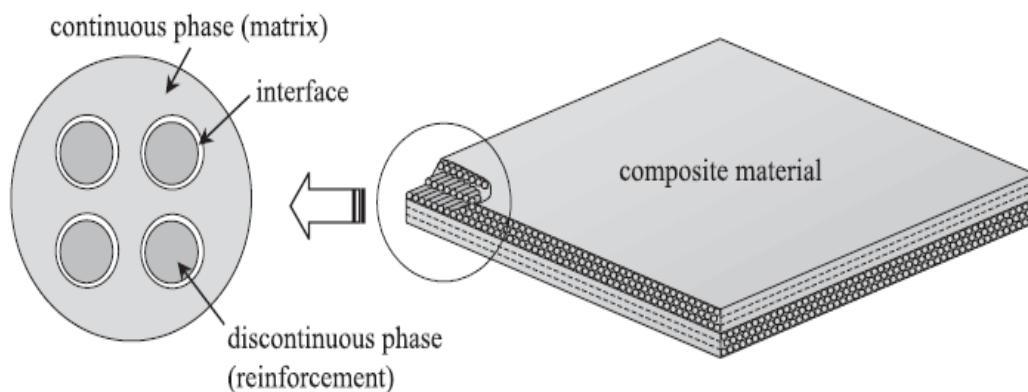
Figure 2.11. Structure of composite material (Lee and Suh 2006)

Composite materials are classified into two primary categories; based on reinforcing materials and matrix materials (Masoud et al.2020) (See in Figure 2.12). According to the matrix materials, composite structures can be categorized into three classification. These are polymer matrix composite materials (PMC), metal matrix composite materials (MMC) and ceramic matrix composite materials (Sezgin 2018).

The other group is based on reinforcing materials. Composite materials in this group are classified as fiber reinforced composite, particle reinforced composite and structurally reinforced composites (Priyanka et al.2017, Rajak et al.2019).
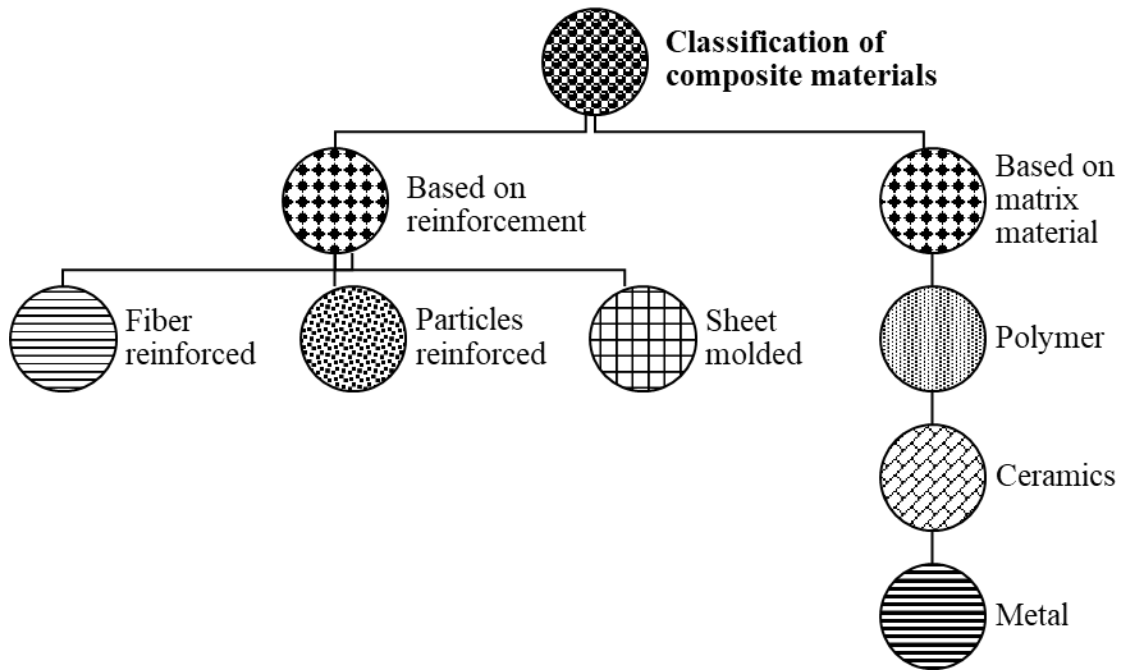
Figure 2.12. Classification of composite materials (Rajak et al.2019)

Composite materials have excellent properties such as corrosion resistance, light-weight, better strength, ability to be designed according to specifications (Koniuszewska 2016, Sezgin 2018, Rajak et al.2019). Due to these superior properties, composite materials are used in aerospace and military, automotive, medical, marine industry, etc. (Al-Oqla and Sapuan 2014, Saçak 2014, Koniuszewska 2016, Sezgin 2018, Rajak et al.2019).

Fiber and fabric reinforced composites

Fibers are unique substances due to their strength, better stiffness, and anisotropy properties (Steinmann and Saelhoff 2016). In this regard, different fibers such as synthetic or natural, continuous or discontinuous, short or long, are used to reinforce composite materials.

The mechanical strength of the fiber used as reinforcement should be considerably higher than the matrix. Primary component that resists against external loads is the fiber, while the polymer matrix forms the environment that holds the fibers together in the desired geometry in fiber-reinforced composites. In preparing fiber-reinforced polymeric composite, some essential points such as mechanical properties of fiber, amount of fiber, fiber orientation and fiber thickness should be taken into consideration (Saçak 2014).

Weaving is a method of fabric production in which fabrics are woven by interlacing of weft and warp yarns at right angles to each other by using weaving machine (Eren 2009). The main benefits of woven composites are their dimensional stability, integrity and packing density of yarn (Alavudeen et al.2015, Sezgin 2018). Because of these advantages, woven fabric is the most used reinforcement material compared to fiber, yarn or 2-Dimensional preforms such as knitted fabric and nonwoven (Misnon et al.2014, Sezgin 2018). There are different forms of woven fabric structures like plain weave, twill weave, satin/sateen weave based on their patterns (Figure 2.13) (Sezgin 2018).

Plain Weave   Twill Weave   Satin Weave
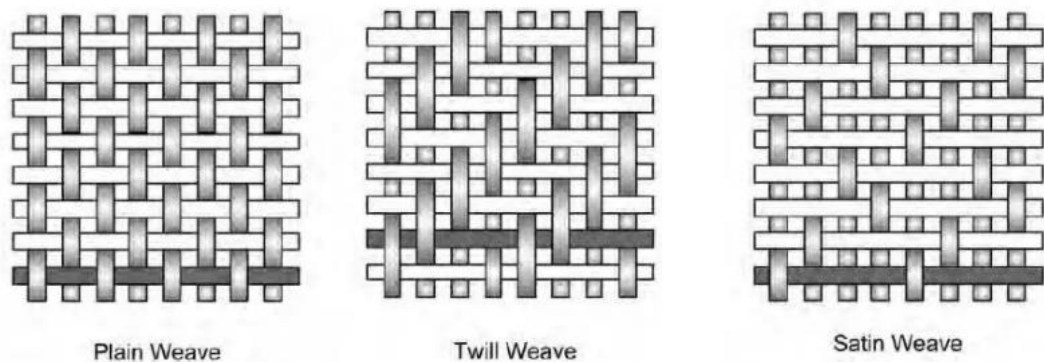
Figure 2.13. Different types of weave structures (Campbell 2010)

Composite materials have been produced by two main methods, open mold and close mold composite manufacturing methods. There are three types open mold composite manufacturing techniques, namely called as hand layup, filament winding, spray up, whereas vacuum bag molding, vacuum infusion processing, resin transfer molding, compression molding, pultrusion are widely used types of closed mold (Liquid Composite Molding–LCM) methods (Saçak 2014, Zin et al.2016, Gül and Kuruca 2017).

Vacuum bagging

In vacuum bagging method, laminate or parts are exposed to mechanical pressure during the curing process. Firstly, oil layers such as wax, plastic, etc. are applied to the mold surface because oil layer enables composites to be removed from the mold. Then, release film is placed on the mold. The breather and bleeder layer absorbs excess resin from the laminate. Later, the mold is covered with a heat-resistant vacuum bagging film. The air between the vacuum bag and the mold is removed by vacuuming. Thus, the material inside the mold is compressed with 1 atm pressure from the outside while the resin is being hardened (Figure 2.14) (Aboubakr 2013, Saçak 2014, Zin et al.2016, Gül and Kuruca 2017).
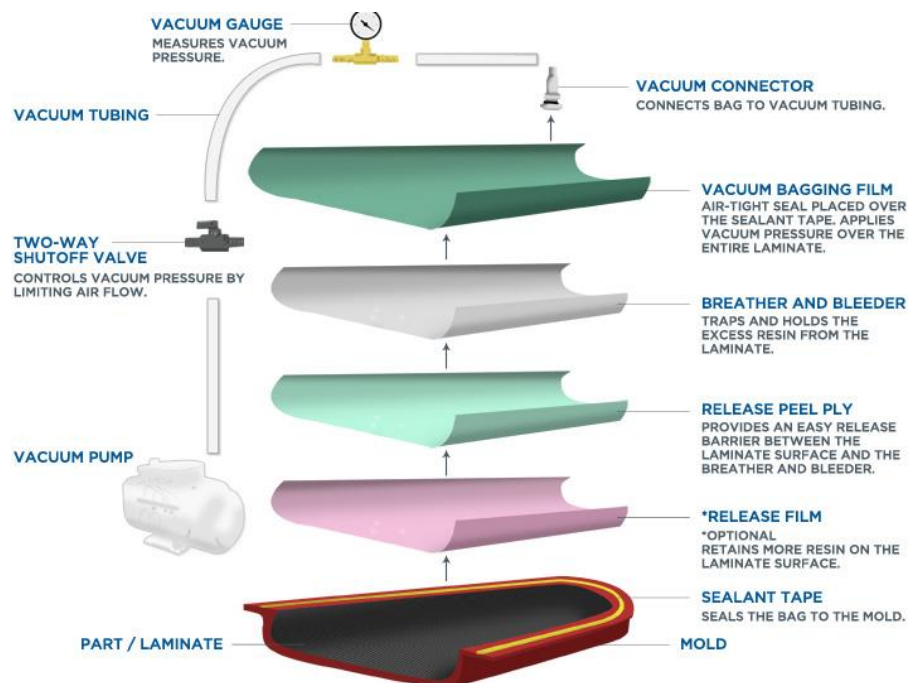
Figure 2.14. Vacuum bagging process set up (Zin et al.2016)

The vacuum bagging method provides better mechanical properties in the material due to its high reinforcement ratio compared to the hand lay-up method (Saçak 2014, Gül and Kuruca 2017).One major drawback of vacuum bagging method is that vacuum bagging film, release peel ply, release film, sealant tape are not being reused (Abdurohman et al.2018).

Filament winding

Filament winding technique has four stages: These are; a) fibre feeding mechanism, b) passing through the resin bath, c) wounding on rotating mandrel, d) curing process (Figure 2.15) (Zin et al.2016, Quanjin et al.2018).

Filament winding has many advantages. Some of which are;
- Controllability of resin usage.
- Least fiber cost.
- Excellent structural laminates properties (Zin et al.2016).

Filament winding also has some disadvantages such as;
- Overcosting of mandrel for big components.
- Changing fiber path is difficult (Miracle and Donaldson 2002, Zin et al.2016).
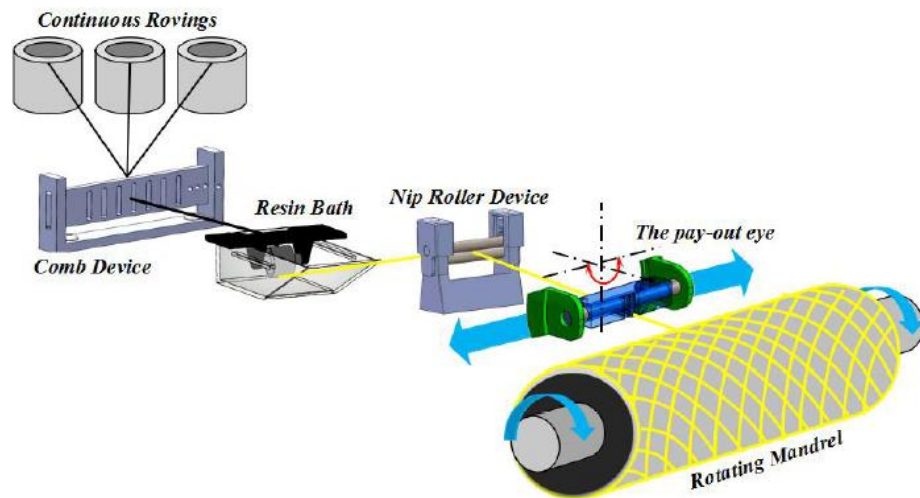
Figure 2.15. Filament winding method (Quanjin et al.2019)

Properties of fiber reinforced composite materials depend on different parameters such as fiber types, structure of textile fibers and properties of the fiber/matrix interface (Illeperuma et al.2014, Martin and Youssef 2018). For example; different fibers such as cotton, E-glass, UHMPWE and PVA have been combined with hydrogels. The hydrogel matrix reinforced by fibers or nanofibers result in robust composite hydrogels (Agrawal et al.2013).

2.7.1. Fiber reinforced composite hydrogels

Hydrogels are brittle materials due to the swelling of polymer structures in water and this situation affects the mechanical performance of composite hydrogel. There are different hydrogels with increased mechanical behaviors to overcome this problem, such as double network (DN) hydrogels, hybrid crosslinking hydrogels, hydrogels with crystalline domains, and fiber-reinforced hydrogels (Lin et al.2014). Studies about fiber-reinforced composite hydrogels are given below.

In one of the studies, Illepurıma et al. (2014) have investigated the mechanical performance of composites that include a tough alginate-polyacrylamide hydrogel matrix reinforced by stainless steel wool. It was noticed that mechanical behaviors such as stiffness and strength were enhanced by the addition of steel wool fibers to alginate-polyacrylamide (PAAm), in comparison with brittle alginate hydrogel composite (Figure 2.16).
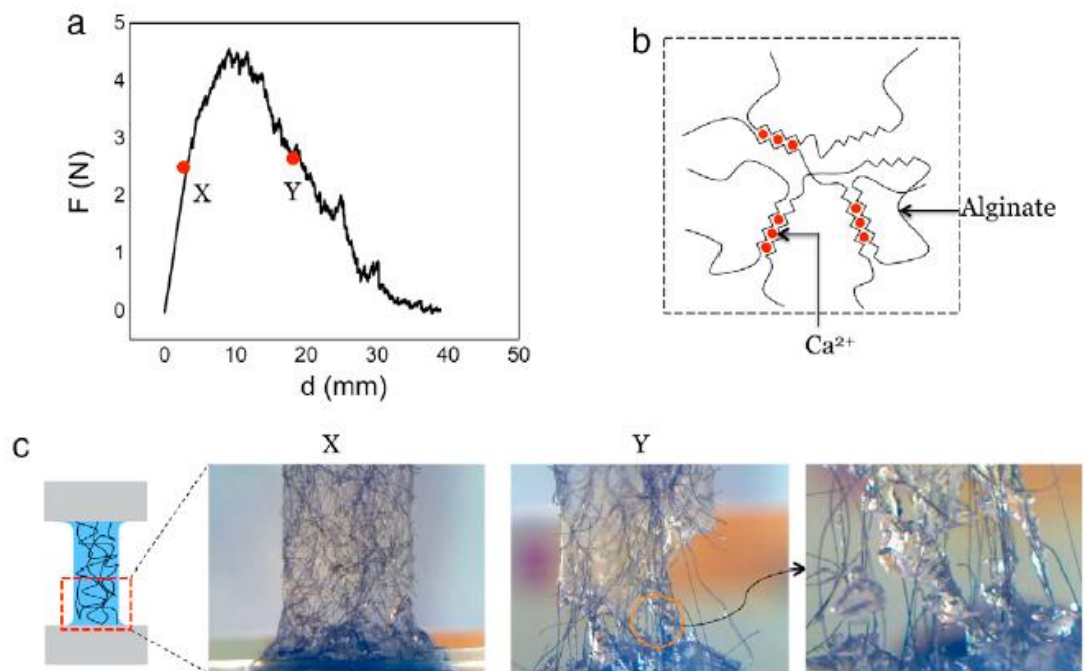
Figure 2.16. Brittle and weak alginate hydrogel composite failure mechanism. (a) Force-displacement curve of an alginate hydrogel composite. (b) Schematic of the molecular structure of alginate hydrogel. (c) Photos at two stages during the tensile test. At small deformations (point X), the fibers are bonded to the matrix. After reaching a maximum force, the composite starts to fail by fibers cutting through the matrix (point Y) (Illepurıma et al. 2014)

In another study, Lin et al. (2014) reinforced polyacrylamide (PAAm)-alginate hydrogel matrix with a stretch fiber mesh produced from thermoplastic polymers. The results indicated that fiber fracture resulted in mechanical energy dissipation, whereas the stretchable hydrogel matrix continued to hold the integrity of composites (Figure 2.17).
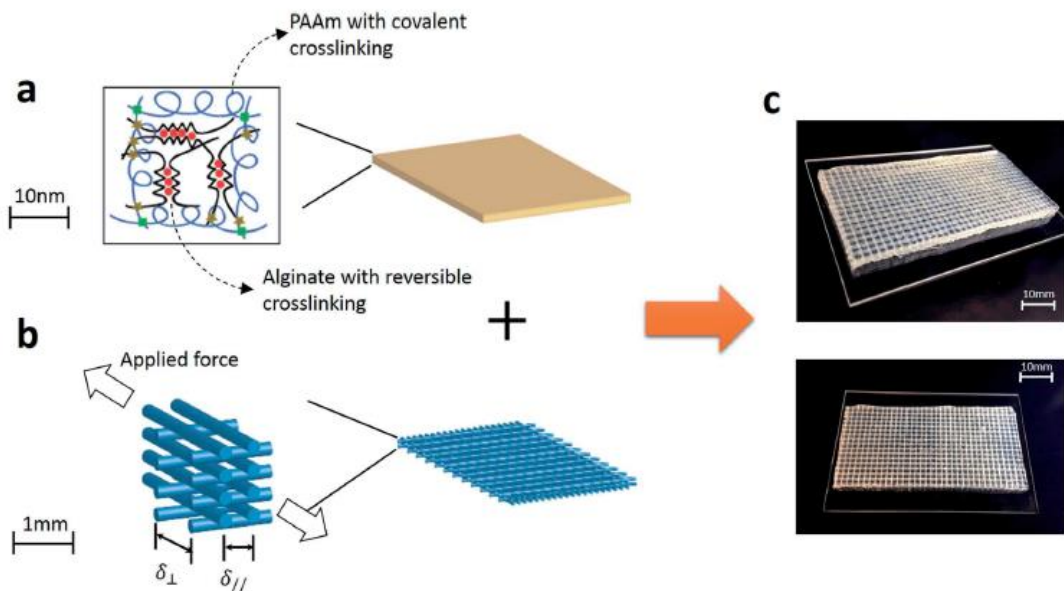
Figure 2.17. Schematic representation of the manufacturing process and the multiscale structure of the fiber-reinforced tough hydrogel: (a) the polyacrylamide-alginate hydrogel with hybrid crosslinking at the nanoscale. (b) the Flex EcoPLA thermoplastic-elastomer fiber mesh reinforcement hydrogel at the macroscale. (c) the polyacrylamide-alginate tough hydrogel reinforced with the fiber mesh photos (Lin et al.2014)

Martin and Youssef (2018) fabricated alginate/polyacrylamide (PAAm) hydrogels by reinforcing E-glass fiber. Divalent (Ca, Sr and Ba) cations or trivalent (Al and Fe) cations were used to crosslink E-glass fiber reinforced alginate/PAAm hydrogels. The dynamic mechanical properties such as storage modulus, loss moduli of the structures were measured. The results indicated that %3 wt. E-glass fiber reinforcement exhibited higher storage modulus than %2 wt. glass fibers. Moreover, the addition of E-glass fiber reinforcement enhanced storage and loss moduli of hydrogel compared to neat hydrogels. The alginate/PAAm hydrogels which contain Fe and Ba cations had higher loss moduli than other divalent or trivalent crosslinked hydrogels because the hydrogels dissipated energy effectively during the crosslinking with heavy elements (Figure 2.18).
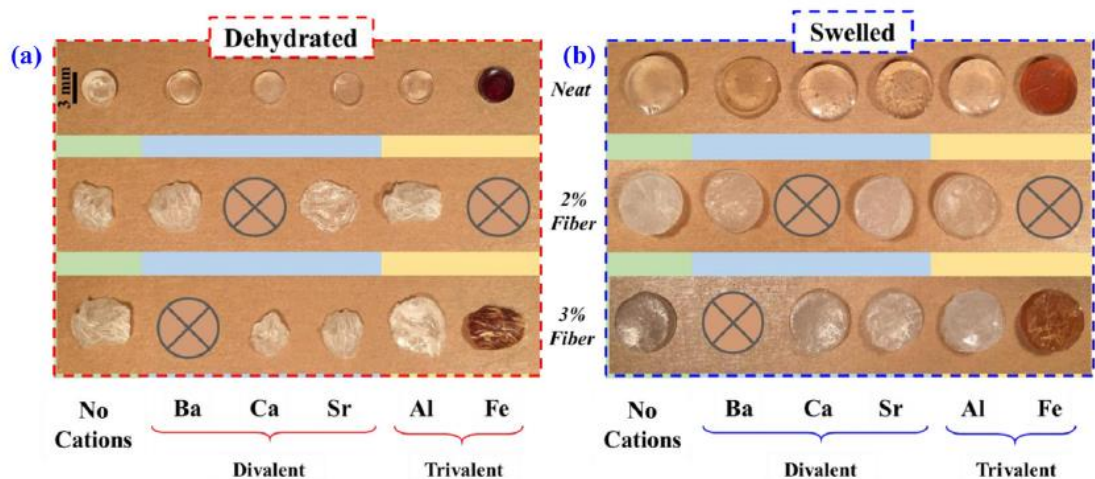
Figure 2.18. Comparison between dehydrated and swelled of hydrogels samples showing effect of multivalent and fiber-glass reinforcement on dried geometry (Martin and Youssef 2018)

No et al. (2020) fabricated artificial tendons made of fiber-reinforced hydrogel (FRH). Ultrahigh molecular weight polyethylene (UHMWPE) fibers were absorbed with either polyvinyl alcohol/gelatin hydrogel or polyvinyl alcohol/gelatin strontium-hardystonite composite hydrogel. UHMPW fibers imitated the collagen fiber bundles, whereas polyvinyl alcohol/gelatin (PG) hydrogel or polyvinyl alcohol/gelatin strontium-hardystonite (PGS) hydrogel imitated the extracellular matrix of the native tendon. When FRH-PG and FRH-PGS were compared with the human Achilles tendon's tensile strength, it was seen that FRH-PG and FRH-PGS had 77- 81 MPa tensile strength value (Figure 2.19). Overall, these results indicated that FRH-PG and FRH-PGS could be used as artificial tendon material.
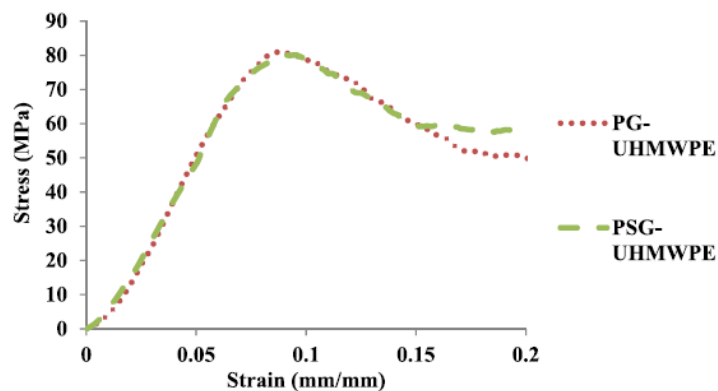
Figure 2.19. Representative Stress−strain curve for FRH-PG (dotted red) and FRH-PGS (dashed green) (No et al.2020)

2.7.2. Fabric reinforced composite hydrogels

Hydrogels possess low mechanical properties (Hubbard et al.2019). For this reason, textile structures such as nonwovens, fabrics etc. are used to improve mechanical properties of hydrogels. Also, such novel composite hydrogels, which are reinforced with fabric or nonwoven, have been extensively used for load-bearing biomedical applications (Holloway et al.2010, Zhang et al.2020). There have been some studies involving fabric, fiber mats reinforced materials that have given below.

Huang et al. (2017) combined polyampholyte (PA) gels with E-glass woven fabrics. They preferred PA hydrogel as matrix material. The glass fabric was selected because it could compose with PA hydrogels. Their results showed that fiber-reinforced composite fracture resistance was associated with the energy dissipation of the matrix during the fiber pull out process.

Holloway et al. (2010) prepared ultrahigh molecular weight polyethylene (UHMWPE) and polypropylene (PP) fiber mats reinforced with polyvinyl alcohol (PVA) hydrogels. According to Halloway et al. (2010) mechanical results of composite showed that UHMWPE reinforced PVA hydrogels could mimic modulus of anisotropic characteristics in the native meniscus.

Zhang et al. (2020) obtained stiff and tough PVA composite hydrogels with reinforced fabric. During the external forces on composite structures, fracture of fibers resulted in the dissipation of mechanical energy whereas mechanical dissipation energy caused increasing hydrogel toughness. Swelling properties of PVA composite hydrogels decreased the stiffness due to interfiber friction (Figure 2.20)
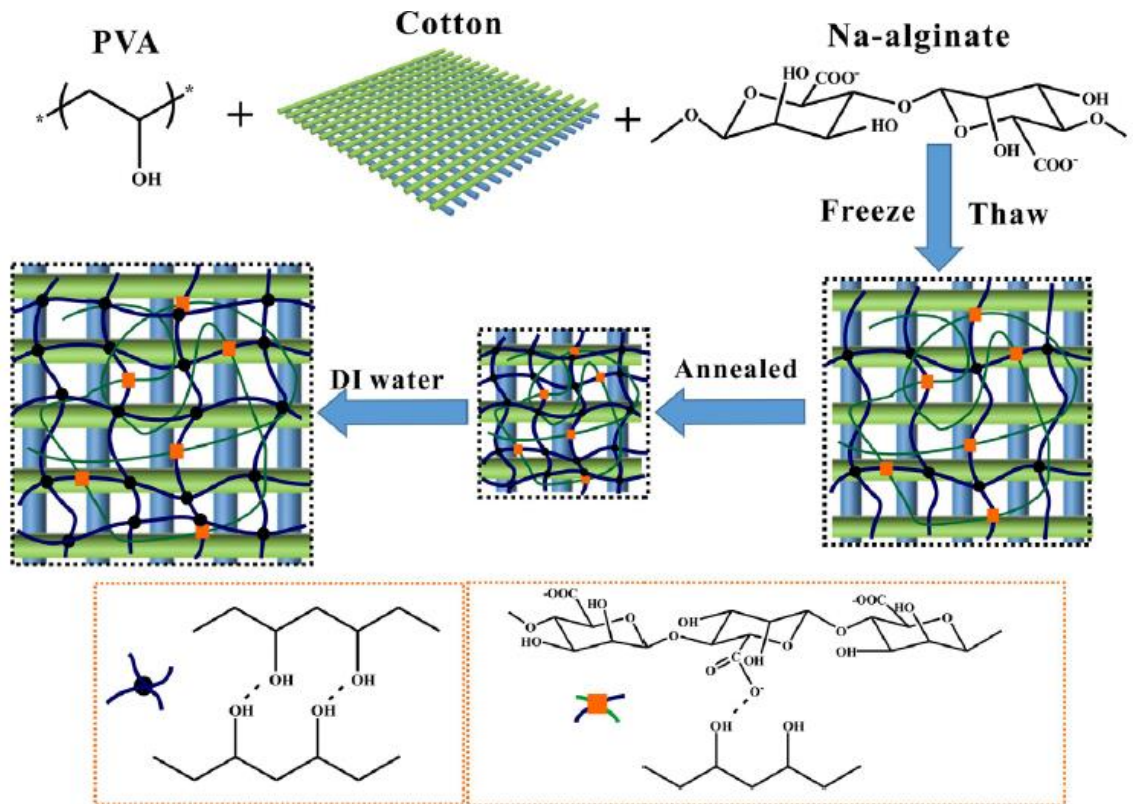
Figure 2.20. The preparation of physically cross-linked PVA–SA hydrogels with cotton fabric reinforced (Zhang et al.2020)

3. MATERIALS AND METHODS

3.1. Materials

3.1.1. Raw materials

Ne40/1 polyvinyl alcohol (PVA) yarns used in the research were obtained from KURABO Marugone Mill, Japan. Ne60/2 Open-end Cotton (Co) yarns was provided from Batmaz Tekstil company (Kestel OSB, Bursa, Turkey) (Koc et al.2019a, b, Koc et al. 2020a, b). Nm33/1 flax yarn, and Nm56/2 wool yarn were used as natural yarns (Koc et al.2020b). Nm10 viscose ring, Nm14 viscose OE (open-end), Nm30 viscose CF (continue filament) yarns were purchased from internal market.

3.1.2. Chemicals

Glutaraldehyde (50wt %) solution was obtained from Amresco (Koc et al.2019a). Borax also known as sodium tetraborate decahydrate ($Na_2B_4O_7.10H_2O$) was provided from Galenik Ecza ve Kimyevi Maddeler Deposu (Batch no: 1408H0048). Distilled water was used in all processes. All raw materials were employed without further purification (Koc et al.2019a, b, Koc et al.2020a, b).

3.2. Methodology

3.2.1. Weaving process of yarn reinforced hydrogel composites

Before production of the woven fabrics, two sets of PVA yarns of Ne40/1 were doubled (combined) into one single yarn at 4850 rev/min spindle speed and 300 t/m twist. Warp was prepared using Ne60/2 Co open-end yarn. A reed number of 12 (dents) was employed with two ends drawn between two reed dents. Hence 24 ends cm^{-1} warp density was obtained. Ne40/2 PVA weft was inserted. Fabric samples were woven by using 10 shafts with the plain draft (Koc et al.2020a).

A weave repeat of 10 warps and 30 wefts were obtained to hold firmly and cover the Co warp from both bottom and upper surfaces by PVA weft yarns. In this way, the Co warp was covered by PVA yarns in top and bottom sides and embedded in hydrogel after gelation of PVA yarns. Fabrics were woven in a sample weaving machine at 400 mm width (Koc et al.2020a).

3.2.2. Weaving process of fabric reinforced hydrogel composites

In this section, weaving process of cotton (Co), PVA, hybrid yarns are presented (Koc et al.2019a). Weaving process was conducted to produce the woven fabric samples (Marks and Robinson, 1976).

Before woven fabric production, two Ne40/1 PVA yarns were doubled and then twisted at 4850 rev/min spindle speed and 300 t/m twist to form Ne 40/2 PVA yarns. These doubled and twisted PVA yarns were further doubled with Ne 60/2 cotton yarn and twisted together to form a hybrid yarn.

The warp of woven fabrics was prepared using Ne60/2 cotton open-end yarn. A reed number of 12 (dents/cm) was employed in weaving with two ends drawn between two red dents. Hence 24 ends/cm warp density was obtained. The hybrid and PVA yarns were inserted as the weft. A weave repeat of 10 warp and 30 weft yarns were obtained as shown in Figure 3.1 to hold firmly and cover the cotton warp from both bottom and upper surfaces by hybrid and PVA weft yarns, respectively. Fabric samples were woven by using 10 shafts with the plain draft. As seen from the weave repeat, there are three different weft yarn movements. 1., 4., 7., . . . PVA weft yarns make one up four downs movement, 2., 5., 8., . . . hybrid weft yarns make one up and one down while 3., 6., 9., . . . PVA weft yarns make movements of four ups and one down. In this way, the cotton warp was covered by PVA and hybrid yarns from the top and bottom surfaces and embedded in hydrogel after gelation of PVA yarns. Fabric thus designed was woven at 36 picks/cm weft density and 184.7 g/m^2 of weight per square meter.

This fabric construction includes around 40% cotton and 60% PVA. Drafting and dobby plans are also seen in Figure 3.1. Fabrics were woven in a sample weaving machine at 400mm width.
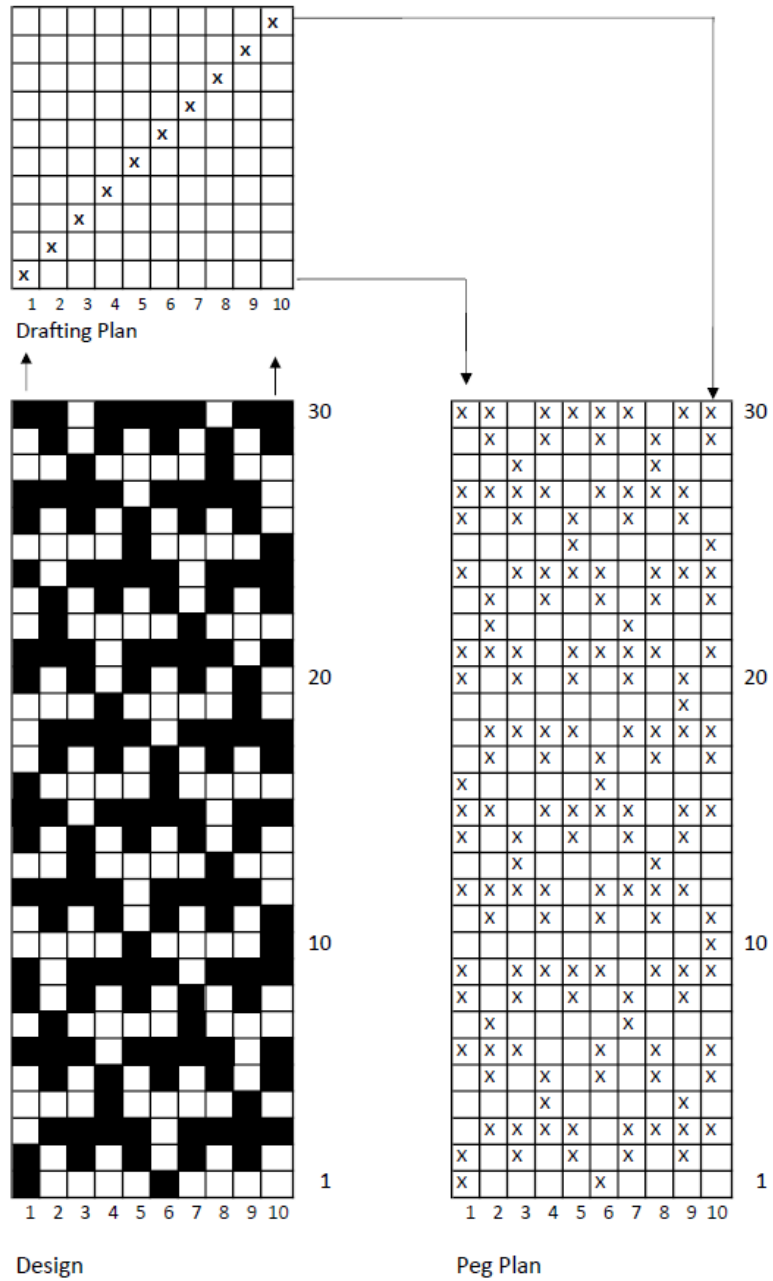
Figure 3.1. Weave, drafting and peg plans (lifting plan) of neat polyvinyl alcohol/cotton fabric

3.2.3. Weaving process with flax, OE cotton and wool warp

In this section, three types of warp yarn were prepared for weaving fabrics to produce natural fabric reinforced hydrogel composites (Koc et al.2020b).

As seen from Figure 3.2, these are Nm33/1 flax, Ne60/2 open-end cotton and Nm56/2 wool natural fiber yarns, Ne40/2 PVA and doubled and then twisted yarns of Nm33/1 flax+Ne40/2 PVA, Nm56/2 wool+Ne40/2 PVA and Ne60/2 open-end cotton+Ne40/2 PVA hybrid yarns. As a first step, two bobbins of Ne40/1 PVA yarns were doubled and then twisted to produce Ne40/2 PVA yarn. Later, Ne40/2 PVA yarns were further doubled and twisted together with Nm33/1 flax, Ne60/2 open-end cotton and Nm56/2 wool yarns to produce three different hybrid yarns. Both Ne40/2 PVA and hybrid yarns were twisted at 4850 rev/min spindle speed and 300 t/m twist values. Hybrid and Ne40/2 PVA yarns were inserted to the fabric as weft yarns.
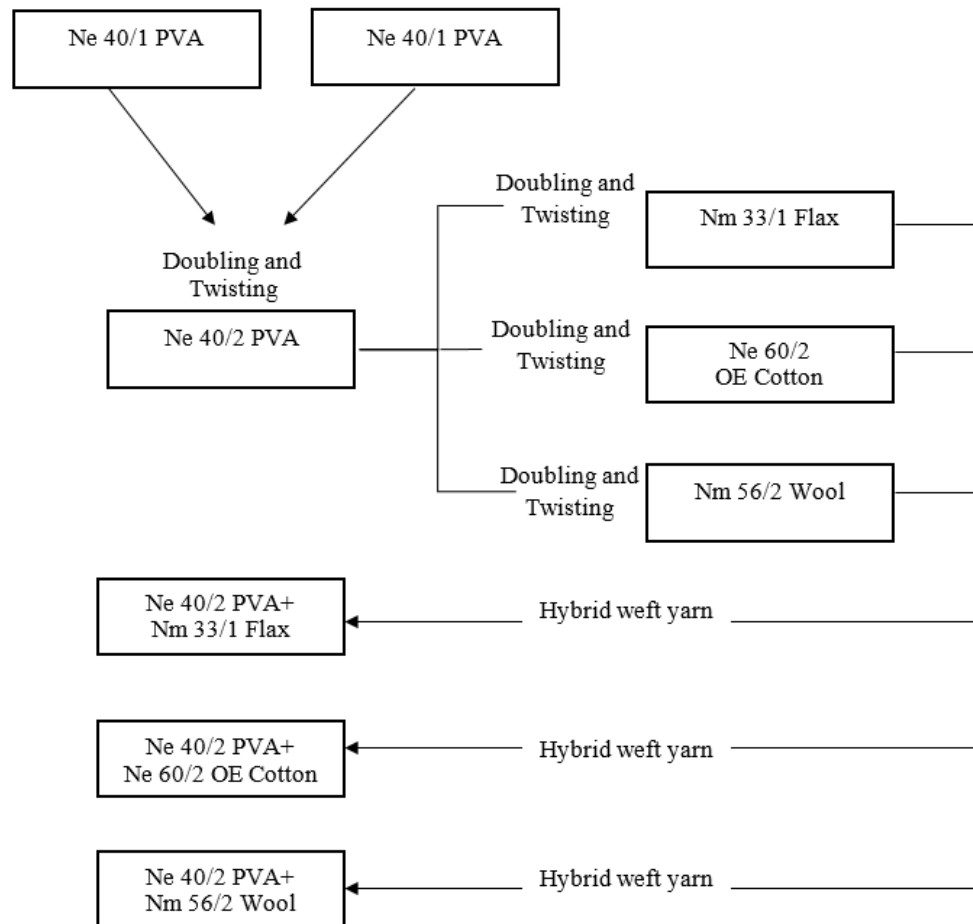
Figure 3.2. Hybrid weft yarn manufacturing process

As shown in Figure 3.3, warp was prepared from Nm33/1 flax, Nm56/2 wool and Ne60/2 open-end cotton natural fiber yarns respectively for the production of three different fabrics.

Hybrid weft with flax yarn component was inserted to the fabric produced with flax warp, hybrid weft with cotton yarn component to the fabric with cotton warp and with the wool component to the fabric with wool warp. Hence, each fabric had only one type of natural fiber (flax, cotton and wool respectively) in addition to PVA yarn. A reed number of 12 (dents/cm) was employed and the warp yarns were prepared at 12 ends/cm warp density for all three fabric types. Weft yarns were inserted at 20 picks/cm for flax warp fabric and 36 picks/cm for both cotton and wool warp fabrics. Fabrics were woven in a sample weaving machine at 400mm width. Weft yarns were inserted to the fabrics with 2 PVA and 1 hybrid yarns order. In this way, the fabric constructions included around 40% cotton-60% PVA, 40% flax-60% PVA and 40% wool-60% PVA material ratios.

After fabrics were woven, they were removed from the loom and made ready for the final step: gelation processing. The weave pattern used in our previous study (Koc et al.2019a) was also preferred in the production of these fabrics (Koc et al.2020b).
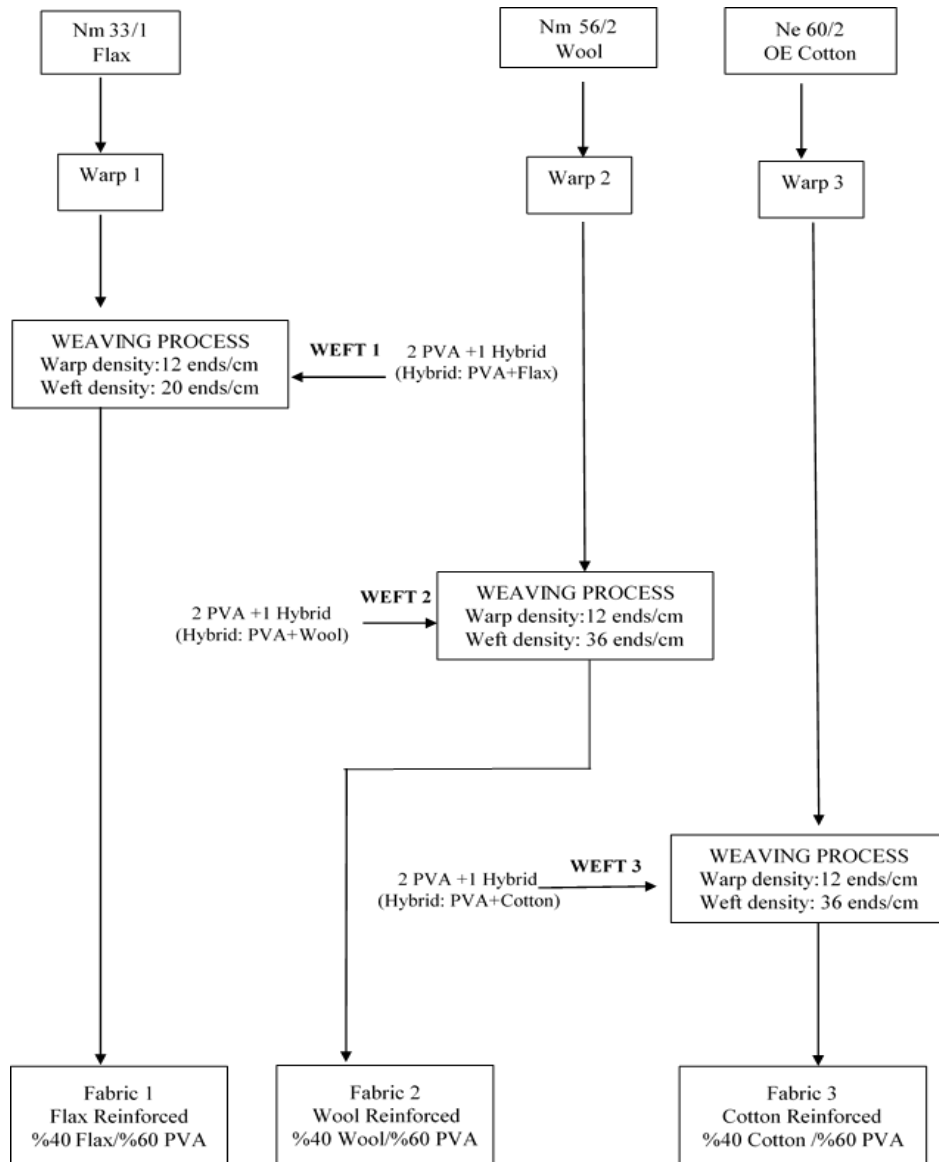
Figure 3.3. The manufacturing process of woven fabric of three types

3.2.4. Weaving process of regenerated cellulose fibers

In this subsection, three types of regenerated cellulose yarns were doubled and twisted with PVA yarn to manufacture woven fabrics and then regenerated cellulose fabric reinforced hydrogel composite to investigate the effect of yarn structure on fabric reinforced hydrogel composite mechanical properties. These are Nm10 viscose ring, Nm14 viscose OE, and Nm30 viscose CF, doubled and then twisted together with Nm33

PVA to produce Nm10 viscose ring + Nm33 PVA, Nm14 viscose OE + Nm33 PVA and Nm30 viscose CF + Nm33 PVA hybrid yarns.

In the first phase, two bobbins of Nm67 PVA yarns were doubled and then twisted to produce Nm33 doubled PVA yarn. Later, Nm33 PVA yarns were further doubled and twisted together with Nm10 viscose ring, Nm14 viscose OE, and Nm 30 viscose CF to manufacture three different hybrid yarns. Both Nm33 PVA and hybrid yarns were twisted at 4850 rev/min spindle speed and 300 t/m twist value. Hybrid and Nm33 PVA yarns were inserted to the fabric as weft yarns. The warp was prepared from Nm10 viscose ring, Nm14 viscose OE and Nm30 viscose CF regenerated cellulose fiber yarns respectively for three different fabrics. Hybrid wefts with viscose ring, viscose OE, and viscose CF yarn components respectively were inserted to fabrics manufactured with viscose ring, viscose OE, and viscose CF warp yarns. There are three types of woven fabrics made of PVA/viscose OE, PVA/viscose ring and PVA/viscose CF weft yarns (Fabric1, Fabric2 and Fabric3). A reed number of 12 (dents/cm) was used and the warp yarns were drawn at 12 ends/cm warp density for all three fabric types. Weft yarns were inserted at 30 picks/cm for viscose ring, viscose OE, and viscose CF warp fabrics. Fabrics were woven in a sample weaving machine at a 400 mm width. Weft yarns were inserted to the fabrics with 2 PVA and one hybrid yarns order. The fabric constructions contained around 40% viscose OE-60% PVA, 40% viscose ring-60% PVA and 40% viscose CF-60% PVA material ratios. After the production, woven fabrics were prepared for gelation processing.

3.2.5. Gelation of PVA in cotton yarn reinforced hydrogel composite

Borax/water solutions were prepared by the magnetic stirring process at 50°C with different concentrations (0.1, 0.3, 0.5, 1, 1.5, and 2.0 wt. %). 5 cm x 10 cm fabric samples were cut at both warp and weft directions. Each fabric sample was put on a petri dish and the prepared borax/water solutions were poured on the fabric samples to transform PVA yarns into hydrogel by crosslinking PVA molecules in the fabric structure. The samples were kept at ambient conditions during 24 hours for the further gelation. Then, excess borax/water solution was removed and all the samples were washed with distilled water

at least five times to remove the uncrosslinked borax from hydrogel composite structure. All the hydrogel composites were dried for the performance tests (Koc et al.2020a).

3.2.6. Gelation of PVA in cotton fabric-reinforced hydrogel composite

Aqueous GA solution preparation, a different volume of GA solutions (0.25, 0.5, 1.5, 2.0, and 3.5 ml) were added into 20 ml of water, whereas borax/water solutions were prepared by magnetic stirring process at 50 $^\circ$C with different concentrations (0.1, 0.3, 0.5, 1, 1.5, and 2.0 wt %). One mililiter of HCl was added into each solution. Since borax was in the solid state at the beginning, borax/water solutions were prepared in terms of weight percent. The received GA was in the liquid state, and GA solutions were prepared depending on volume (ml). About 5 cm x 10 cm fabric samples were cut in the warp directions and used to prepare fabric-reinforced hydrogel composite samples. Each fabric sample was put on a petri dish, and the prepared borax/water solutions and GA/water solutions (including HCl as the catalyst) were spilled on the fabric samples to transform PVA yarns into hydrogel form by crosslinking PVA molecules in the fabric structure. PVA is a semi-crystalline polymer, and it always requires some heating for an appropriate dissolution when the polymer was used in the granular form (Koski et al.2004). In this study, since PVA was in the form fibers in the yarn and fabric structure, the surface area of PVA was high and the water molecules were very easily approached to PVA molecules and whole PVA fibers were dissolved quickly just after pouring the water. So, with the existence of crosslinker molecules in the water, PVA yarns in the fabric were simultaneously dissolved and crosslinked leading to transformation into hydrogel structure. The samples were kept at ambient conditions during 24 h for further gelation.

Then, the excess borax/water and GA/water solutions were removed, and all the samples were washed with distilled water several times to remove the uncrosslinked borax and GA from the hydrogel composite structure. All the hydrogel composites were dried for the performance tests. The thickness of the neat fabric before the gelation was about 0.796 +/- 0.02 mm. When the fabric was treated with the crosslinkers and hold in the water in 90 min, the thickness of the composite hydrogels was about 2.3mm (borax sample) and

1.6mm (GA sample). When the samples were dried, the thickness decreased but never be less than the thickness of neat fabric (Koc et al.2019a).

3.2.7. Gelation of PVA in cotton, flax and wool reinforced hydrogel composite

Aqueous borax solutions were prepared with the addition of different concentrations (0.5, 1.0, 1.5, and 2.0 w/v %) and magnetic stirring process at 50°C. After production of PVA/Cotton, PVA/Wool, and PVA/Flax woven fabrics with PVA and hybrid weft and cotton/wool/flax warp yarns, the fabric samples were cut as 5 cm x 10 cm dimensions in the warp and weft directions. Each fabric sample was put on a petridish and the prepared borax/water solutions were spilled on the fabric samples to transform PVA yarns into hydrogel form by crosslinking PVA molecules in the fabric structure. The samples were kept at ambient conditions for 24 hours for the further gelation. Then, the excess borax/water was removed and all the samples were washed with distilled water several times to remove the uncrosslinked borax hydrogel from composite structure. All the hydrogel composites were dried for the performance tests (Koc et al.2020b).

3.2.8. Gelation of PVA/viscose OE, PVA/viscose ring, PVA/viscose CF Fabrics

The fabric samples were cut at warp and weft directions (5 cm × 10 cm dimensions). Each fabric sample was placed in the petri dish and treated with different borax-water solutions (0.5, 1, 1.5, and 2 w/v %). As mentioned in our previous studies (Koc et al.2019a, Koc et al.2020b), PVA molecules crosslinked in the fabric structure. Therefore PVA yarns transformed into hydrogel form in the fabric (Figure 3.4). To remove the uncrosslinked borax hydrogel from viscose OE, viscose ring, viscose CF reinforced hydrogel composite structure, all samples washed the distilled water for several times.
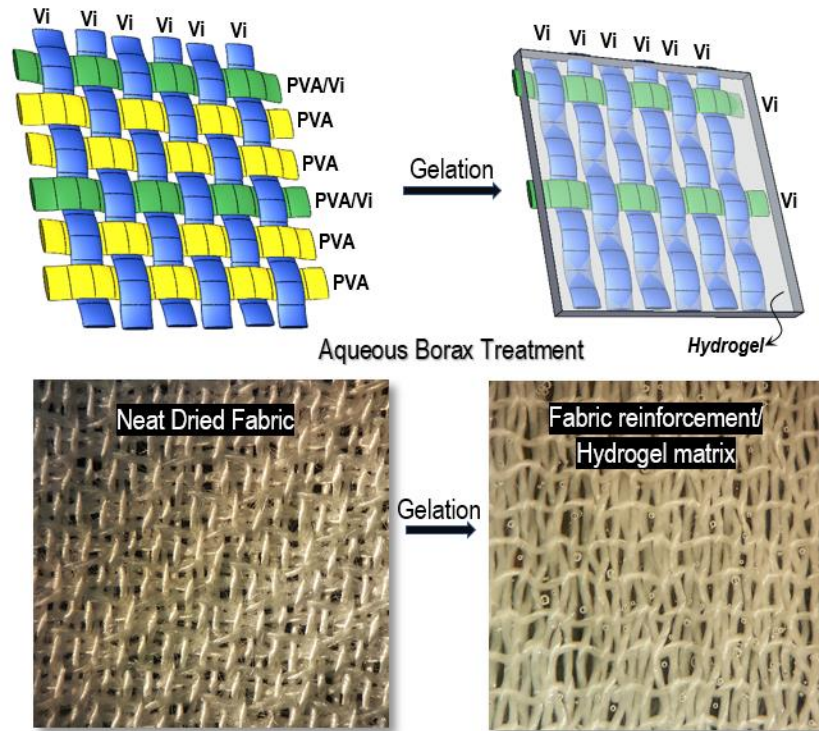
Figure 3.4. Conversion of neat fabric to regenerated cellulose fabric reinforced hydrogel composite via aqueous borax treatment

3.2.9. Chemical analysis of hydrogel

Chemical analysis of neat PVA and PVA/cotton fabrics (Koc et al.2019a, Koc et al.2020a) and composite hydrogel due to cross linker ratio have been carried out using ATR–FTIR (ATR-FTIR; Bruker IFS 66, Middle East Technical University Central Laboratory, Ankara, Turkey).Chemical analysis of neat PVA/Cotton fabrics, neat cotton yarn, neat PVA/Wool fabrics, neat wool yarn, neat PVA/Flax fabrics, neat flax yarn (Koc et al.2020b), neat PVA/regenerated cellulose fibers and neat woven PVA/ regenerated cellulose fabrics and their borax/water treated and dried counterparts and composite hydrogel due to cross linker ratio were recorded using Attenuated Total Reflection and Fourier Transform Infrared Spectroscopy (ATR-FTIR, Nicolet iS50) and measurements were performed at 20°C and relative humidity of 65%.

3.2.10. Morphology analysis of hydrogel

Scanning Electron Microscopy (SEM) Carl Zeiss Evo 40 was used to analyze the surface and the section morphologies. The samples were sputter coated with a conducting layer for better imaging (Koc et al.2020b).

3.2.11. Microstructural analysis of hydrogel

Microstructural characterization of neat PVA/Co fabrics and their borax/water-treated and dried counterparts (Koc et al.2019a, Koc et al.2020a) and GA/water treated and dried counterparts (Koc et al.2019a) were conducted using Rigaku Ultima IV X-ray diffractometer (2Θ between 10°and 60° with the scanning speed of 0.03^o/s).

3.2.12. Thermal characterization of hydrogel

Thermal properties of yarn-reinforced and fabric reinforced hydrogel composites in dried form were evaluated by measuring weight losses with temperature in air environment using a thermogravimetric analyzer (TA SDT 650, Middle East Technical University Central Laboratory, Ankara, Turkey), heating from 50°C to 800°C (heating rate of 10°C min^{-1}) (Koc et al.2019a, Koc et al.2020a). Thermal properties of natural woven fabric and regenerated cellulose fibers reinforced hydrogel composites in dried form were assessed by measuring weight losses in nitrogen environment using a thermogravimetric analyzer (TA Q600) by heating from 50 to 800°C (heating rate of 10°C min^{-1}) (Koc et al.2020b).

3.2.13. Swelling and water removal test

Each dried sample was immersed in a distilled water pool in Petri dishes and held for 90 min. Samples absorbed the water and swelled. After the swollen samples were taken from the water, excess water was removed with paper tissues and then yarn-reinforced hydrogel composite samples were weighed.

It was assumed that the first measurement of the sample contained 100% of water. Then, the samples were kept at ambient conditions to allow water evaporation. Weight measurements were repeated after every 15 min to observe water removal by time. This process was also conducted for neat fabric containing no hydrogel.

The degree of swelling was calculated with the following equation in percentage (Sonker et al.2016)

$$Swelling\ (\%) = (w_s - w_d) \times 100/w_d \tag{3.2}$$

where ws is the weight of hydrogel composite with water and wd is the weight of dried hydrogel composite.

3.2.14. Mechanical measurements of textile reinforced hydrogel composite

Tensile testing was carried out by using Shimadzu tensile tester with AG-X plus model and load cell capacity of 5000 N (Bursa Uludag University Textile Engineering Test and Analysis Laboratory, Bursa, Turkey). Exactly the same sample size was used after the gelation process without cutting them. Gauge length and testing speed were adjusted to 30 and 200 mm/min, respectively. Tensile tests were performed for dried and swollen fabric-reinforced hydrogel composite. Then the samples were waited in the deionized water to obtain the swollen samples. All the measurements were conducted at both neat fabrics and their hydrogel composites analogs in warp direction and weft direction (Koc et al.2019a, Koc et al.2020a, b).

3.2.15. Tensile strength measurements of the yarns and hydrogel composite yarns

In this subsection, tensile testing of hydrogel composite yarns which has been produced from PVA/Co hybrid yarn, Ne40/2 PVA, Ne60/2 Cotton were carried out by using Shimadzu tensile tester of AG-X plus model and load cell capacity of 50N (Bursa Uludag University Textile Engineering Test and Analysis Laboratory, Bursa, Turkey) (Koc et al.2019b).

Twenty yarns of 35 cm length were taken from each yarn type (Ne40/2 PVA, PVA/Co Hybrid yarn, Ne60/2 Cotton yarns) and tensile test was performed one by one. Gauge length and testing speed were adjusted to 30 and 100 mm/min, respectively. In order to wet the samples, the samples were kept in the deionized water for 15 minutes.

After treatment with borax, the samples were dried and then hold in deionized water for 15 minutes. The samples were considered to have 100 wt. % of water. All the measurements were conducted with both neat yarns and their hydrogel composite analogs.

3.2.16. Statistical Analysis

The primary purpose of Statistical Analysis for this study was to decide the relationship between borax-water concentrations and breaking force at the breaking points of regenerated cellulose (viscose ring, viscose OE, viscose CF) woven fabric reinforced hydrogel composites both in warp and weft directions.

To achieve this aim, the questions below were examined:
➢ Is there a significant relationship between borax-water concentration and breaking force hydrogel composite samples (in warp direction)?
➢ Is there a significant relationship between borax-water concentration and breaking force hydrogel composite samples (in weft direction)?

In this study, the data were analyzed with SPSS 25 Computer Package Program. Before starting data analysis, firstly it was checked whether the scores of borax-water concentration (borax-water conc.), breaking force at the breaking points of regenerated cellulose (viscose ring, viscose OE, viscose CF) woven fabric reinforced hydrogel composites showed normal distribution. The normality values of the data were calculated with the Shapiro-Wilks test due to the number of 5 samples in the normality test.

As a result of the normality test (normal distribution test), it was seen that the distribution was normal and the (Skewness-Kurtosis) values of the scores were less than 1.96. Correlation analysis was used to evaluate between the variables were linear or not. In this regard, the correlation coefficient explained (r) the level, amount and direction of the relationship between the variables (Büyüköztürk 2002).

Consequently, Pearson's correlation analysis was used to determine the relationship between borax-water concentration and breaking force at the breaking points in the warp direction or in weft direction scores.

The correlation coefficient of 1.00 is perfectly positive; -1.00 is the perfect negative; 0.00 indicates that there is no relationship.

As the absolute value of the correlation coefficient (r);

Being between 0.70-1.00 (high)

Being between 0.30-0.70 (middle)

Being between 0.00-0.30 (low level relationship)

For the statistical test significance level, (Sig.) $p < 0.05$ value was accepted

4. RESULTS AND DISCUSSIONS

4.1. Yarn-Reinforced Hydrogel Composite Produced from Woven Fabrics by Simultaneous Dissolution and Cross-Linking[1]

4.1.1. Concept study of the fabric-reinforced hydrogel composite

Schematic illustration and high magnification photograph images of PVA/Cotton (Co) fabric construction (before borax treatment), yarn-reinforced hydrogel composite (after borax treatment), and the dried and swollen forms along with mirror images of yarn-reinforced hydrogel composite are shown in Figure 4.1.

After production of PVA/Co woven fabric with PVA weft and Co warp yarns, fabric samples were prepared by cutting woven fabric as 5 x 10 cm^2 dimensions in the warp and weft directions. Samples were treated with previously prepared borax/water solution as explained in the "Materials and methods" section. As seen from Figure 4.1, when PVA/Co fabrics were treated with borax/water solution, PVA yarns (Figure 4.1(a)) totally lost their structures and turned to transparent gel form by simultaneous dissolution and gelation of PVA in the fabric. In this way, PVA forms matrix structures of Co yarn reinforced hydrogel composite (Figure 4.1(b)). Aligned Co yarns in the hydrogel composite structure can be clearly seen in dried (Figure 4.1(c1)) and wet forms (Figure 4.1(c2)). Since the matrix is a transparent hydrogel, yarns in the composite can be seen from both sides as in the mirror image (Figure 4.1(d)).

When the previously prepared borax/water solutions were poured on the fabric samples (10 x 5 cm^2), fabrics were extended in the Co yarn direction (warp) and shrunk in the weft direction; 10 cm (warp) x 5 cm (weft) and 5 cm (warp) x 10 cm (weft) cut samples turned to 11 cm (warp) x 2 cm (weft) and 8 cm (warp) x 7 cm (weft) size, respectively. This

---

[1] This subsection is based on the paper "Koc, U., Eren, R., Aykut, Y. (2020). Yarn-reinforced hydrogel composite produced from woven fabrics by simultaneous dissolution and cross-linking. *Polymers and Polymer Composites*. https://doi.org/10.1177/0967391120903648"

extension and shrinkage can be explained with the cross-linking of PVA molecules and partial opening of the crimp in Co yarns in fabric structure.

PVA yarns lost their structure with borax/water treatment and as a result of the simultaneous dissolution of PVA molecules and crosslinking of these dissolved molecules.
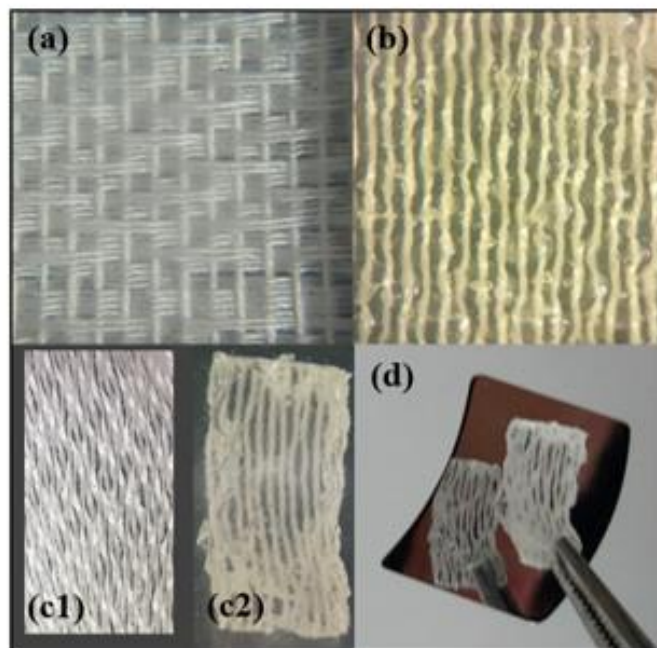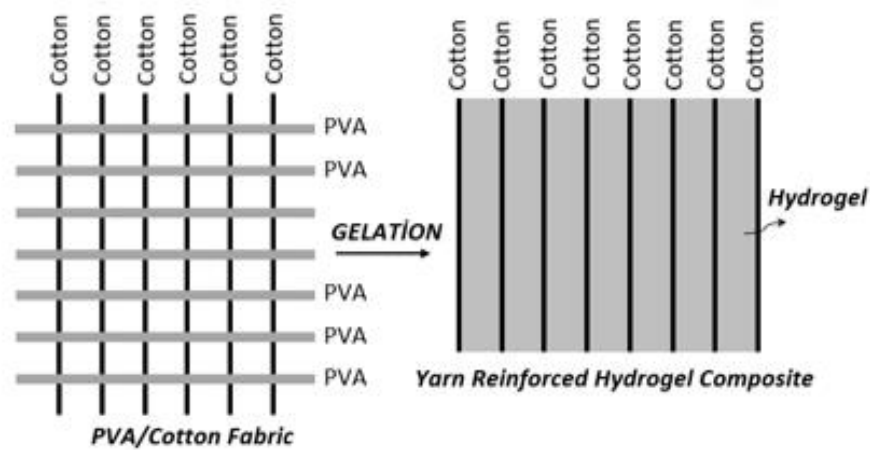
Figure 4.1. Schematic illustration and high magnification photograph images of (a) PVA/cotton fabric construction (before borax treatment), and (b) yarn reinforced hydrogel (after borax treatment),(c1) dried yarn reinforced hydrogel, (c2) swollen yarn reinforced hydrogel with water, and (d) mirror images yarn reinforced hydrogel composite

4.1.2. Chemical analysis of hydrogel composite via FTIR

In order to investigate the chemical change of the fabric samples when treated with different ratio of borax/water solutions, ATR-FTIR measurements were carried out with dried samples and the results are presented in Figure 4.2.

Cellulose molecules at Co yarn have plenty of -OH groups and can form many hydrogen bonds with the hydrogel matrix on the surface of the cotton yarn (Wang and Chen 2011, Han et al.2017). So, investigation of the transformation of PVA to hydrogel structures with borax cross-linking was carried out with FTIR analysis. All samples exhibited broad characteristic OH stretching vibration peak between 2971 cm^{-1} and 3637 cm^{-1} with the highest peak point around 3300 cm^{-1} (Lim et al.2015). This peak corresponds to hydrophilic hydroxyl groups in PVA and Co, and also increasing borax content of borax/water solution, the intensity of this peak gradually decreases because of the complexation (cross-linking) of borax and hydroxyl groups (Spoljaric et al.2014). Treatment of samples with borax leads to a new peak detected at 662 cm^{-1}. This corresponds to the stretching vibrations of O-B-O bonds (Spoljaric et al.2014). The peak at 2924 cm^{-1} can be attributed to C-H stretching vibration in CH_2 groups (Spoljaric et al.2014). The peak at 1088 cm^{-1} assigned to the C–O in stretching mode for PVA (Han et al.2017) and this peak shifts to 1107 cm^{-1} after formation of hydrogel structure. Both types of complexes as trigonal (around 1425 cm^{-1}) and tetrahedral (around 1335 cm^{-1}) were formed between PVA and borax molecules (Spoljaric et al.2014). The ratios of these peaks are not distinctively changed by increasing borax ratio. It can be assessed that the ratios of these complexes are not changed by increasing borax ratio. Free hydroxyl groups on trigonal complexes can also allow more hydrogen bonding between PVA and Co molecular chains (Spoljaric et al.2014).
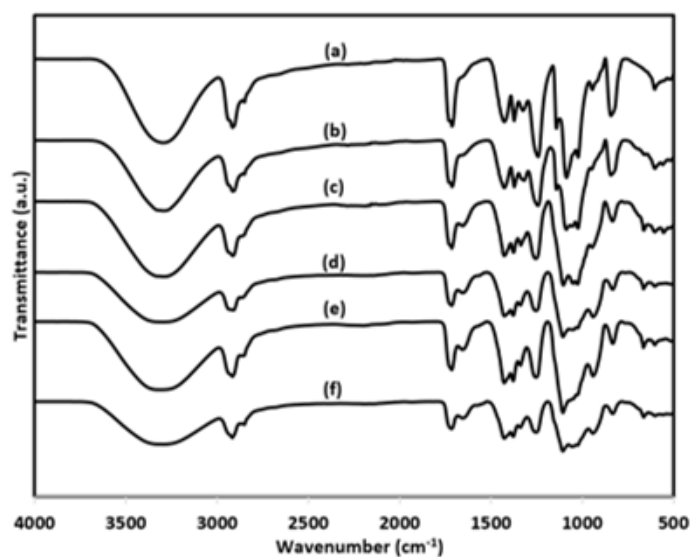
Figure 4.2. FTIR spectra of (a) PVA fabric, (b) neat PVA/cellulose fabric; PVA/cellulose fabric treated in different wt.% of borax/water solutions: (c) 0.5%, (d) 1.0%, (e) 1.5% and (f) 2.0%

4.1.3. Thermal analysis of hydrogel composite via thermogravimetric measurement

Thermogravimetric analysis (TGA) of neat PVA/Co fabric and different concentration of borax/water treated PVA/Co fabric, so-called yarn reinforced hydrogel composites in the air atmosphere, is shown in Figure 4.3. Initial weight loss step up to around 100 °C arises from water evaporation from the sample. The following sharp weight loss results from the removal of volatiles because of the degradation of materials. By increasing borax/water concentration, the thermal stability of yarn reinforced hydrogel composites increases and thermal degradation temperatures shift to higher degrees as a result of the restriction of segmental motion originated from cross-linking of PVA molecules (Lim et al.2015). So, the enhancement of thermal stability is obvious. Residual material content increases by increasing borax content in the structures after TGA measurement. As seen from the inset figure in Figure 4.3, residual contents were 3.95 wt.% for untreated fabric sample and 3.22, 2.66, 4.43, 8.58, 9.01, and 11.17 wt.% for 0.1, 0.3, 0.5, 1, 1.5, and 2 wt. % borax/water- treated and dried samples, respectively.
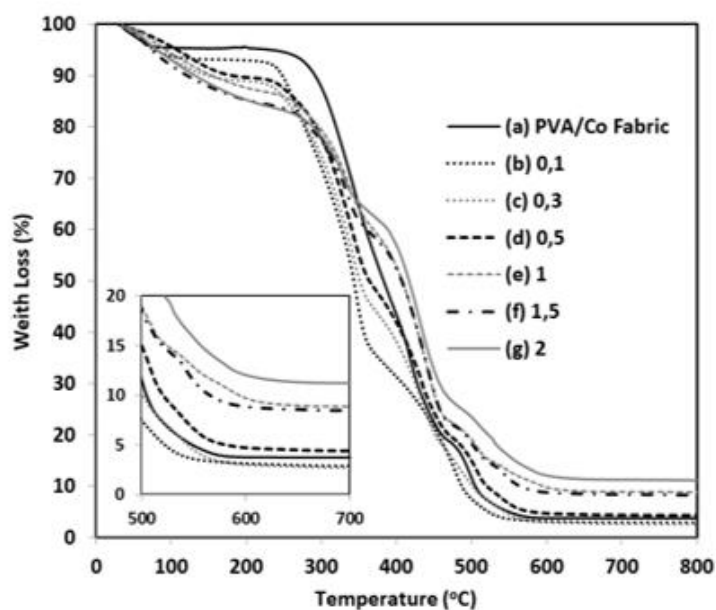
Figure 4.3. (A) TGA plots of (a) neat PVA/Co fabric; PVA/Co fabric treated in different wt.% of borax/water solutions: (b) 0.1, (c) 0.3, (d) 0.5, (e) 1.0, (f) 1.5 and (g) 2.0

4.1.4. Microstructural analysis of hydrogel composites via X-ray diffraction method

X-Ray diffraction measurements were conducted to study crystal formation and transformation after the borax/water treatment of the PVA/Co fabric samples (Figure 4). Neat PVA fabric exhibited two obvious diffraction peaks at 19.45° and 22.69°, which corresponded to the orthorhombic lattice structure of semi-crystalline PVA (Chen et al.2008, Han et al.2014). The peak at 19.45° shifts to 20.2° when the sample was treated with 0.1wt. % of borax/water solution and then dried. Increasing borax concentration up to 2wt. % fluctuated the location of this peak between 20.2° and 20.46°. On the other hand, increasing borax concentration decreases the intensity of the peaks of 19.45° and 22.69° as a result of the strong interaction of borax with hydroxyl group of PVA and complexation among them (Han et al.2014). These don't allow organized arrangement of PVA chains and hence reduce crystallization. A sharp peak at 22.6° and the peaks at 15.33° and 16.9° are caused by the crystalline structure of cellulose of Co in the fabric (Han et al.2014). Intensities of these peaks do not change homogeneously depending on borax concentration since the density of the materials is not homogeneous at a specific thickness.
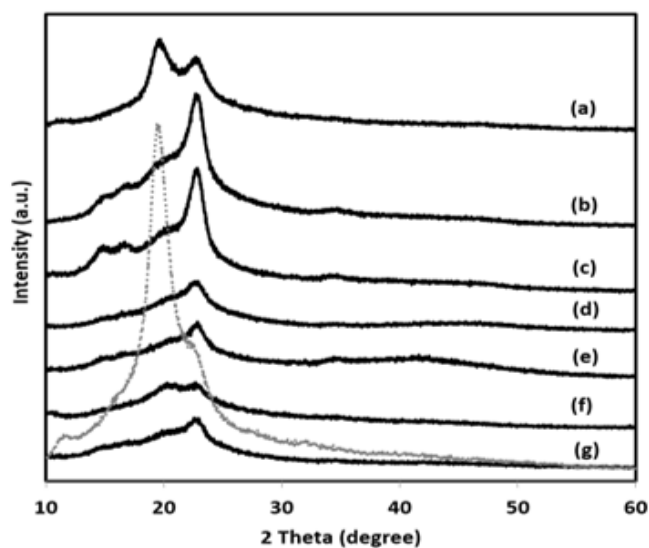
Figure 4.4. XRD patterns of (a) neat PVA/Co fabric; PVA/Co fabric treated in different wt.% of borax/water solutions: (b) 0.1, (c) 0.3, (d) 0.5, (e) 1.0, (f) 1.5 and (g) 2.0 (Gray dotted line is neat PVA fabric)

4.1.5. Water loss and swelling percentages yarn-reinforced hydrogel composites

After keeping the dried yarn-reinforced hydrogel composites in water for 90 minutes, samples were weighed for every 15 minutes to investigate weight loss of the samples depending on water evaporation and the results were demonstrated in Figure 4.5.

As seen from the figure, weight loss speed of borax-free neat PVA/Co fabric is higher than borax- treated fabric samples. Increasing borax concentration up to 1.0 wt.% decreases water evaporation rate, because partial cross-linking occurred up to 1.0 wt.%, then continuously increasing borax concentration increases the water evaporation rate from the hydrogel composites as chains are mostly cross-linked after this point.
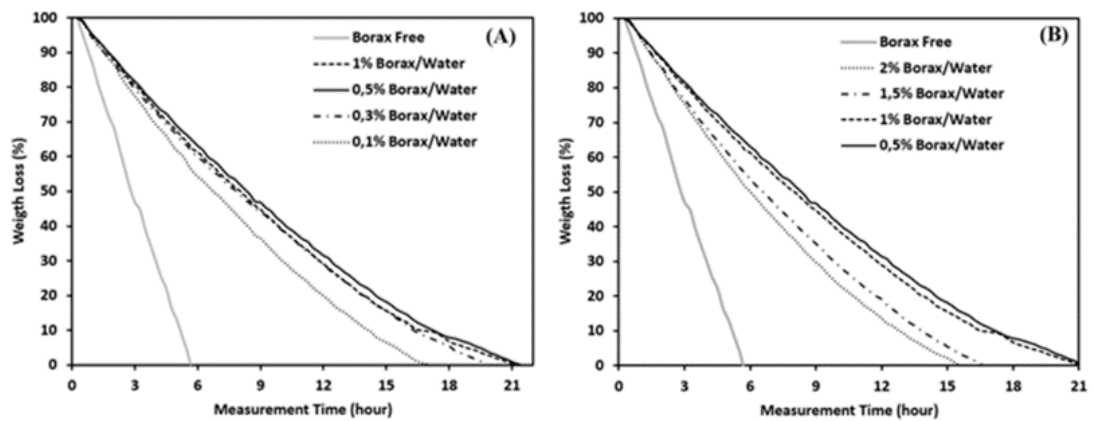
Figure 4.5. Water loss percentage by time of different borax ratio treated yarn reinforced hydrogel composites

Swelling percentage depending on cross-linker borax/water concentration and water evaporation from the hydrogel composites by time was calculated from the Equation (3.2) as given in "Materials and methods" section, and the plots are presented in Figure 4.6 (See 3.2 for details). As seen from the figure, the swelling percentage decreases by time at any borax concentration applied to the samples. On the other hand, measuring the different borax concentration treated samples at the same time frames and depending on the water removal from the hydrogel composites, swelling percentage continuously increases up to 1 wt. % and then decreases with increasing borax concentration. Swelling of PVA-based hydrogel depends on the amount of hydroxyl group and the chain mobility in the structure (Sonker et al.2018). When PVA molecules are crosslinked, chain mobility and the number of hydroxyl group decrease.

Amount of hydroxyl group decreases (can be seen from FTIR results) by increasing cross-linker concentration, but since partial cross-linking occurs up to 1 wt.% still chain mobilities are not restricted tremendously and therefore swelling increases. On the other hand, when cross-linker concentrations continuously increased after 1 wt. % borax concentration, the swelling percentage decreased as a result of the restriction of chain mobilities and mostly cross-linking of PVA molecules.
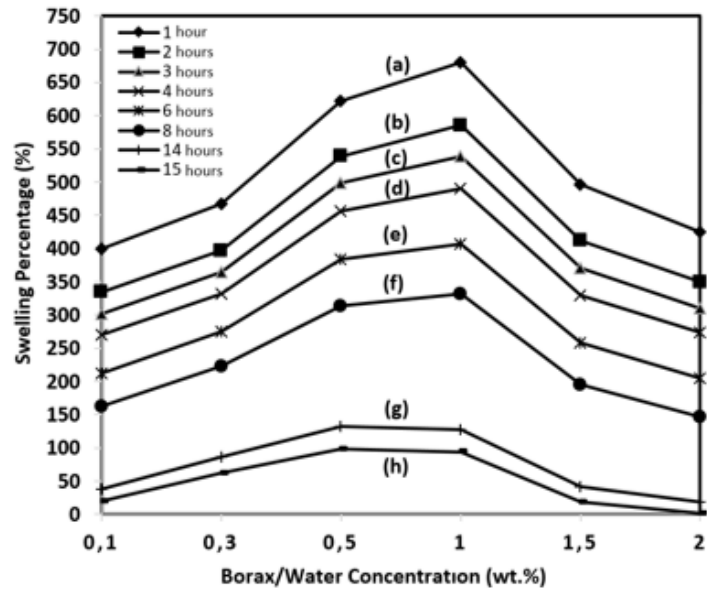
Figure 4.6. Swelling percentage of the yarn reinforced hydrogel composites due to borax/water treatment concentration: PVA/Co fabric treated in different wt. % of borax/water solutions: (b) 0.1, (c) 0.3, (d) 0.5, (e) 1, (f) 1.5 and (g) 2.0

4.1.6. Mechanical analysis of hydrogel composites due to water contents

Mechanical properties of yarn-reinforced hydrogel composites have been investigated due to the water content of the samples by measuring force-elongation plots in the warp (Figure 4.7(a)) and weft (Figure 4.7(b)) directions. As seen from the plots, breaking force tremendously increases when the water content decreases in the samples in both warp and weft directions. Water molecules are inserted among the cross-linked molecular chain and diverged from each other by swelling the hydrogel structure. On the other hand, when the hydrogel structure releases water, molecules come close to each other and tend to crystallize at the certain points. So, breaking forces for the dried samples are higher than the wet samples. Mechanical properties are much higher in the warp direction than in the weft direction since Co yarns are aligned in the warp direction and reinforced the hydrogel composite structure.

In order to compare the breaking point depending on water content in both warp and weft directions, the results are demonstrated in the same plots as given in Figure 4.8. Breaking force in the warp direction was 26,8 N when the hydrogel composite contained 90% of water and increased to 366,3 N when it was fully dried. Breaking force in the weft

direction was 1, 22 N when the hydrogel composite contained 90% of water and increased to 225,9 N when it was fully dried.
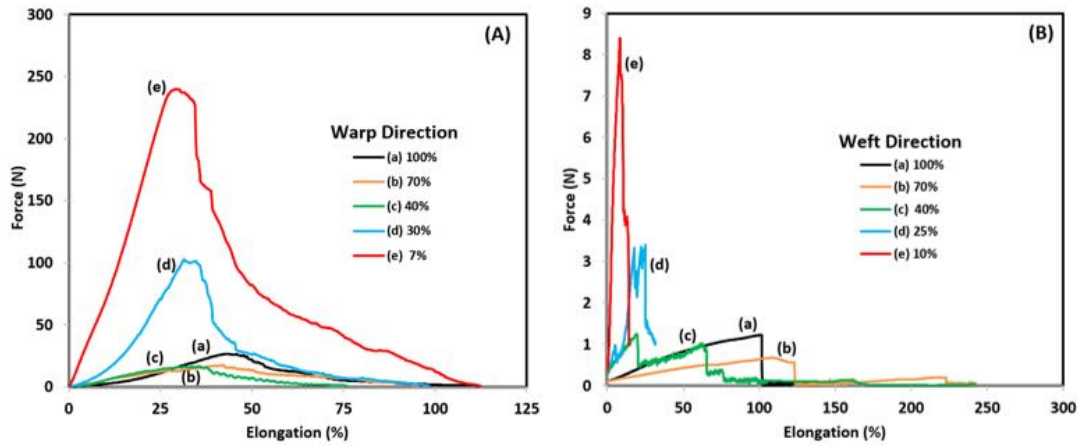
Figure 4.7. Tensile properties of yarn reinforced hydrogel composite (1.0 wt. % borax/water treated) when contain different content of water at (A) warp and (B) weft directions

Breaking force of PVA/Co fabric in the warp and weft directions are 212,7 N and 1055, 9 N respectively. Co yarns are withstood against breaking when the measurements were conducted in the warp direction, and PVA yarns are withstood against breaking when the measurements were conducted in the weft direction. Since perfectly spun PVA yarns were totally dissolved and then transformed to hydrogel structure after borax/water treatment, a tremendous mechanical loss in the weft direction was observed. Since also some hydrogels were formed among the Co fibers in the Co yarns (inset figure 4.8 (a), (b)), Co fibers have been moved away from each other and Co yarn resembles a roving. Because friction decreases between Co fibers and fibers can slide easily in the hydrogel, mechanical properties dramatically decrease with increasing water content in hydrogel composite in the warp direction. Dried hydrogel composites show maximum breaking force in both warp and weft directions since hydrogel turned to a brittle rigid structure in the dry form.
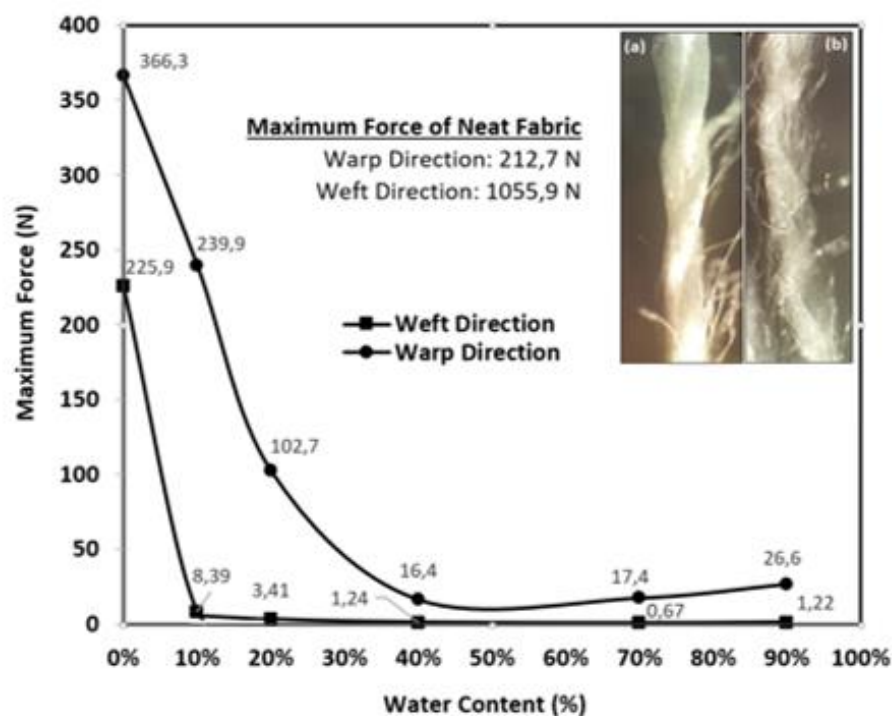
Figure 4.8. Breaking force comparison of the hydrogel composite sample (1.0 wt. % borax/water treated) at warp and weft direction due to water content. Inset figure: (a) cotton yarn in the neat fabric before gelation, (b) cotton yarn in hydrogel composite

4.2. One-step preparation of woven fabric reinforced hydrogel composite for enhanced mechanical properties[2]

4.2.1. Concept study of the fabric-reinforced hydrogel composite

Test samples were prepared by cutting the samples as 5 cm x 10 cm fabric in warp direction from as-produced woven fabric. Schematic illustration of neat PVA/cotton fabric and cotton fabric-reinforced hydrogel composite structure after gelation is demonstrated in Figure 4.9. As seen from the schematic illustration, the warp was made of cotton yarns, but the weft was inserted with the order of two PVA and one cotton yarns.

---

[2] This subsection is based on the paper "Koc, U., Aykut, Y., Eren, R. (2019a). One-step preparation of woven fabric-reinforced hydrogel composite. *Journal of Industrial Textiles*. https://doi.org/10.1177/1528083719850832"

When the fabric samples were treated with aqueous borax or GA solutions, PVA yarns in the fabric structures dissolved and transformed into gel form.

Since cotton yarns did not dissolve, they kept their position in the structure and stayed as the reinforcement material in the as-produced hydrogel composites. High magnification photograph images of neat PVA/cotton fabric (Figure 4.9 (A)) and its aqueous GA (Figure 4.9 (B) and borax (Figure 4.9 (C)) solution-treated analogs are shown in Figure 4.9. Mirror images of the hydrogel composite samples were given to show how cotton fabric positioned inside the hydrogel matrix (inset images in Figure 4.9 (B), (C)). As seen from the images, PVA transformation into gel structure when borax was used as crosslinker is seen more obviously than GA crosslinking at the proposed condition.
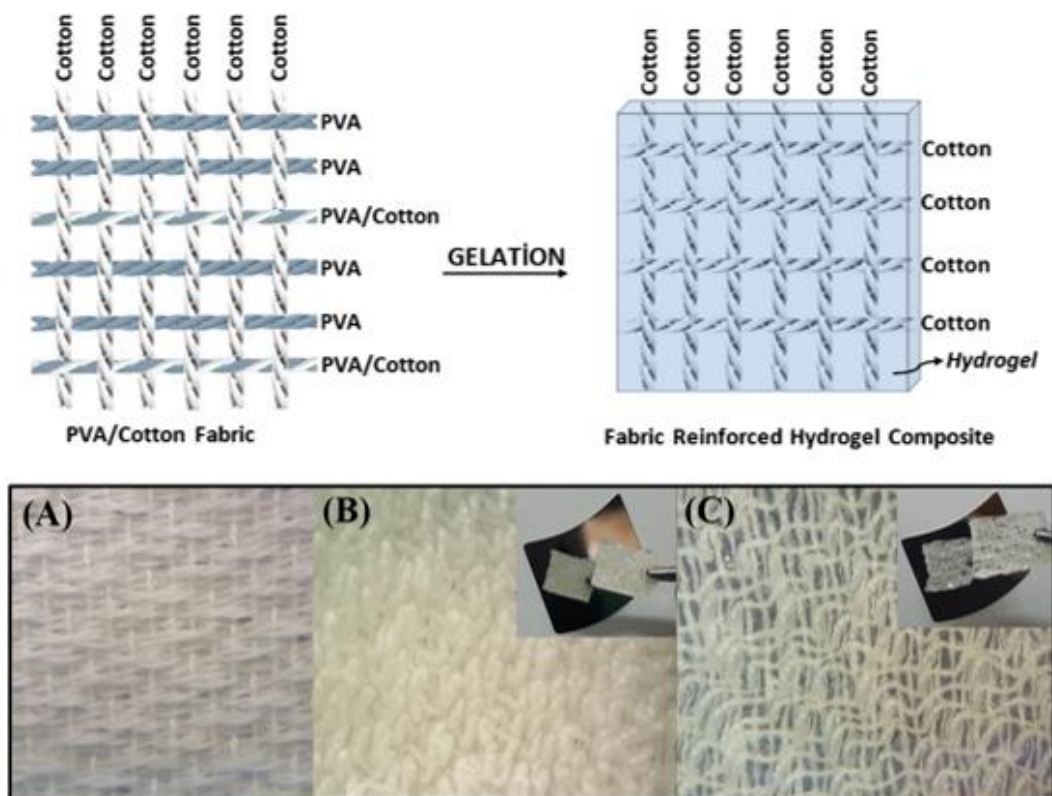
Figure 4.9. Schematic illustration and high magnification photograph images of (A) neat PVA/cotton fabric construction, (B) GA treated PVA/cotton fabric, (C) borax treated PVA/cotton fabric. Insets are the mirror images of the hydrogel composite samples

4.2.2. Chemical analysis of hydrogel composite via FTIR

In order to investigate the crosslinking of PVA by borax and GA in PVA/cotton fabric structure, ATR-FTIR characterizations were performed for the neat fabric and their different concentration of borax (Figure 4.10 (A)) and GA (Figure 4.10 (B)) treated fabric analogs. Pure fabric (before water or crosslinker solutions treatments) sample exhibiting a broad peak with the highest peak point around 3308 cm^{-1} corresponded to OH stretching vibration in PVA or cellulose molecules (Lim et al.2015).

In Figure 4.10 (A), the reduction of the OH peak with the addition of borax was one of the evidence of crosslinking occurring via OH groups (Spoljaric et al.2014). The reduction of this peak is not so much since cellulose was not dissolved and mostly OH groups on the cotton fiber surfaces complexed with borax, and OH groups in the fibers were mostly conserved. C-H stretching vibration was detected at 2924 cm^{-1} (Spoljaric et al.2014, Rudra et al.2015). The peak seen at 1088 cm^{-1} corresponded to C–O stretching (Han et al.2017).

The new peak detected at 658 with the addition of borax to the structure could be attributed to stretching vibrations of O-B-O bonds (Spoljaric et al.2014, Han et al.2017). With GA treatment in Figure 4.10 (B), OH groups were consumed, and the intensity of OH decreased as a result of possible formation of acetal bridges when crosslinking was formed (Mansur et al.2008). Broad OH peak shifted to higher wavenumber at GA sample compared to borax samples. Also, peak intensity of 1716 cm^{-1} related to C=O carbonyl stretching comes from GA molecules increased with increasing GA ratio, which implied that GA was not completely reacted with the molecules in the fabric structure, and some residuals of GA have still exited after gelation (Reis et al.2006).
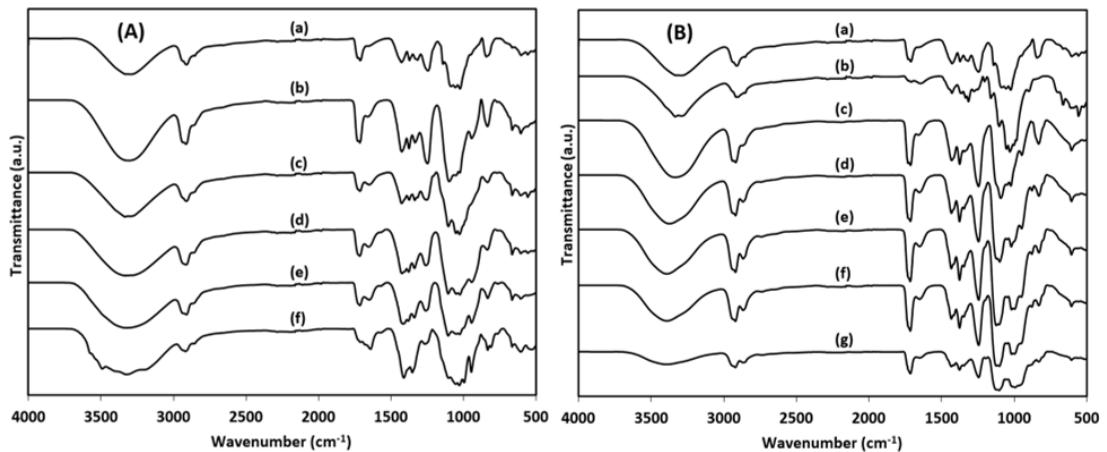
Figure 4.10. FTIR spectra of (a) neat PVA/Co fabric; and PVA/Co fabric treated in different (A) wt.% of borax/water solutions: (b) 0.3, (c) 0.5, (d) 1.0, (e) 1.5 and (f) 2.0; and (B) GA solution contents in water/HCl solution: (b) 0, (c) 0.25 ml, (d) 0.5 ml, (e) 1.5 ml, (f) 2.0 ml and (g) 3.5 ml

4.2.3. Thermal analysis of hydrogel composite via TGA measurement

Thermogravimetric analysis (TGA) of neat PVA/cotton fabric and borax/water and GA-treated PVA/cotton fabric, so-called fabric-reinforced hydrogel composites in the air atmosphere, are shown in Figure 4.11. Initial weight loss up to around 100 ^{o}C corresponded to water evaporation from the samples. Prominent weight loss was observed mainly between 267-389 ^{o}C and 389-665 ^{o}C for borax-treated samples and between 302-496 ^{o}C for GA-treated sample. This can be related to the removal of volatiles as a result of the degradation of the dried hydrogel composite by heating. Prominent weight loss started at a lower temperature in the borax-treated sample compared to neat fabric up to around 400 ^{o}C, and then increasing temperature made the degradation slower in borax-treated samples. Increasing borax content made the process slower because of the restriction of segmental motion by crosslinking (Lim et al.2015). Residual of the material after the TGA test increased because borax components stayed in the system, and contents were 0 wt.% for untreated fabric sample and 1.11, 2.53, 3.89, 8.36, 8.47 and 13.94 wt.% for 0.1, 0.3, 0.5, 1, 1.5, and 2 wt. % borax/water treated and dried samples sequentially (Figure 4.11(a)). GA- treated hydrogel composites were completely degraded up to 800 ^{o}C regardless of the GA content (Figure 4.11(b)).

GA treatment did not have a very significant effect on thermal stability of the neat fabric in this study comparing to borax-treated samples, but the degradation continued at higher temperatures with increasing GA content after around 500 °C. This can also be explained by the restriction of segmental motion by crosslinking (Lim et al.2015).
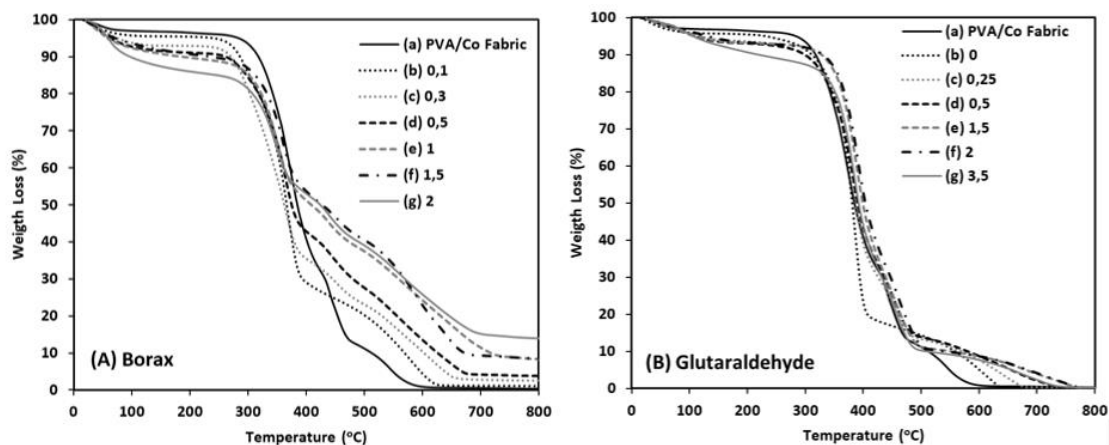
Figure 4.11. TGA plots of (a) neat PVA/Co fabric; and PVA/Co fabric treated in different (A) wt.% of borax/water solutions: (b) 0.1, (c) 0.3, (d) 0.5, (e) 1, (f) 1.5 and (g) 2.0; and (B) GA solution contents in water/HCl solution: (b) 0, (c) 0.25 ml, (d) 0.5 ml, (e) 1.5 ml, (f) 2.0 ml and (g) 3.5 ml

4.2.4. Microstructural analysis of hydrogel composites via X-ray diffraction method

X-Ray diffraction measurements were conducted on the dried hydrogel composite samples to investigate how gelation affected the crystalline microstructural changes with both borax and GA treatments, and the XRD plots were demonstrated in Figure 4.12 (A) (borax-treated samples) and (B) (GA-treated samples). Two distinct peaks detected at 19.52° and 22.8° at neat PVA/cotton fabric are related to the orthorhombic lattice structure of semi-crystalline PVA (Chen et al.2008, Han et al.2014).

Peak intensity at 19.52° extremely decreased even with a small amount of borax treatment. Peak intensity at 22.8° also decreased with the initial treatment of low concentration of aqueous borax solution, and increasing borax concentration in the treatment solution caused to reduce this peak even more.

58

The intensity reduction of these peaks could be related to strong interaction and complexation of borax with hydroxide radical of PVA chains that diminished the rearrangement of PVA chains and did not allow a proper crystallization (Han et al.2014).The overlapping peak at 22.8° can also come from crystalline structure of cellulose in cotton yarns in the hydrogel composite (Adanur 2000).Intensity of the peaks coming from cellulose mostly decreased because mostly dried hydrogel matrix was face to experimental section rather than cotton yarns in the dried composite hydrogel. Pure borax peaks at 35.2° were also seen at high borax concentration treatment sample since excess borax didn't go into crosslinking reaction and crystallized again after drying the composite hydrogel samples (Baron et al.2019).A similar trend was observed at GA-treated samples as the peak intensity at 19.52° tremendously decreased (Figure 4.12 (b)). Crystallinity also decreased with GA treatment as a result of crosslinking of PVA (Rudra et al.2015). The decrease in the peak intensity of 19.52° after both borax and GA treatments is another evidence of the crosslinking of PVA chains.
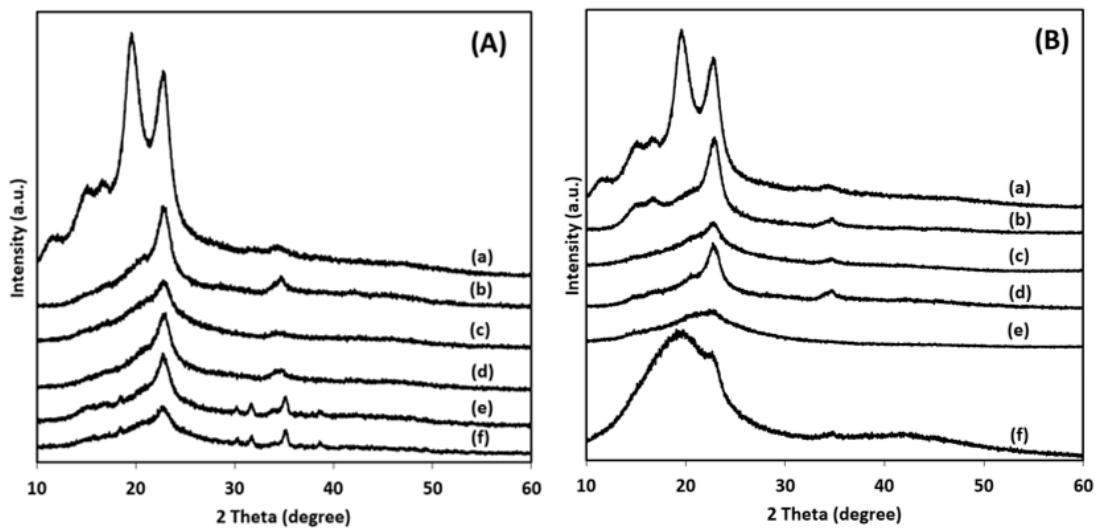
Figure 4.12. XRD patterns of (a) neat PVA/Co fabric; and PVA/Co fabric treated in different (A) wt.% of borax/water solutions: (b) 0.1, (c) 0.5, (d) 1, (e) 1,5 and (f) 2.0; and (B) GA solution contents in water/HCl solution: (b) 0, (c) 0.25 ml, (d) 0.5 ml, (e) 2.0 ml and (f) 3.5 ml

4.2.5. Mechanical analysis of hydrogel composites due to crosslinker and water contents

The same size of PVA/cotton-woven fabrics were cut at warp directions. The maximum applied force of the neat fabric was measured as 227.32 N. Appropriate ratio of aqueous borax and GA solutions were poured on the fabrics and waited for 24 hours in order to allow a proper crosslinking of the PVA molecules in the fabric structure, and as-obtained woven fabric-reinforced hydrogel composites were rinsed with distilled water several times. Finally, composite structures were left to laboratory condition (50% relative humidity and temperature to 24°C) to release water, and then mechanicals tests were performed. Mechanical properties of the dried woven fabric-reinforced hydrogel composites were demonstrated in Figure 4.13 (A) (borax treated) and (B) (GA treated). As seen from Figure 4.13 (A), the rigidity of dried composite hydrogel increased with the initial addition of borax and then decreased gradually by increasing borax ratio in the aqueous treatment solution. Breaking elongation also decreased by increasing borax ratio. Inset tables in Figure 4.13 (A) and (B) have demonstrated the maximum applied force to failure depending on cross linker ratios. Breaking force increased first from 301.48 to 340.4 N when borax ratio increased from 0.1 to 0.3 wt% and then it decreased properly to 312.26, 256.71, 254.89, and 165.83 N by increasing the borax ratio to 0.5, 1, 1.5, and 2 wt. %, respectively.

When the cross linker concentrations were increased, the amount of crosslinked chains increased and crystallized PVA chains were reduced (this can be seen from XRD data). This is the main reason for the dramatically decrease the mechanical properties. The breaking was observed from the single place as seen in the inset picture of Figure 4.13(A) as shown with the black arrow. On the contrary, gradual and consecutive breaking occurred at multiple places of the composite at GA-treated sample at high concentrations (Figure 4.13(B) (c) to (f)). These multiple failing points were shown with black arrows as inset picture in Figure 4.13(B). Single place breaking was observed at low aqueous GA concentration (Figure 4.13 (B) (a)). Breaking force also first increased from 280.04 to 293.07 N when GA ratio increased from 0 to 0.25 wt. %. It then decreased to 228.2, 247.6,

185.1, and 188.04 N not in proper order as in borax treated samples with the increase in GA ratio to 0.5, 1.0, 1.5, and 2.0 wt. %.

Comparing with borax samples, higher breaking elongations were found with GA samples. This can be attributed to flexibility of GA comparing to crystallizable borax. Optimum cross linker concentrations for borax and GA samples were determined as 1.0 wt% for borax and 0.25 ml GA samples. Since most of the PVA chains already crosslinked and no more borax required, after 1 wt. % aqueous borax, additional borax crystallized by itself in the composite structure. This can be clearly seen from the XRD spectra Figure 4.12 (A) (e) and (f). About 0.25 ml GA sample was selected for mechanical analysis depending on water contents because consecutive breaking observed at multiple places during the mechanical test after this concentration (Figure 4.13 (B)).
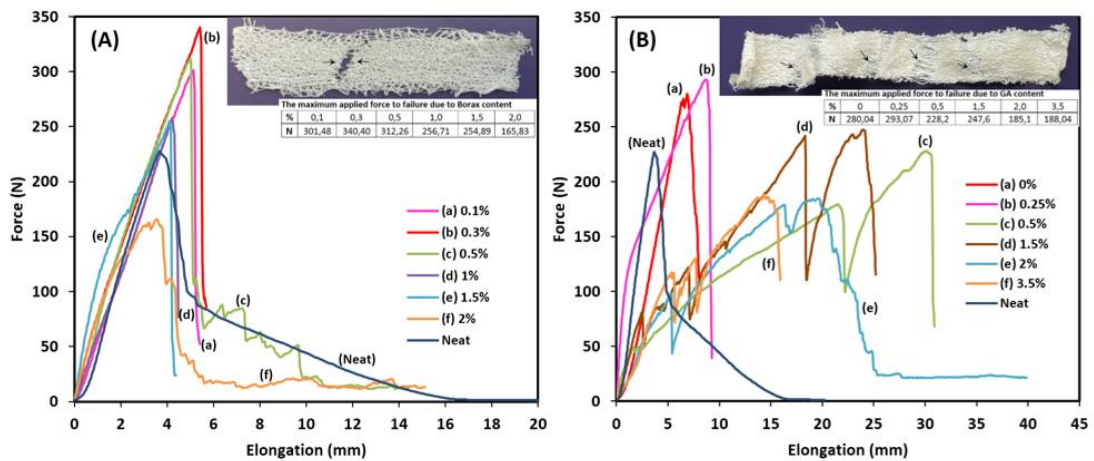
Figure 4.13. Tensile properties of dried fabric reinforced hydrogel composites: ((A) wt.% of borax/water solutions: (a) 0.1, (b) 0.3, (c) 0.5, (d) 1.0, (e) 1.5 and (f) 2.0; and (B) GA solution contents in water/HCl solution: (a) 0, (b) 0.25 ml, (c) 0.5 ml, (d) 1.5 ml, (e) 2.0 ml and (f) 3.5 ml

Mechanical properties of fabric-reinforced hydrogel composite depending on water content in the composite structures have been investigated by observing force-elongation plots, and the results were shown in Figure 4.14 (a) (borax treated) and (b) (GA treated). As seen from Figure 4.14 for borax-treated samples, the rigidity of the fabric-reinforced hydrogel composite dramatically increased by releasing water from the structure. Breaking force gradually increased by releasing water from the structure. Breaking force was 40.8 N when the hydrogel composite contained 100 wt. % water and increased to 277 N when it contained 5 wt. % water. At the same time, breaking elongation gradually

decreased with decreasing water content in the composite structure. At GA-treated samples, a very high breaking elongation was obtained at high ratio GA treatment but it did not change in proper order in all the samples. This could be caused by the organic nature of the molecular structure of the GA. Breaking force first decreased and then gradually increased when the water content in the composite structure increased.

Breaking force was 246.4 and 285.9 N when the hydrogel composite contained 70 and 100 wt% water and increased to 325 N when it contained 5 wt. % water. PVA yarns in the neat fabric structure were dissolved and transformed into hydrogel structure after pouring the crosslinking aqueous borax and GA solution on the fabric. So, the applied force was mostly withstood by the reinforced cotton yarns in the hydrogel composite. Additionally, in Figure 4.14, breaking force at borax-based hydrogel composite decreased more by increasing water content comparing to GA-based hydrogel composite.
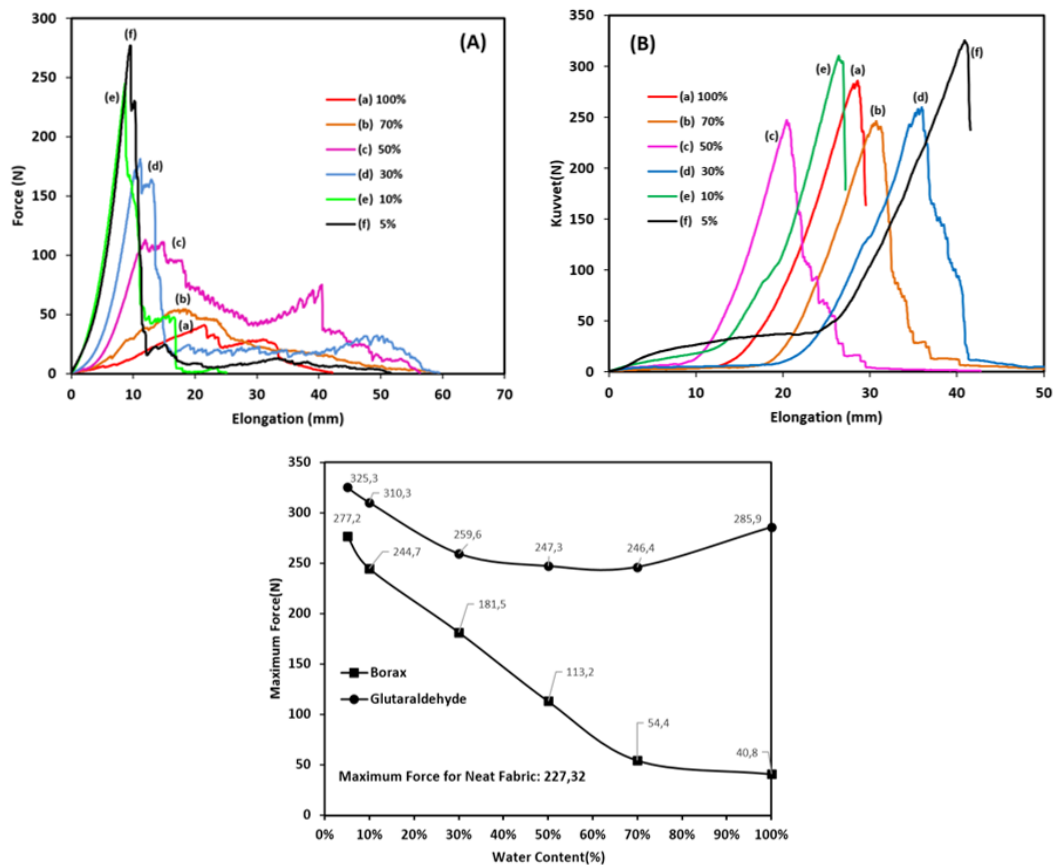
Figure 4.14. Tensile properties of fabric reinforced hydrogel composite when contain different content of water: (A) 1wt. % aqueous borax treated samples, (B) 0.25 ml GA solution contents in water/HCl solution treated sample, (C) Breaking force comparisons

4.3. Natural fibers woven fabric reinforced hydrogel composites for enhanced mechanical properties[3]

4.3.1. Concept study result of the gelation of cotton, flax and wool fabric reinforced hydrogel composites

The woven fabric samples were cut in the warp and the weft directions with a dimensions of 5 cm x 10 cm. As seen from Figure 4.15, when PVA/W, PVA/C, PVA/F fabrics were treated with borax/water solution, PVA yarns totally lost their construction and turned to transparent hydrogel form by simultaneous dissolution and crosslinking of PVA molecules as yarn in the fabrics. Since cotton, wool, flax yarns did not get dissolved by borax-water solution, they kept their position in the structure and stayed as the reinforcement material in the hydrogel composites

.
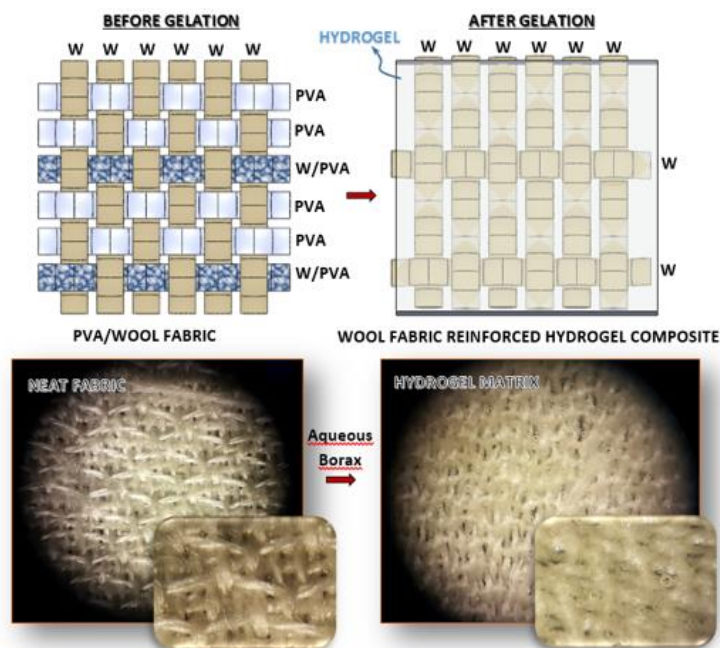
Figure 4.15. Schematic illustration and optical microscopy images of neat PVA/W fabric and its hydrogel matrix form of aqueous borax treated analog

---

[3] This subsection is based on the paper "Koc, U., Aykut, Y., Eren, R. (2020). Natural fibers woven fabric reinforced hydrogel composites for enhanced mechanical properties. https://doi.org/10.1177/1528083720944485"

4.3.2. Morphology analysis of cotton, flax and wool fabric reinforced hydrogel composites

In order to investigate the interaction between hydrogel matrix and yarns in the fabrics as reinforcement, morphological observation with SEM imaging was carried out. Incorporation of hydrogel into fabric structures varied due to the nature of the reinforced fabric structures. Inspecting SEM images as seen in Figure 4.16, since the wool has wax materials on the surface structure, borax-water solutions could not penetrate properly into the yarn structures in the fabric. Moreover, during the production of wool yarn, the yarns are treated with oil to eliminate the potential breakage between the fibers and reduction of friction developed between fibers within yarns. This is the reason for having the lower penetration of borax water solutions. The simultaneous dissolution and crosslinking of PVA smoothened the surface of wool fibers by clogging the cuticle cells layers on the fiber surfaces. On the other hand, when observing flax and cotton samples, the borax-water solutions penetrated inside the yarn structure. Comparing wool, flax and cotton samples, hydrogels were mostly collected on the junctions of wool yarns, but the hydrogels penetrated inside of flax and cotton yarns among their fibers due to low amount of wax (as compared with wool fiber) in their physical surface composition.

WOOL	COTTON	FLAX
[1]WF-RHC	[2]CF-RHC	[3]FF-RHC

[1]WF-RHC: Wool Fabric Reinforced Hydrogel Composite, [2]CF-RHC: Cotton Fabric Reinforced Hydrogel Composite, [3]FF-RHC: Flax Fabric Reinforced Hydrogel Composite
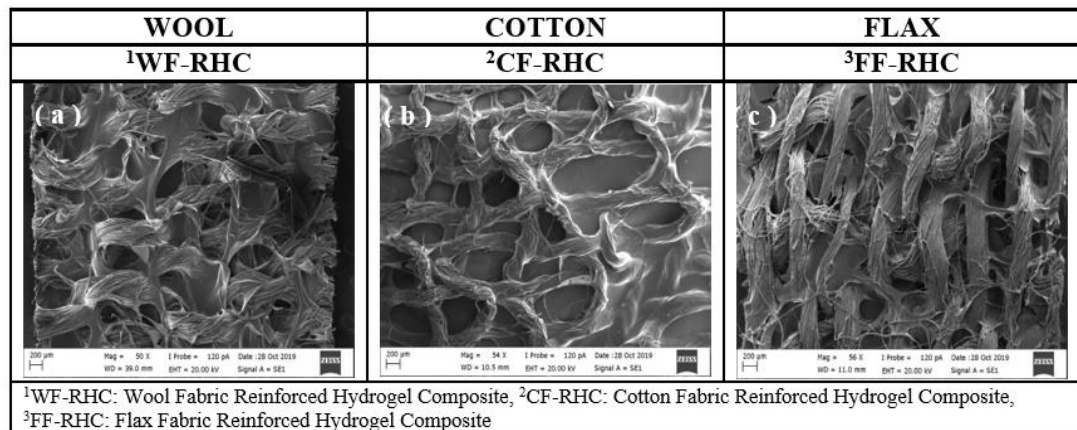
Figure 4.16.SEM images aqueous borax treated PVA/W, PVA/C and PVA/F fabrics after hydrogel matrix formation

4.3.3. Chemical analysis of cotton, flax and wool fabric reinforced hydrogel composites

Chemical investigation of fabric reinforced hydrogel composites with different concentrations of aqueous borax treatment, and their neat fabric counterparts were examined with FTIR spectra and given in Figure 4.17 (A1, A2) for Cotton based, Figure 4.17 (B1, B2) for flax based, and Figure 4.17 (C1, C2) for wool based. For the better comparison and investigation, neat cotton, neat flax and neat wool yarns also treated with the same solution and analyzed with FTIR as shown in the same figures. All the FTIR measurement were conducted with the dried samples. FTIR spectra for PVA/C fabric before and after aqueous borax treatment were presented in Figure 4.17 (A1). The peak at 2930 cm^{-1} could be assigned to C-H stretching of CH$_2$ group (Lu et al.2017). A broad band showing up between 3033 and 3606 cm^{-1} with a maximum peak point around 3295 cm^{-1} belonged to O-H stretching vibration from the hydroxyl groups in PVA and cotton (Al-Emam et al.2019). Decrease of this peak could be attributed to formation of hydrogel structure. The new peak detected at 667 cm^{-1} with addition to borax to the structure could be attributed to stretching vibration B-O-B bond in the borate network (Huang et al.2019). The peak at 1083 cm^{-1} assigned to the C–O in stretching mode for PVA (Lu et al.2017). But no significant effect of aqueous borax on cotton yarns was observed (Figure 4.17 (A2)). FTIR spectra of PVA/F fabrics and neat flax yarns before and after aqueous borax treatment were demonstrated in Figure 4.17 (B1) and (4.17 B2) respectively. The FT-IR spectra of yarn treated spectra (Figure 4.17 (B1) revealed that there is no significant change after borax treatment, so the changes on borax treated PVA/F sample (Figure 4.17 (B1)) could be attributed to changes on PVA molecules as in PVA/C sample. FTIR spectra of PVA/W fabrics and neat wool yarns before and after aqueous borax treatment were shown in Figure 4.17 (C1) and (C2) respectively. A distinct broad parabolic OH peak is seen at aqueous borax treated PVA/W around between 3012 and 3655 cm^{-1} comparing the neat PVA/W fabric. This is another evidence to formation of PVA based hydrogel structure. As cotton and flax yarn samples, no significant change was not observed at aqueous borax treated neat wool yarns at the applied condition.
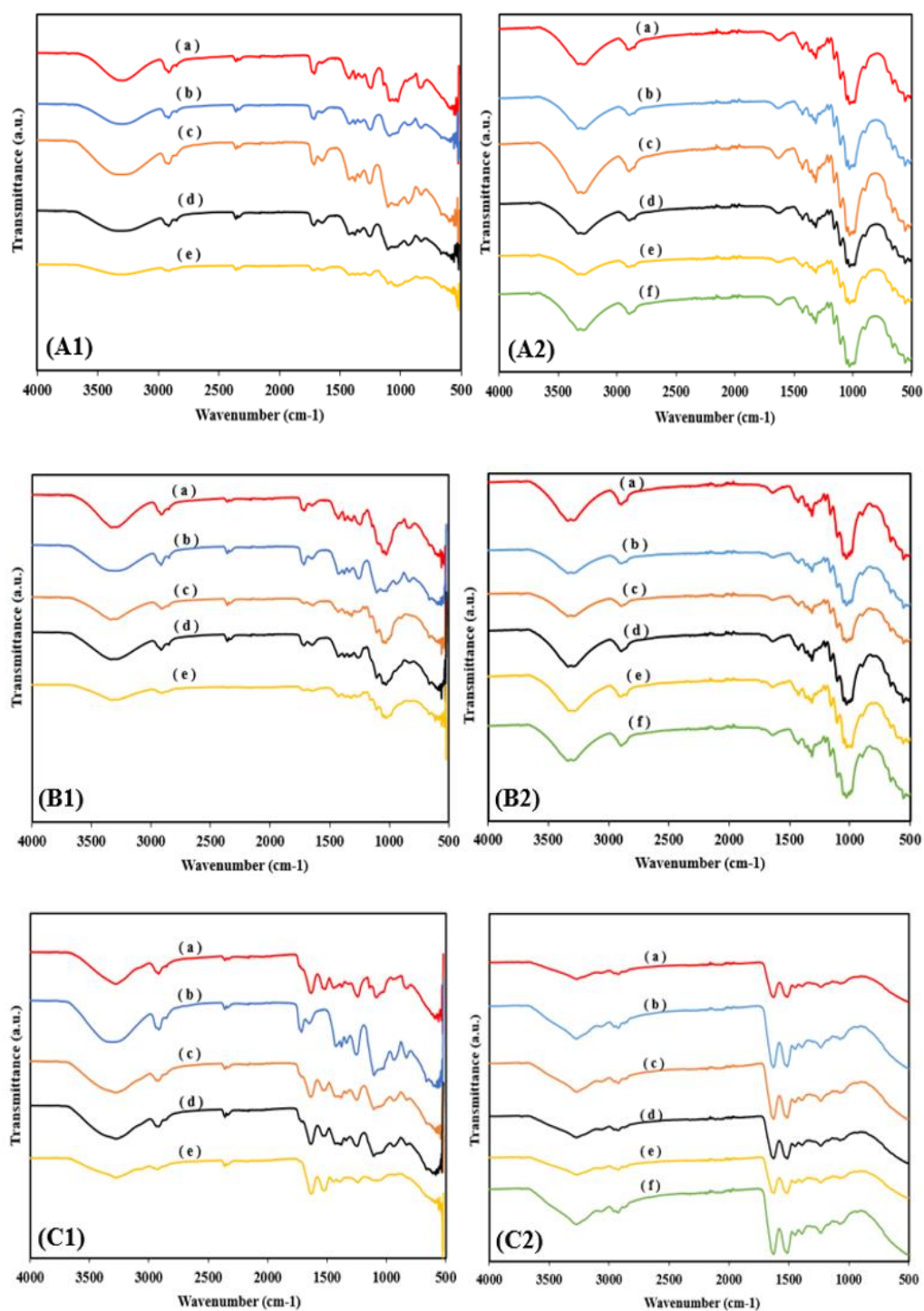
Figure 4.17. FTIR spectra of aqueous borax treated (A1) PVA/C fabrics, (A2) cotton yarn only, (B1)PVA/F fabrics, (B2) flax yarn only, (C1) PVA/W fabrics and (C2) wool yarn only. Treated with different w/v% of borax/water solutions ((A1, B1, C1): (a) without treatment, (b) 0.5, (c) 1.0, (d) 1.5 and (e) 2.0), ((A2, B2, C2): (a) without treatment, (b) 0,1 , (c) 0.5 , (d) 1 , (e) 1.5, (f) 2.0)

4.3.4. Thermal analysis of cotton, flax and wool fabric reinforced hydrogel composites

Thermogravimetric analysis of neat PVA/C fabric, neat PVA/F fabric, neat PVA/W fabric, and their aqueous borax treated counterparts, so-called fabric reinforced hydrogel composites, in dried form were performed under nitrogen atmosphere, and the results are shown in Figure 4.18 and Table 4.1. Main water loss of all hydrogel composite samples occurred up to 100 $^{\circ}$C. The amount of water loss for all sample groups increased after gelation process compared to their neat counterparts. Water loss for cotton samples up to 100 $^{\circ}$C being higher than flax and wool samples revealed that cotton reinforced hydrogel sample takes more time for fully drying, see Figure 4.18 (A). Treating the neat samples with aqueous borax even at low concentration, reduced thermal stability a little bit at all samples. Increasing the amount of borax concentration after 0.5 w/v % didn't change the degradation temperatures significantly at PVA/F samples as seen in Figure 4.18 (B). This difference is even smaller at PVA/W hydrogel composite samples as seen in Figure 4.18 (C). For PVA/C samples, the amount of water loss with respect to borax content is gradually increased due to the percentage of borax concentration as seen in Figure 4.18 (A,(a) to (e)). The untreated PVA/C neat fabric started to degrade thermally at temperatures of 301 to 469°C, whereas the borax-water treated samples started thermal degrade mainly between 271 and 498 $^{\circ}$C for 0.5 w/v % borax-water concentration and between 293 and 485 $^{\circ}$C for 1.0 w/v %. For the concentration of 1.5 w/v % and 2.0 w/v % borax-water solutions, thermal degradation was observed at the temperature range between 281 and 492°C and between 293 and 485°C respectively. When PVA/C fabrics were treated with borax-water solution having a concentration between 0.5 and 2.0% w/v, hemicellulose degradation started at temperature of 280°C ,while the cellulose structure was degraded at temperature of 490°C and lignin started to decompose at a temperature of 795°C (Yang et al.2007) . Residual contents were 15 wt. % for untreated PVA/C fabric sample and 14, 24, 20, 23 wt. % for 0.5, 1.0, 1.5, 2.0 w/v % borax-water treated samples respectively (Figure 4.18 (A). Inspecting Figure 4.18 (B), the untreated PVA/F neat fabric mainly thermally degraded at the temperature between 286 and 472°C, whereas the borax-water treated samples' thermal degradation occurred mainly between 248 and 493 $^{\circ}$C for 0.5 w/v % borax-water concentration and between 273 and 470 $^{\circ}$C for 1.0 w/v%.

For the concentration of 1.5 w/v% and 2.0 w/v% borax-water solutions, thermal degradation was observed at the temperature range between 274 and 473°C and between 274 and 484°C respectively. Like PVA/C fabrics, the PVA/C fabrics have the same fashion because of their similar structural properties. Residual contents after TGA measurements were 11 wt. % for untreated PVA/F fabric sample and 23, 25, 33, 23 wt. %, and for 0.5, 1.0, 1.5, 2.0 w/v % borax/water treated samples sequentially (Figure 4.18(B)). In Figure 4.18 (C), the untreated neat PVA/W fabric thermally degraded at the temperatures between 263 and 480°C, whereas the borax-water treated samples' thermal degradation occurred mainly between 244 and 481°C for 0.5 w/v % borax-water concentration and between 249 and 488 °C for 1.0 w/v%. For the concentration of 1.5 and 2.0 w/v% borax-water solutions, thermal degradation was observed at the temperature between 240 and 466 °C and between 251 and 484 °C respectively. Residual contents were 15 w/v% for untreated PVA/W fabric sample and 21, 21, 22, 26 wt. % for 0.5, 1.0, 1.5, 2.0 w/v % borax/water treated samples sequentially (Figure 4.18 (C)).
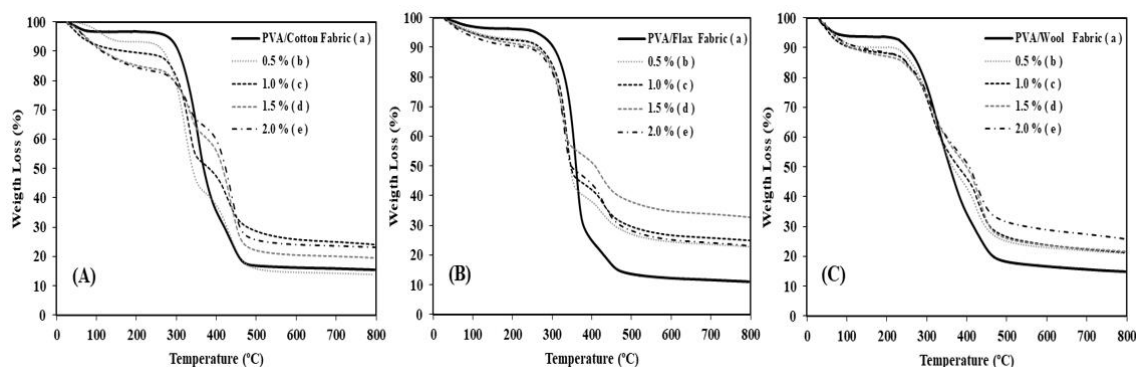
Figure 4.18. TGA plots of (A) PVA/C, (B) PVA/F and (C) PVA/W fabrics treated in different w/v% of borax/water solutions: (a) neat fabrics, (b) 0.5, (c) 1.0, (d) 1.5 and (e) 2.0

Table 4.1. Data points obtained from TGA plots of PVA/C, PVA/F and PVA/W fabrics treated in different w/v % of borax/water solutions

Sample	Borax water concentration (w/v %)	Degradation Temperature (°C)	Residual weight (wt. %)
PVA/F	0.5	271-498	14
	1.0	293-485	24
	1.5	281-492	20
	2.0	293-485	23
	Neat	301-469	15
PVA/C	0.5	248-493	23
	1.0	273-470	25
	1.5	274-473	33
	2.0	274-484	23
	Neat	286-472	11
PVA/W	0.5	244-481	21
	1.0	249-488	21
	1.5	240-466	22
	2.0	251-484	26
	Neat	263-480	15

4.3.5. Mechanical analysis of cotton, flax and wool fabric reinforced hydrogel composites due to cross linker and water contents

Mechanical properties of the cotton, flax and wool woven fabric reinforced hydrogel composites at both warp and weft direction were investigated via force-elongation curves due to cross linker borax content, and the plots were demonstrated in Figure 4.19 (Cotton), Figure 4.20 (Flax), and Figure 4.21 (Wool). When the cotton samples were examined, the maximum applied force of the wetted (with just water) neat PVA/C fabric was measured as 227 N at warp direction while the maximum applied force of the wetted neat PVA/C fabric was measured as 223 N at weft direction.

As seen from the Figure 4.19 (a), the breaking force of the hydrogel composite in the warp direction was 162 N when the neat fabric was treated with 0.5 %w/v of borax-water solution, and it was decreased further to 100 N when the borax-water concentration was changed to 1.0 % w/v, due to the crosslinking of PVA in the PVA/C blend woven structure.

Inter and intra friction developed with in the cotton based woven hydrogel structure could be decreased. The breaking force was increased from 225 to 262 N by changing the borax-water concentration from 1.5 to 2.0 w/v % in the warp direction. Due to the formation of more stable hydrogels within and between the yarns, inter and intra friction of yarns were developed and enhanced the mechanical performance of PVA/C with borax-water treatment. Since the composites were tested in wet form, elongation at the break is higher in this study comparing with our previous study at warp direction (Koc et al.2019a). Additionally, breaking strength increase with increasing borax concentration in the treatment solution at wet samples in this study, but breaking point decreased at dried composites except initial increase of borax concentration in the previous study (Koc et al.2019a). In another study, it was also confirmed that breaking strength gradually increased when the hydrogel composite released its water content (Koc et al.2020a). On the other hand, as seen in Figure 4.19 (B) the breaking force in the weft direction was 108 N when the treatment concentration was 0.5 w/v %. Likewise, the force was gradually decreased from 96 to 84 N when the concentration of borax-water was changed from 1.0 to 1.5 w/v%. The breaking force was 162 N when the aqueous borax treatment concentration was 2.0 w/v%.
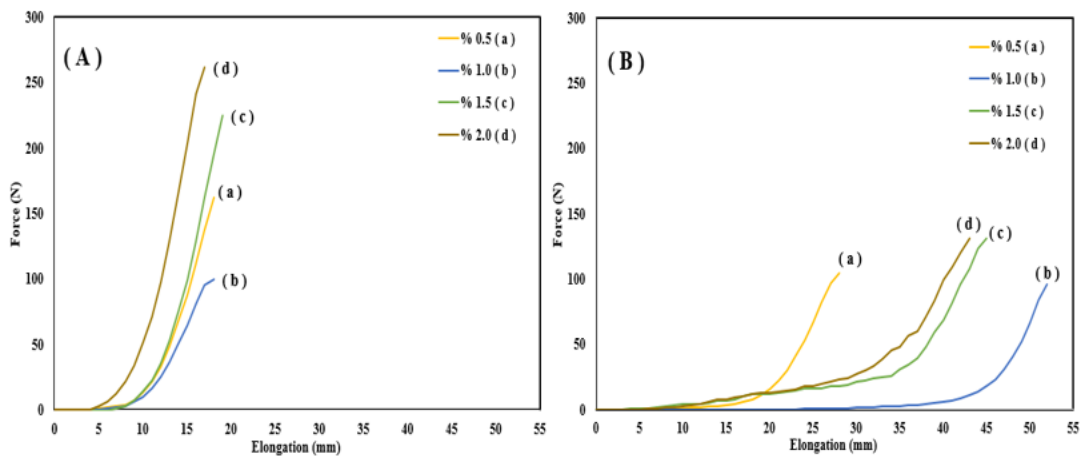
Figure 4.19. Tensile properties of cotton fabric reinforced hydrogel composites ((A) warp and (B) weft directions) after held in water for 15 min: Treatment with different w/v % of borax/water solutions ((a) 0.5, (b) 1.0, (c) 1.5, (d) 2.0)

Observing the mechanical performance of flax sample, the maximum applied force of the wetted (with just water) neat PVA/F fabric was measured as 115 N in the warp direction.

While, the maximum applied force of the wet neat PVA/F fabric was measured as 95 N in the weft direction. Mechanical properties of wet woven flax-reinforced hydrogel composite were demonstrated in Figure 4.20 (A) at warp direction and in Figure 4.20 (B) weft direction. The breaking force in warp direction was increased from 157 to 239 N proportional with the increasing of borax-water treatment concentration from 0.5 to 1.0 % w/v whereas it was gradually decreased from 105 to 101 N, when the concentration borax-water is changed from 1.5 to 2.0 % w/v in the warp direction respectively. As seen from Figure 4.20 B, the breaking forces in the weft direction were 132 N (0.5 w/v %), 88 N (1.0 w/v %), 99 N (1.5 w/v %), 82 N (2.0 w/v %), respectively.
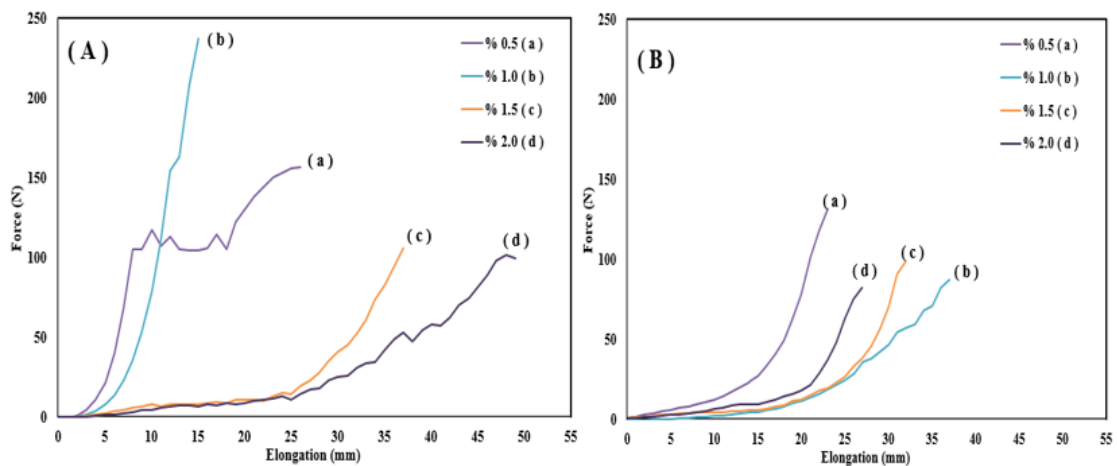
Figure 4.20. Tensile properties of flax fabric reinforced hydrogel composites ((A) warp and (B) weft directions) after held in water for 15 min: Treatment with different w/v % of borax/water solutions ((a) 0.5, (b) 1.0, (c) 1.5, (d) 2.0)

When the mechanical performance of the wool samples were examined, the maximum applied force of the wetted (just water) neat PVA/W fabric was measured as 284 N at warp direction while the maximum applied force of the wet neat PVA/W fabric was 85 N at weft direction. The physic mechanical property of PVA/W fabric was influenced by aqueous borax treatment.

The mechanical properties of wool fabric reinforced hydrogel composites have been investigated due to concentration of the cross linker treatment by using the force elongation plots in the warp (Figure 4.21 (A)) and the weft (Figure 4.21 (B)) directions.

The breaking force in the warp direction was increased from 290 to 320 N when the used borax-water concentration was increased from 0.5 to 1.5 w/v%, whereas, when the

concentration of borax-water was 2.0 w/v%, the force decreased to 313.42 N in warp direction. When the amount of borax concentration was increased it enhanced the crosslinked chains and reduced crystallized PVA chains, this would reduce mechanical performance of the hydrogel composite (Han et al.2014). As seen from Figure 4.21 (B), the breaking forces in the weft direction were 83 N (0.5 w/v %), 85 N (1.0 w/v %), 92 N (1.5 w/v %), 98 N (2.0 w/v %), respectively.
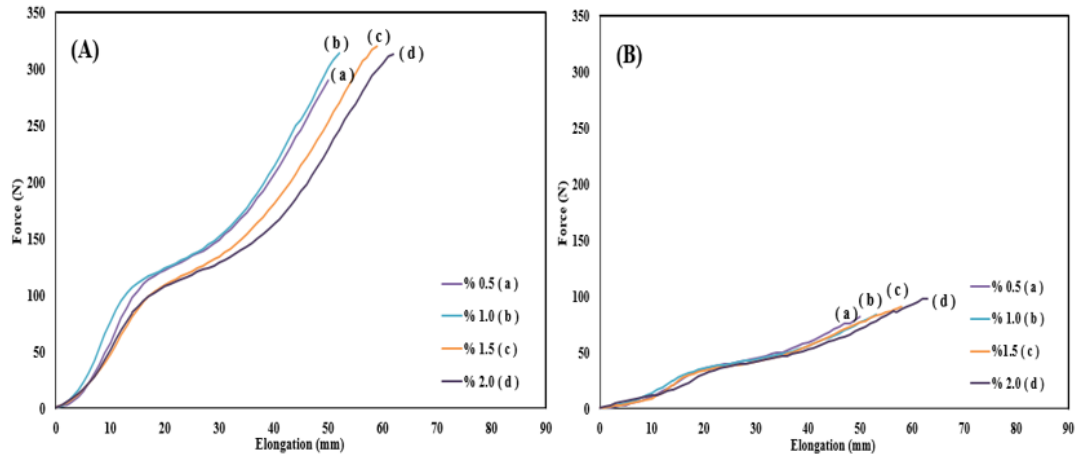
Figure 4.21. Tensile properties of wool fabric reinforced hydrogel composites ((A) warp and (B) weft directions) after held in water for 15 min: Treatment with different w/v % of borax/water solutions ((a) 0.5, (b) 1.0, (c) 1.5, (d) 2.0)

4.4. Regenerated cellulose woven fabric reinforced hydrogel composite[4]

4.4.1. Morphology analysis of viscose ring, viscose open end and viscose continue filament fabric reinforced hydrogel composites

Morphological observations with SEM imaging were analyzed to carry out the interaction between the hydrogel matrix and yarns in the fabrics as reinforcement. The penetration of borax-water solutions into fabric structures varied depending on the manufacturing technique of the reinforced fabric structures. The images taken from the SEM were shown in Figure 4.22a and 4.22b; the interaction between hydrogel matrix and yarns in the

---

[4] This subsection is based on the paper "Koc, U., Aykut, Y., Eren, R. 2020. Regenerated cellulose woven fabric reinforced hydrogel composite. The paper prepared from the research of the section was submitted to The Journal of the Textile Institute and it is at the reviewing process."

viscose filament fabrics as reinforcement can be observed more uniformly spread than that of the viscose ring.

Due to the compact structure of viscose ring fabric, borax-water solutions could not penetrate inside part of ring-spun yarns (Nikolić et al.2003).
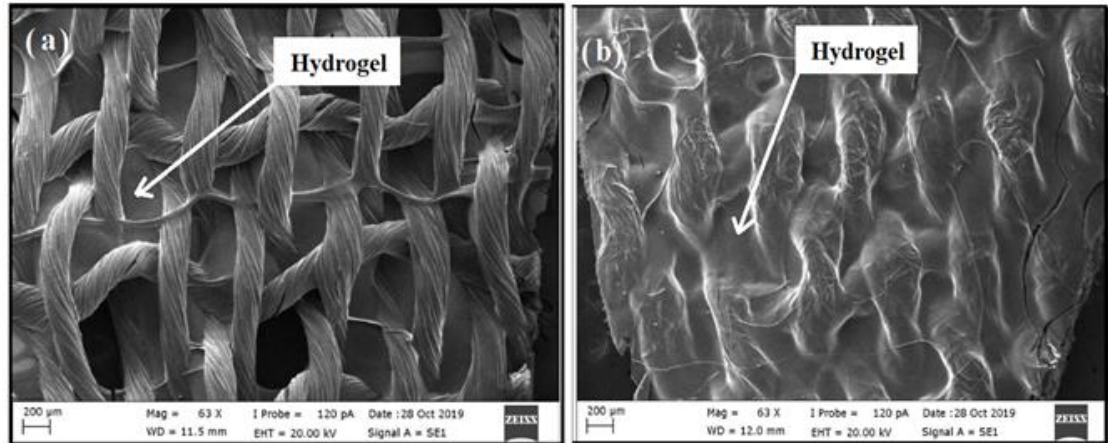
Figure 4.22. SEM images of (a) viscose continue filament fabric and (b) viscose ring fabric reinforced hydrogel composites

4.4.2. Chemical analysis of (viscose ring), (viscose OE) and viscose CF fabric reinforced hydrogel composites

Viscose ring, viscose OE and viscose CF fabric reinforced hydrogel composite structures were treated with different concentrations of borax water solutions. And untreated and aqueous borax treated woven fabrics were characterized by FTIR, as shown in Figure 4.23a1 for viscose ring, Figure 4.23b1 for viscose OE, and Figure 4. 23c1 for viscose CF.

The observation made from Figure 4.23(a2, b2, c2) showed that the same borax solution did not chemically affect viscose ring (Figure 4.23 a2), viscose OE (Figure 4.23 b2), and viscose CF (Figure 4.23 c2), yarns. FTIR spectra for PVA/viscose ring fabric untreated and aqueous borax treated were demonstrated in Figure 4.23 a1. All samples exhibited a broad band between 3100 and 3600 cm^{-1} corresponded to OH stretching vibration from hydroxyl groups in PVA and viscose ring (Abdulkhani et al.2013, Célino et al.2013). The peak seen at 2933 cm^{-1} in Figure 4.23 a1 belonged to C-H stretching vibration in CH$_2$ groups (Koc et al.2020, Spoljaric et al.2014). The peak

at 1088 cm^{-1} assigned to the C-O in stretching mode for PVA (Koc et al.2019a, Taleb et al.2009) and this peak changed to 1103 cm^{-1} after the formation of hydrogel structure. The peak at 1420 cm^{-1} can be attributed to CH$_2$ symmetric bending vibration (Dong et al.2020, Carrillo et al.2004).

FTIR spectra of PVA/viscose OE fabrics and neat viscose OE yarns untreated and aqueous borax treated were demonstrated in Figure 4.23b1 and 4.23b2, respectively. The findings revealed that there is no significant interaction between aqueous borax and viscose OE yarns structure as seen in (Figure 4.23b2) Result obtained from borax treated PVA/viscose OE samples in Figure 4.23b1 showed a similar trend with changes on PVA molecules as in PVA/viscose ring sample. PVA/viscose CF fabrics and viscose CF yarns, which were borax water treated and untreated, were analyzed by FTIR spectra as observed in Figure 4.23c1 and 4.23c2, respectively. The OH peak was observed between 3100 and 3550 cm^{-1} (Alhosseini et al.2012, Awada and Daneault 2015) for borax treated PVA/viscose CF fabric.

Overall results revealed that borax treated samples transformed PVA molecules into crosslinked hydrogel structure, but borax-water solutions did not affect regenerated cellulose fibers.
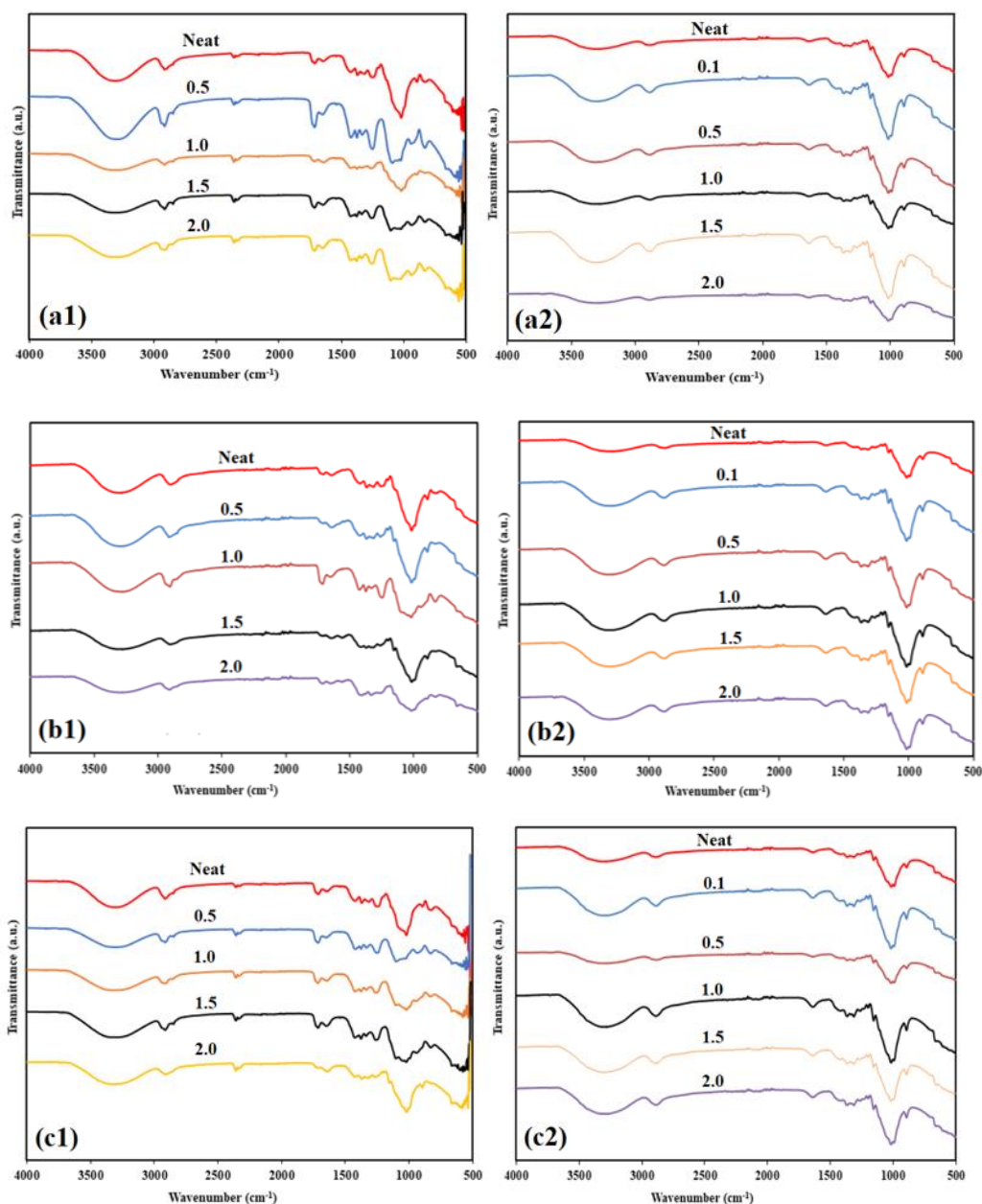
Figure 4.23. FTIR spectra of aqueous borax treated (a1) PVA/viscose ring fabrics, (a2) viscose ring yarn only, (b1) PVA/viscose OE fabrics, (b2) viscose OE yarn only, (c1) PVA/viscose CF fabrics and (c2) viscose CF yarn only. Treated with different w/v% of borax/water solutions ((a1, b1, c1): without treatment (neat), 0.5, 1.0, 1.5 and 2.0, ((a2, b2, c2): without treatment (neat), 0.1, 0.5, 1.0, 1.5, 2.0

4.4.3. Thermal analysis of viscose ring, viscose open end and viscose continue filament fabric reinforced hydrogel composites

Thermogravimetric analysis of neat PVA/viscose ring fabric, neat PVA/viscose CF fabric and their aqueous borax treated fabrics so-called fabric reinforced hydrogel composites,

were performed under nitrogen atmosphere. The tests were was conducted in dried samples forms, and the results are shown in Figure 4.24.

The quantity of moisture loss of specimens raised after the formation of gelation compared to raw materials. Water loss for neat PVA/viscose CF samples up to 100°C became higher than the neat PVA/viscose ring shown in Figure 4.24a. Treating the neat samples with aqueous borax with the solutions of minimum concentration might reduce the thermal stability of the sample. Increasing the amount of borax concentration after 0.5 w/v % did not have a noticeable influence on the thermal stability of PVA/viscose ring samples, as seen in Figure 4.24a. But thermal stability of PVA/viscose CF fabric was changed after 1.5 w/v % borax concentration, as seen in Figure 4.24b. The borax-water treated PVA/viscose CF and PVA/viscose ring samples demonstrated slower weight loss between 400 and 500 °C because of the crosslinking of PVA and aromatization (Venkateswaran et al.1990, Wang et al.2014).

The quantity of moisture loss in viscose R fabrics with respect to amount of used borax contents was improved shown   in Figure 4.24a. The untreated PVA/viscose R neat fabric started to degrade thermally at temperatures of 283 to 472 °C, while the borax-water treated samples started to thermally degrade mainly between 273 and 481 °C for 0.5 w/v % borax-water concentration. In the same manner, for 1.0 w/v % borax water concentration the thermal degradation happened between 273 and 479 °C. For the concentration of 1.5 w/v % and 2.0 w/v % borax-water solutions, thermal degradation was observed at the temperature range between 254 and 497 °C and between 255 and 466 °C, respectively (Lee et al.2015). Residual contents were 17 wt. % for untreated PVA/viscose ring fabric sample and 17, 22, 24, 25 wt. % for 0.5, 1.0, 1.5, 2.0 w/v% borax-water treated samples respectively (Figure 4.24a).

As observed in Figure 4.24b, the untreated PVA/viscose CF neat fabric mainly thermally degraded at the temperature between 287 and 481°C, whereas the 0.5 w/v % of borax-water treated samples thermally degraded between 258 and 489 °C. For 1.0 w/v% of borax water concentration treated PVA/viscose CF fabric thermally degraded in between 273 and 451 °C.

Likewise, for the concentration of 1.5 w/v% and 2.0 w/v% borax-water solutions, thermal degradation was observed at the temperature range between 273 and 476 °C and between 273 and 464 °C, respectively (Lee et al.2015).Residual contents after TGA measurements were 10 wt. % for untreated PVA/viscose CF fabric sample and 19, 25, 26, 26 wt. % for 0.5, 1.0, 1.5, 2.0 w/v % borax/water treated samples respectively (Figure 4.24b).
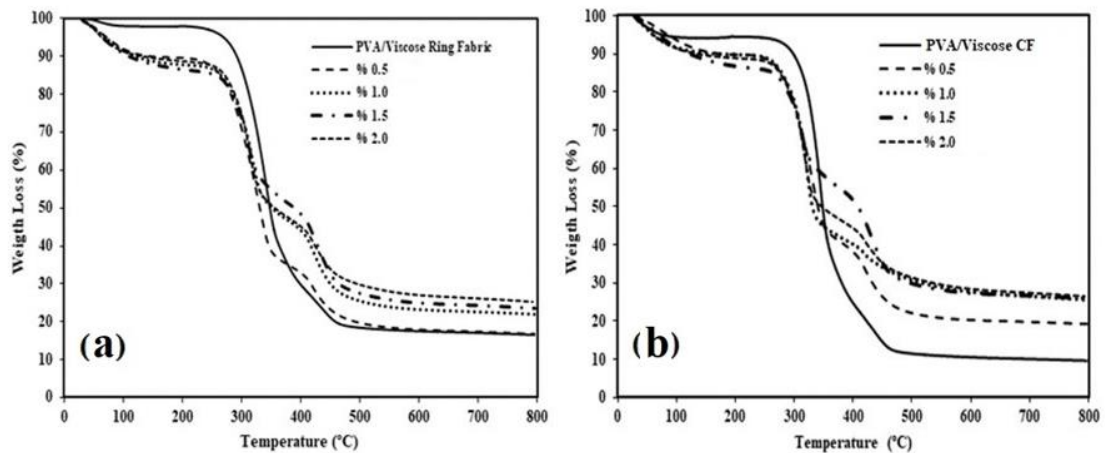
Figure 4.24. TGA curves of (a) PVA/viscose ring fabric treated in different wt. % of borax-water solutions: neat PVA/Viscose ring fabric, 0.5, 1.0, 1.5 and 2.0; (b) PVA/viscose CF fabric treated in different wt. % of borax-water solutions: neat PVA/viscose CF fabric, 0.5, 1.0, 1.5 and 2.0

4.4.4. Effect of the cross-linker and water contents on mechanical properties of viscose ring, viscose OE and viscose CF fabric reinforced hydrogel composites

Mechanical analysis of the viscose ring, viscose OE and viscose CF woven fabric reinforced hydrogel composites were examined due to content of borax solubility in water by measuring force-elongation plots in the warp direction (Figure 4.25a (viscose ring), Figure 4.26a (viscose OE) and Figure 4.27a (viscose CF)) and weft direction (Figure 4.25b (viscose ring), Figure 4.26b (viscose OE) and Figure 4.27b (viscose CF)).

When the mechanical performance of viscose ring samples was investigated, the breaking force of the wetted (just water) neat PVA/viscose ring in the warp and weft directions were 205 and 103 N, respectively. As shown from Figure 4.25a, when the borax-water concentration was increased from 0.5 w/v to 1.0 w/v, the breaking force of the hydrogel composite in the warp direction decreased from 258 to 218 N.

The breaking force for the 1.5 to 2.0 w/v % borax-water concentration in the warp direction was 243 to 225 N, sequentially. As described previously we obtain that decreasing mechanical properties of samples was related to the crystallization of PVA chain (Koc et al.2019a). As seen from Figure 4.25b, the breaking forces in the weft direction were 112 N (0.5 w/v %), 109 N (1.0 w/v %), 120 N (1.5 w/v %), 144 N (2.0 w/v %), respectively.
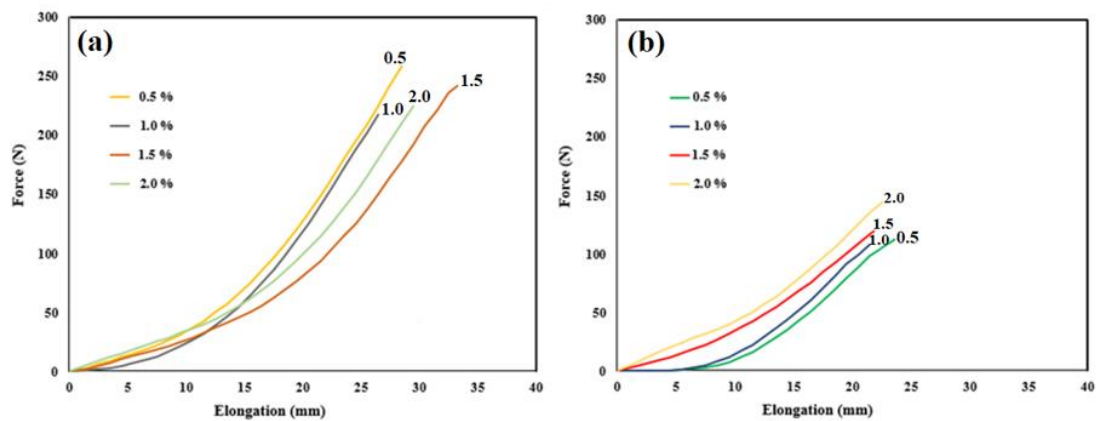
Figure 4.25. Tensile properties of Viscose R fabric reinforced hydrogel composites ((a) warp and (b) weft directions) after held in water for 15 min: Treatment with different w/v % of borax/water solutions (0.5, 1.0, 1.5 and 2.0)

When the results of viscose OE samples were evaluated, the maximum applied force of the wetted neat PVA/viscose OE fabric was measured as 202 N at warp direction. In contrast, the maximum applied force of the wetted neat PVA/viscose OE fabric was 93 N at weft direction. The mechanical properties of aqueous borax treated viscose OE fabric reinforced hydrogel composites were demonstrated in the warp direction (Figure 4.26a) and the weft direction (Figure 4.26b). While the breaking force in the warp direction was increased from 245 to 318 N when the used borax-water concentration was increased from 0.5 to 1.5 w/v %. Then the breaking force decreased to 292 N in warp direction when the concentration of borax-water was 2.0 w/v %.As seen from Figure 4.26b, the breaking forces in weft direction were 65N (0.5 w/v %), 95N (1.0 w/v %), 94N (1.5 w/v %), 73N (2.0 w/v %), respectively.
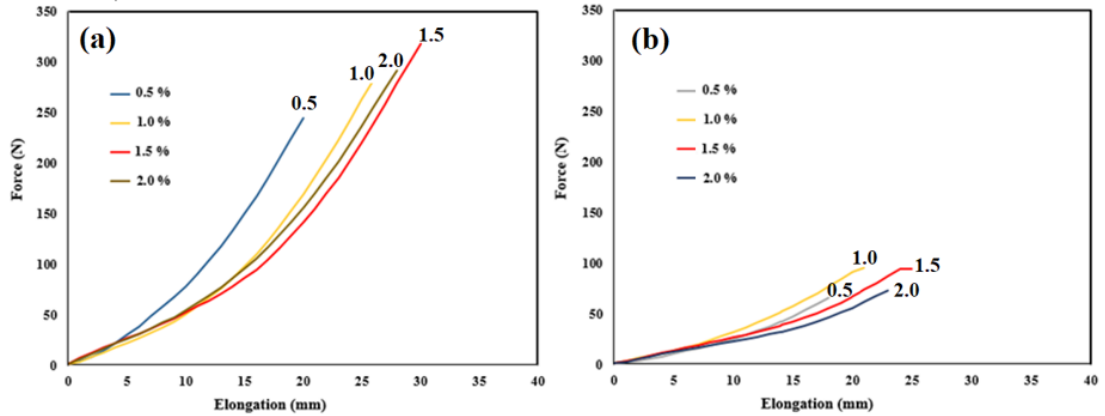
Figure 4.26. Tensile properties of viscose OE fabric reinforced hydrogel composites ((a) warp and (b) weft directions) after held in water for 15 min: Treatment with different w/v % of borax/water solutions (0.5, 1.0, 1.5, and 2.0)

According to the description of mechanical performance of viscose continue filament sample, the maximum applied force of the wetted neat PVA/viscose CF fabric was 271 N in the warp direction while the maximum used force of the wetted neat PVA/viscose CF fabric was 80 N in the weft direction. The mechanical properties of viscose CF fabric reinforced hydrogel composites have been indicated depending on the concentration of borax treatment by measuring force-elongation plots in the warp direction (Figure 4.27a) and the weft direction (Figure 4.27b) .It was increased from 333 to 380 N when the concentration of borax-water increased from 1.5 to 2.0 w/v%. As seen from Figure 4.27b, the breaking forces in the weft direction were 93 N (0.5 w/v %), 85 N (1.0 w/v %), 93 N (1.5 w/v %), 92 N (2.0 w/v %), respectively.
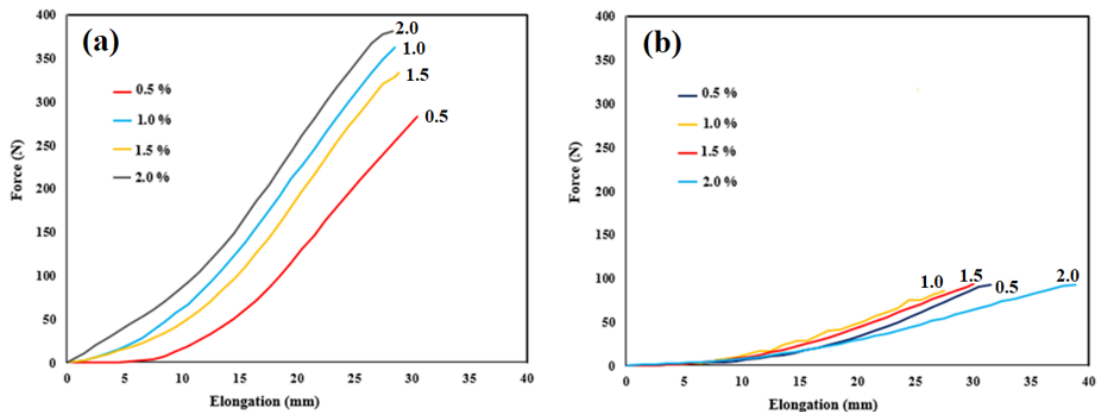
Figure 4.27. Tensile properties of viscose CF fabric reinforced hydrogel composites ((a) warp and (b) weft directions) after held in water for 15 min: Treatment with different w/v % of borax/water solutions (0.5, 1.0, 1.5, and 2.0)

The mechanical properties of yarns as well as their fabrics were significantly affected by different fiber and yarn properties such as fiber length, variation and distribution, twist, yarn manufacturing mechanism (technology) and fiber strength. Moreover, the arrangement of filament fibers in the yarns structure has valuable influence on the overall mechanical performance of yarns and fabrics (Jahan 2017).The inter and intra friction developed in the yarn structures affect both physical and mechanical properties of yarns as well as their fabrics. Longer staple natural as well as synthetic fibers give higher strength to the yarn than short fibers. Likewise for a single spun yarn, increases in the twist gives a higher strength up to a certain limit (Morton and Hearle 2008).

All in all, fabric reinforced hydrogel composites made from PVA/viscose CF gave better mechanical performance than its viscose ring and viscose OE counterparts due to the length of fiber (staple or filament). According to the length of fiber, fiber was influenced by water absorption (Chung and Kim 2016). Absorption of water can lead to transverse and axial directions swelling of fibers. At the same time, porosity of woven fabrics was blocked after swelling of fibers and so fibers swelling reduced water permeability (Morton and Hearle 2008).

Therefore, swelling is an important component in the woven fabrics and plays a vital role for mechanical performance of fabric reinforced hydrogel composite. Woven fabrics made from PVA/viscose R, PVA/viscose OE, PVA/viscose CF were swollen with aqueous borax treatment after changing of the yarn from PVA to hydrogel structure that resulted in some shrinkage of fabrics and enhancing yarn crimp because of crosslinking process and swelling.

The mechanical performance of fabric reinforced hydrogel composite has been negatively affected by the shrinkage of fabrics. The shrinkage of wetted (with just water) viscose fabrics depend on swelling of fibers, the residual moisture content in the fabrics and type of fabric (staple or filament). Shrinkage of filament viscose fabric was lower than staple viscose fabric after water treatment (Chung and Kim 2016). In this context, the results show that viscose CF based hydrogel composites had better mechanical performance than viscose ring and viscose OE hydrogel composites

4.4.5.SPSS Analysis

There is a high level positive and significant relationship between borax-water concentration and breaking force at the breaking points of regenerated cellulose (viscose ring ,viscose OE ,viscose CF) woven fabric reinforced hydrogel composites in the warp direction (r =0.89; r =0.89; r =0.89, p <0.05). According to this, it can be said that as the borax-water concentration increased, breaking force at the breaking points of regenerated cellulose woven fabric reinforced hydrogel composites in the warp direction increased. Considering the determination coefficient ($r^2 = 0.79$), it can be interpreted that 79% of the total variance (variability) in breaking force at the breaking points of regenerated cellulose was due to borax-water concentration.

There was no significant relationship between borax-water concentration and breaking force at the breaking points of regenerated cellulose (viscose ring, viscose OE, viscose CF) woven fabric reinforced hydrogel composites in weft direction (r =0.82; r = -0.12; r =0.65, p>0.05). Accordingly, it can be said that it did not matter if borax-water concentration increased or decreased, it was not related to breaking force at the breaking points of regenerated cellulose woven fabric reinforced hydrogel composites in weft direction. Viscose ring, viscose OE, viscose CF yarns resisted against breaking when the measurements were carried out in the warp direction, while PVA and hybrid yarns resisted against breaking when the measurements were carried out in the weft direction. Therefore, PVA yarns changed to hydrogel structure after gelation process, mechanical properties reduced in weft direction (Koc et al.2020a).

4.5. Hydrogel Composite Yarn Prepared From Polyvinyl Alcohol/Cotton Hybrid Yarn[5]

4.5.1. Concept study of the hydrogel composite yarn

First of all, single hybrid yarn was prepared from two PVA and one Co yarn by twisting them together (Figure 4.28 A), then the hybrid yarn was dipped in the prepared aqueous borax solution. After aqueous borax treatment, PVA yarns transformed into hydrogel yarn in the structure by swelling a little bit, but cotton yarns protected their yarn structures. Cotton yarn was slightly crimped with aqueous borax treatment after the transformation of the yarn from PVA to hydrogel structure that caused some shrinkage due to crosslinking process (Figure 4.28 B and 4.28 C). Hydrogel and cotton yarn phases could be easily distinguished from each other (Figure 4.28 D). As seen from the images, when a force is applied to the hydrogel composite yarn, first hydrogel phase will be mostly subjected to the force. The crimped form of the cotton yarn will not properly reinforce in the hydrogel phase because continuous force with the elongation will open the crimping first.
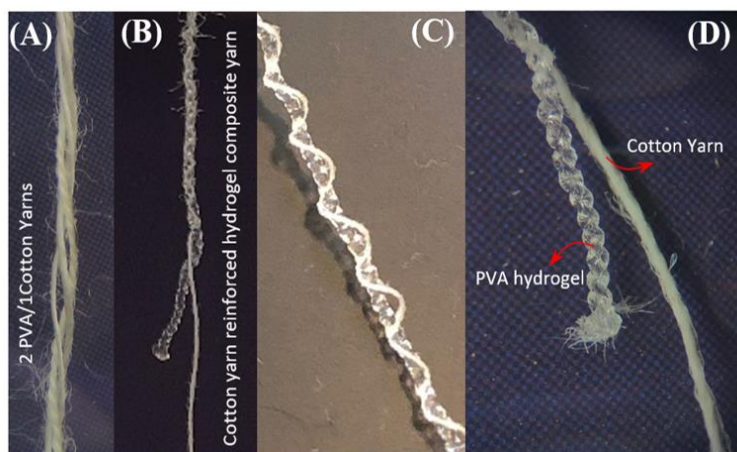
Figure 4.28. Photograph images of (A) PVA/Cotton hybrid yarn, (B, C and D) cotton yarn reinforced hydrogel composite yarn

---

[5] This subsection is based on the conference paper "Koc, U., Eren, R., Aykut, Y.2019.Hydrogel Composite Yarn Prepared From Polyvinyl Alcohol/Cotton Hybrid Yarn. 17th National 3rd International the Recent Progress Symposium on Textile Technology and Chemistry, 20-22 November, 2019, Bursa, Turkey."

4.5.2. Chemical analysis of hydrogel composite yarns

The broad peak between 3000-3500 cm^{-1} corresponds to –OH stretching and its intensity dramatically decreases after hydrogel production from PVA because of crosslinking of PVA molecules via borax and hydroxyl groups (Spoljaric et al.2014). It is the main evidence to express the consumption of OH groups on PVA molecules and the formation of hydrogel from PVA. Peak at 663 at hydrogel can be attributed to stretching vibrations of O-B-O bonds coming from the added borax (Spoljaric et al.2014).
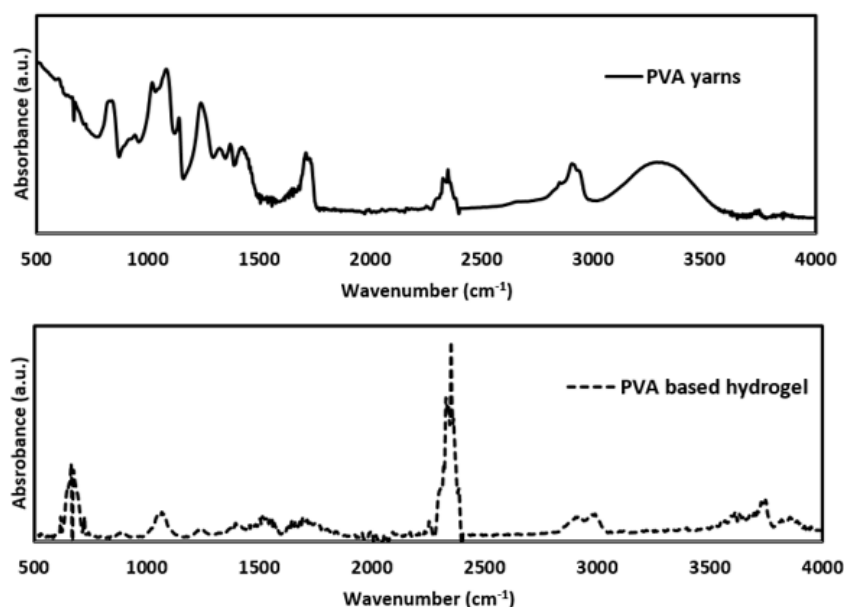
Figure 4.29. ATR-FTIR spectra of PVA yarns and their aqueous borax treated then dried analogs

4.5.3. Thermal analysis of hydrogel composite yarns

PVA yarns exhibited a glass transition temperature at 70.9 ºC, and it shifted to 75.3 ºC at hydrogel sample since borax crosslinked the PVA molecules in the amorphous region and limited the molecular motion and caused the enhancement of glass transition temperature (Lim et al.2015). Melting temperature of PVA yarns were detected at 200.9 ºC. This temperature was detected at 201.9 ºC for hydrogel sample corresponding to PVA based crystalline domains in the sample (Lim et al.2015).

In order to observe thermal stability, TGA measurements were carried out in air atmosphere, and the results were demonstrated in Figure 4.30 B. Even though thermal weight loss started at low temperatures for hydrogel sample, sharp and distinct decompositional weight loss occurred at high temperature.

Thermogravimetric analysis revealed that the structure became thermally more stable after forming crosslinked structure. PVA yarn sample was almost consumed until 700 $^{\circ}$C, but about 20 wt. % residual material was observed after the test for hydrogel sample even the temperature reached to 850 $^{\circ}$C. This residual was the products of borax compounds after thermal decomposition.
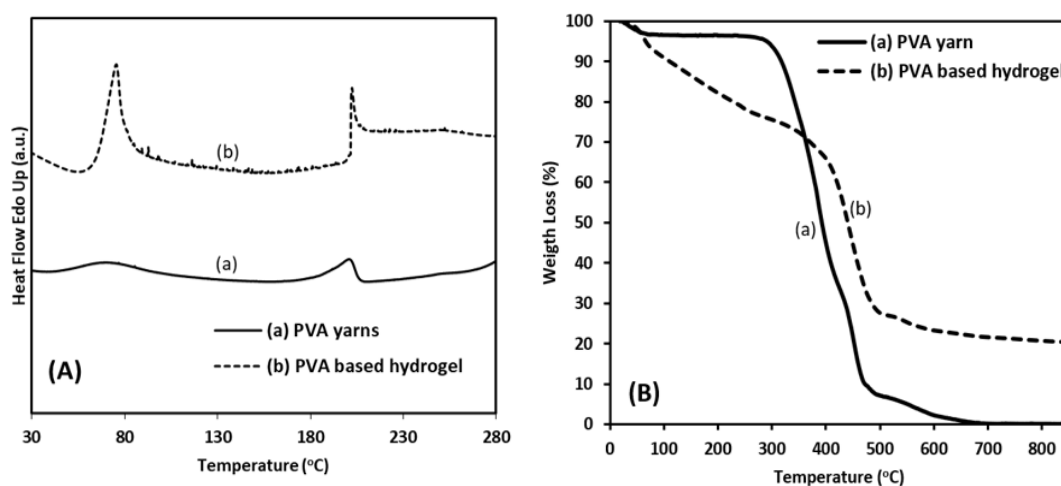
Figure 4.30. Thermal analysis of PVA yarns and their aqueous borax treated and dried analogs: (A) DSC and (B) TGA plots

4.5.4. Mechanical analysis of hydrogel composite yarns

Mechanical properties of the PVA, cotton (Co) and hybrid yarns before and after aqueous borax treatment were investigated by examining tensile strength measurements. Tensile test results were given in Figure 4.31. As seen, PVA and cotton yarns break after almost a linear increase of the force with elongation, but PVA/Co hybrid yarn was broken after a zigzag type of increase. Breaking strength of the yarns were 7.05, 5.03 and 5.09 N for dry PVA, cotton and PVA/Co hybrid yarns respectively. When the yarns were wetted with water, PVA yarn was completely dissolved and the breaking strength of wet cotton and PVA/Co yarns was measured as 5.55 and 6.42 N. When PVA/Co yarn was treated

with aqueous borax solution, a yield point was observed around 2.73 N and the materials was totally broken at 4.68 N. The yielding point was related to breaking of the hydrogel part. After hydrogel part was broken, force didn't increase obviously with continuous increase of elongation.

The materials was elongated gradually as a result of the opening of the crimped structure of cotton yarn formed after aqueous borax treatment of PVA/Co hybrid yarn. Breaking strength of aqueous borax treated cotton yarn was obtained as 4.40 N which was quite lower compared to the wetted cotton yarn.
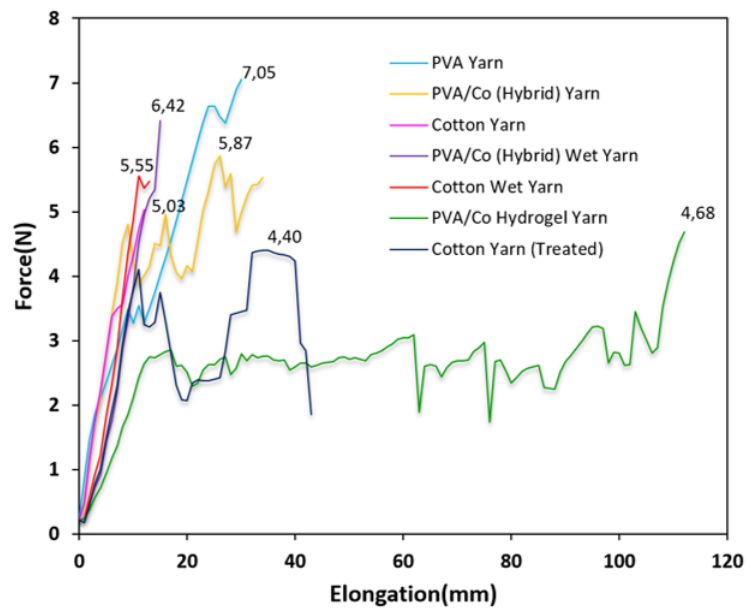
Figure 4.31. Tensile strength measurement of neat, water and aqueous borax treated yarns

5. CONCLUSION

This thesis is composed of articles, each of them presents scientific argument to enhance the mechanical performance of textile reinforced hydrogel composites for hydrogel applications. The results produced in this thesis can be summarized as follows;

Firstly, cotton (Co) yarn-reinforced hydrogel composites were prepared from previously produced PVA/Co fabrics by simultaneous dissolution and cross-linking of PVA with borax/water solution. With increasing borax concentration up to 1wt.%, water evaporation rate decreased, then increased with continuously increasing borax concentration. Breaking force of PVA/Co fabric in the warp and weft directions were measured as 212,7 and 1055,9 N, respectively. Breaking force tremendously increased when water content decreased in the samples at both warp and weft directions. During the drying process, there was a geometrical increase in the breaking force after warp direction sample released 90% of its water content. The geometrical increase started for the weft direction sample after it released 60% of its water content. Breaking force in the warp direction was 26,8 N when the hydrogel composite contained 90% of water and increased to 366,3 N when it was fully dried. Breaking force at weft direction was 1,22 N when the hydrogel composite contained 90% of water and increased to 225,9 N when it was fully dried. Because hydrogels also formed among the Co fibers inside Co yarns in the hydrogel composite, Co fibers have been moved away from each other and Co yarn resembled a roving. As a result, friction between Co fibers was reduced and fibers could slide easily in the hydrogel and therefore mechanical properties dramatically decreased with increasing water content in hydrogel composite at warp direction. Maximum breaking force at both warp and weft directions were observed at dried hydrogel composites since hydrogel turned to a brittle rigid structure in the dry form (Koc et al.2020a).

Secondly, cotton/polyvinyl alcohol-woven fabric-based hydrogel composite structures were successfully obtained by treating as-produced woven fabrics with aqueous borax and GA solutions. PVA yarns were directly transformed to hydrogel matrix structure when the crosslinker solutions were poured on the fabrics. The composite structure

became thermally more stable when borax was used as crosslinker comparing to GA treated samples. Force-elongation tests were performed to investigate the effect crosslinker and water content in the hydrogel composite structures on mechanical properties. Maximum applied force to failure decreased by increasing crosslinker content for both borax and GA treated samples. Increasing water content in the structure extensively decreased the breaking strength of the hydrogel composite. The high strength hydrogel composites could be used as hygroscopic materials for planting and erosion control at inclined terrains (Koc et al.2019a).

Third, natural fiber woven fabric reinforced hydrogel composite formation and the suitability of three different natural fibers for reinforcement were investigated. Woven fabrics were produced by mixing PVA yarns with three types of natural fiber yarns, namely cotton, flax and wool. PVA fibers in the fabric structure were simultaneously dissolved and PVA molecules were crosslinked when treated with aqueous borax solution. However cotton, flax and wool fibers kept their position in the fabric structure. A natural fiber woven fabric reinforced hydrogel composite structure was obtained. FTIR result revealed that aqueous borax treatment properly converted PVA molecules into crosslinked hydrogel structure, but no significant chemical change was observed at neat fibers when the neat cotton, flax and wool yarns were treated with the same solution separately. When SEM images were analyzed even though PVA molecules could penetrate inside the flax and cotton yarns and completed their crosslinking processes among the fibers, the penetration didn't happen inside the wool yarns and hydrogel structures were mostly seen at the yarn interlacing points and on the wool fabric surface. Penetration of hydrogel inside the cotton and flax yarns reduced the inter fiber friction and therefore the strength of fabric reinforced hydrogel composite compared to neat fabric strength with most of borax concentrations. But the strength of wool fabric reinforced hydrogel composite remained almost unaffected and stable with all borax concentrations. Overall result suggested that wool fabric reinforcement for PVA based hydrogel composites was better for mechanical performance comparing to cotton and flax fabric reinforcements and could be used as a natural reinforcing material to strengthen hydrogel composites.

Despite a serious strength reduction in the fabric reinforced hydrogels with cotton and flax fabric reinforcement compared to neat cotton and flax fabrics in wet state, the strength levels of cotton and flax fabric reinforced hydrogel composites are much higher than only hydrogel structures and could be sufficient for many applications (Koc et al.2020b).

Fourth, the effects of different borax-water concentrations on regenerated cellulose fabric reinforced hydrogels, the suitability of regenerated cellulose yarn type as the reinforcement material and properties of regenerated cellulose woven fabric reinforced hydrogel composites have been studied by focusing on the mechanical, thermal, morphology and chemical properties and statistical analysis. The SEM micrographs showed that hydrogel structures spread on the surface of viscose ring fabrics due to compact structure of viscose ring yarns while it was seen at the inside of viscose CF yarns and interlacing points of viscose CF yarns. From the FTIR results, aqueous borax treatment changed PVA yarns into crosslinked hydrogel structure, whereas chemical reaction between borax-water solution and the regenerated cellulose did not occur. The results of breaking force at the breaking points of regenerated cellulose woven fabric reinforced hydrogel composites were evaluated according to Pearson's correlation analysis by using SPPS 25 statistical program. The statistical analysis showed that there is a high level positive and significant relationship between borax-water concentration and breaking force at the breaking points of regenerated cellulose (viscose ring, viscose OE ,viscose CF) woven fabric reinforced hydrogel composites in the warp direction. On the other hand, no significant was found between borax-water concentration and breaking force at the breaking points of regenerated cellulose woven fabric reinforced hydrogel composites in weft direction. According to the findings in our previous research, wool fabric reinforcement for PVA based hydrogel composites could improve the mechanical performance compared with cotton and flax reinforcements. The obtained results have shown that the mechanical properties of viscose CF based hydrogel composites have been significantly improved, compared to staple viscose OE and viscose ring counterparts.

In the final stage of the thesis, single cotton yarn reinforced hydrogel composite structure was investigated by aqueous borax crosslinker treatment of PVA/Co hybrid yarn at room temperature. When the hybrid yarn was dipped into crosslinker solution, PVA yarn in the hybrid yarn structure was transformed into hydrogel form via crosslinking of PVA chains with borax. Cotton yarn kept its structure by gaining some crimping and it carried a mission as reinforcement to hydrogel yarn in the structure. Visual images showed that a proper hydrogel composite yarn structure was formed. Chemical analyses supported the formation of crosslinking via OH groups of PVA molecules in the structure. Thermal stability increased after aqueous borax treatment. Tensile measurements demonstrated that after aqueous borax treatment cotton yarn leaded as a reinforcement to the hydrogel yarn (Koc et al.2019b).

REFERENCES

Aboubakr, S.H. 2013. Epoxy-clay nanocomposite for carbon fiber reinforced polymer applications. *Master Thesis*, Department of Civil Engineering, The University of New Mexico, Albuquerque, New Mexico.

Abdurohman, K., Satrio, T., Muzayadah, N. L., Teten. 2018. A comparison process between hand lay-up, vacuum infusion and vacuum bagging method toward e-glass EW 185/lycal composites. *Journal of Physics: Conference Series*, 1130:012018.

Abdulkhani, A., Hojati Marvast, E., Ashori A., Hamzeh, Y., Karimi, A.N. 2013. Preparation of cellulose/polyvinyl alcohol biocomposite films using 1-n-butyl-3-methylimidazolium chloride. *International Journal of Biological Macromolecules.* Nov;62:379-386.

Adanur, S. 2000. Handbook of weaving. CRC Press, New York, USA, 446 pp.

Ahmed, E. M. 2015. Hydrogel: Preparation, characterization, and applications: A review. *Journal of Advanced Research*, 6(2):105–121.

Akhtar, M. F., Hanif, M., Ranjha, N. M. 2016. Methods of synthesis of hydrogels . A review.*Saudi Pharmaceutical Journal*, 24(5):554–559.

Al-Oqla, F. M., & Sapuan, S. M. (2014). Natural fiber reinforced polymer composites in industrial applications: Feasibility of date palm fibers for sustainable automotive industry. Journal of Cleaner Production, 66:347–354.

Al-Emam, E., Motawea, A.G., Janssens, K., Caen, J. 2019.Evaluation of polyvinyl alcohol–borax/agarose (PVA–B/AG) blend hydrogels for removal of deteriorated consolidants from ancient Egyptian wall paintings. *Heritage Science*, 7(1):1–18.

Alhosseini, S. N., Moztarzadeh, F., Mozafari, M., Asgari, S., Dodel, M., Samadikuchaksaraei, A., Jalali, N. 2012. Synthesis and characterization of electrospun polyvinyl alcohol nanofibrous scaffolds modified by blending with chitosan for neural tissue engineering. *International Journal of Nanomedicine*, 7: 25-34.

Alavudeen, A., Rajini, N., Karthikeyan, S., Thiruchitrambalam, M., Venkateshwaren, N. 2015. Mechanical properties of banana/kenaf fiber-reinforced hybrid polyester composites: Effect of woven fabric and random orientation. *Materials and Design*, 66: 246–257.

Amsden, B. 1998. Solute diffusion within hydrogels. Mechanisms and models. *Macromolecules*, 31(23): 8382–8395.

Agrawal, A., Rahbar, N., & Calvert, P. D. 2013. Strong fiber-reinforced hydrogel. *Acta Biomaterialia*, 9(2): 5313–5318.

Aswathy, S. H., Narendrakumar, U., Manjubala, I. 2020. Commercial hydrogels for biomedical applications. *Heliyon*, 6(4):e03719.

Awada, H., Daneault, C. 2015. Chemical modification of poly (vinyl alcohol) in water. *Applied Sciences   (Switzerland)*, 5(4):840–850.

Baghaei, B.2015. Development of thermo-plastic biocomposites based on aligned hybrid yarns for fast composite manufacturing. *Ph.D*. Thesis, School of Engineering, University of Borås, Borås, Sweden.

Baron, R.I., Bercea M., Avadanei, M., Lisa, G., Biliuta, G., Coseri, S. 2019.Green route for the fabrication of self-healable hydrogels based on tricarboxy cellulose and poly(vinyl alcohol). *Int. J. Biol. Macromol*, 123: 744–751.

Basan, H., İmren, D., Gümüşderelioglu, M. 2001. pH'a Duyarlı Hidrojeller ve Kontrollu İlaç, *FABAD J. Pharm. Sci.,* 26: 81-92.

Buwalda, S. J., Boere, K. W. M., Dijkstra, P. J., Feijen, J., Vermonden, T., Hennink, W.E. 2014. Hydrogels in a historical perspective: From simple networks to smart materials. *Journal of Control Release* , 190:254–273.

Butylina, S., Geng, S., Oksman, K. 2016. Properties of as-prepared and freeze-dried hydrogels made from poly (vinyl alcohol) and cellulose nanocrystals using freeze-thaw technique. *European Polymer Journal*, 81:386–396.

Brahıma, S. 2016. Ph ve sıcaklığa duyarlı hidrojellerin sentezlenmesi ve ilaç salım davranışlarının modellenmesi. *Master thesis,* Faculty of Chemical Engineering, Inonu University, Malatya.

Buenger, D., Topuz, F., Groll, J. 2012. Hydrogels in sensing applications. *Progress in Polymer Science*, 37(12):1678–1719.

Caló, E., Khutoryanskiy, V. V. 2015. Biomedical applications of hydrogels: A review of patents and commercial products. *European Polymer Journal*, 65:252–267.

Campbell, F. C. 2010. Structural Composite Materials. ASM International, Ohio, USA,612 pp.

Carrillo, F., Colom, X., Suñol, J.J., Saurina, J. 2004. Structural FTIR analysis and thermal characterization of lyocell and viscose-type   fibres. *European Polymer Journal*, 40(9):2229–2234.

Chiellini, E., Corti, A., D'Antone, S., Solaro, R. 2003. *Biodegradation of poly (vinyl alcohol) based materials*. *Progress in Polymer Science (Oxford)*, 28:963-1014.

Chirani, N., Yahia, L.H., Gritsch L., Motta, F.L., Chirani, S., Faré, S. 2015. History and Applications of Hydrogels. *Journal of Biomedical Sciencies*, 4:2.

Chen, Y., Cao, X., Chang, P.R., Huneault, M. 2008. Comparative study on the films of poly (vinyl alcohol)/pea starch nanocrystals and poly (vinyl alcohol)/native pea starch. *Carbohydrate Polymers,* 73: 8-17.

Chung , H., Kim, J.Y. 2016. Effects of washing parameters on dimensional stability of viscose rayon fabrics. *Fibers and Polymers*, 17(11):1945–1954.

Célino, A., Fréour, S., Jacquemin, F., Casari, P., Célino, A., Fréour, S., Casari, P. 2013. Characterization and modeling of the moisture diffusion behaviour of natural fibres. *Journal of Applied Polymer Science*, 130(1): 297–306.

Çavuşoğlu, J. 2016. Polymeric Tubes Prepared From Poly (Vinyl Alcohol) Fiber Templates. *Ph.D. Thesis*, Department of Chemistry, Boğaziçi University, Turkey.

Dai, W. S., Barbari, T. A. 1999. Hydrogel membranes with mesh size asymmetry based on the gradient crosslinking of poly (vinyl alcohol). *Journal of Membrane Science*, 156(1):67–79.

Dong, Y., Hou, L., Wu, P. 2020. Exploring the diffusion behavior of urea aqueous solution in the viscose film by ATR-FTIR spectroscopy. *Cellulose*, 27(5): 2403–2415.

Duarte, L., Matte, C. R., Bizarro, C. V., Ayub, M. A. Z. 2020. Transglutaminases: part I—origins, sources, and biotechnological characteristics. *World Journal of Microbiology and Biotechnology*, 36(1):15.

Eren, R. 2009. Dokuma Hazırlık Teknolojisi. Marmara kitap merkezi yayınları, 232 s.

Eslahi, N., Abdorahim, M., Simchi, A. 2016. Smart Polymeric Hydrogels for Cartilage Tissue Engineering: A Review on the Chemistry and Biological Functions. *Biomacromolecules*, 17(11): 3441–3463.

Ferreira, N. N., Ferreira, L. M. B., Cardoso, V. M. O., Boni, F. I., Souza, A. L. R., Gremião, M.P.D. 2018. Recent advances in smart hydrogels for biomedical applications: From self-assembly to functional approaches. *European Polymer Journal*, 99 : 117–133.

Garg, S., Garg, A., Vishwavidyalaya, R.D. 2016. Hydrogel : Classification, Properties, Preparation and Technical Features. *Asian Journal of Biomaterial Research*, 2(6):163–170.

Gallego, R., Arteaga, J. F., Valencia, C., Franco, J. M. 2013. Isocyanate-functionalized chitin and chitosan as gelling agents of castor oil. *Molecules*, 18(6):6532–6549.

Gadhave, R. V., Mahanwar, P. A., Gadekar, P. T. 2019. Effect of glutaraldehyde on thermal and mechanical properties of starch and polyvinyl alcohol blends. *Designed Monomers and Polymers*, 22(1):164–170.

Gholamali, I. 2019. Stimuli-Responsive Polysaccharide Hydrogels for Biomedical Applications: a Review. *Regenerative Engineering and Translational Medicine*. https://doi.org/10.1007/s40883-019-00134-1.

Guo, Y., Bae, J., Fang, Z., Li, P., Zhao, F., & Yu, G. 2020. Hydrogels and Hydrogel-Derived Materials for Energy and Water Sustainability. *Chem. Rev.*, 120:7642–7707.

Gül, A., Kuruca, L.2017. Kompozit-CTP el kitabı.Matsaş Matbaacılık A.Ş., İstanbul, 64 s.

Han, J., Lei, T., Wu, Q.2014. High-water-content mouldable polyvinyl alcohol-borax hydrogels reinforced by well-dispersed cellulose nanoparticles: Dynamic rheological properties and hydrogel formation mechanism. *Carbohydr. Polym.*, 102(1):306–16.

Han, J., Yue, Y., Wu, Q., Huang, C., Pan, H., Zhan, X., Xu, X. 2017. Effects of nanocellulose on the structure and properties of poly (vinyl alcohol)-borax hybrid foams. *Cellulose*, 24(10): 4433–4448.

Hassan, C. M., Peppas, N. A. 2000. Structure and applications of poly (vinyl alcohol) hydrogels produced by conventional crosslinking or by freezing/thawing methods. *Advances in Polymer Science*, 153: 37–65.

Hassan, A., Niazi, M. B. K., Hussain, A., Farrukh, S.,Ahmad, T. 2018. Development of Anti-bacterial PVA/Starch Based Hydrogel Membrane for Wound Dressing. *Journal of Polymers and the Environment*, 26(1):235–243.

He, M., Wang, Z., Cao, Y., Zhao, Y., Duan, B., Chen, Y.,Zhang, L. 2014. Construction of chitin/PVA composite hydrogels with jellyfish gel-like structure and their biocompatibility. *Biomacromolecules*, 15(9):3358–3365.

Hennink, W. E., van Nostrum, C. F. 2012. Novel crosslinking methods to design hydrogels. *Advanced Drug Delivery Reviews*, 64:223–236.

Hoffman, A. S. 2012. Hydrogels for biomedical applications. *Advanced Drug Delivery Reviews*, 64:18–23.

Holloway, J. L., Lowman, A. M., & Palmese, G. R. 2010. Mechanical evaluation of poly (vinyl alcohol)-based fibrous composites as biomaterials for meniscal tissue replacement. Acta Biomaterialia, 6(12):4716–4724.

Hortós, M., Viñas, M., Espino, S., & Bou, J. J. 2019. Influence of temperature on high molecular weight poly(Lactic acid) stereocomplex formation. *Express Polymer Letters*, 13(2):123–134.

Hospodiuk, M.,Dey,M.,Sosnoski, D.,Ozbolat, I. T.2017. The bioink: A comprehensive review on bioprintable materials. *Biotechnology Advances*, 35(2): 217–239.

Huang, S. , Shuyi, S. , Gan, H., Linjun, W. , Lin, C. , Danyuan, X. , Qin, Y . 2019. Facile fabrication and characterization of highly stretchable lignin-based hydroxyethyl cellulose self-healing hydrogel .*Carbohydrate Polymers*, 223(May). https://doi.org/10.1016/j.carbpol.2019.115080.

Huang, Y., King, D. R., Sun, T. L., Nonoyama, T., Kurokawa, T., Nakajima, T., Gong, J. P. 2017. Energy-Dissipative Matrices Enable Synergistic Toughening in Fiber Reinforced Soft Composites. *Advanced Functional Materials*, 27(9):1605350.

Hubbard, A. M., Cui, W., Huang, Y., Takahashi, R., Dickey, M. D., Genzer, J., Gong, J. P. 2019. Hydrogel/Elastomer Laminates Bonded via Fabric Interphases for Stimuli-Responsive Actuators. *Matter*, 1(3):674–689.

Idris, I. 2013. News and Views: News and Views. *Diabetes, Obesity and Metabolism*, 15(1):96–98.

Illeperuma, W. R. K., Sun, J. Y., Suo, Z.,Vlassak, J. J. 2014. Fiber-reinforced tough hydrogels. *Extreme Mechanics Letters*, 1: 90–96.

Jahan, I. 2017. Effect of fabric structure on the mechanical properties of woven fabrics. *Advance Research in Textile Engineering*, 2(2):1018.

Kabir, S. M. F., Sikdar, P. P., Haque, B., Bhuiyan, M. A. R., Ali, A., Islam, M. N. 2018. Cellulose-based hydrogel materials: chemistry, properties and their prospective applications. *Progress in Biomaterials*, 7(3) :153–174.

Kishida, A., Ikada, Y., 2001. Hydrogels for Biomedical and Pharmaceutical Applications: Editor: Dumitriu, S. Polymeric Biomaterials, Revised and Expanded. Boca Raton: CRC Press, USA, pp: 133-134.

Kadajji, V. G., Betageri, G. V. 2011. Water soluble polymers for pharmaceutical applications. *Polymers*, 3(4):1972–2009.

Khan, S., Ullah, A., Ullah, K., Rehman, N. U. 2016. Insight into hydrogels. *Designed Monomers and Polymers*, 19(5):456–478.

Kim, J.K., Mai, Y.W. 1998. Engineered interfaces in fiber reinforced composites. Elsevier, Oxford, 416 pp.

Koehler, J., Brandl, F. P., & Goepferich, A. M. 2018. Hydrogel wound dressings for bioactive treatment of acute and chronic wounds. *European Polymer Journal*, 100:1–11.

Koc, U., Aykut, Y., Eren, R. 2019a.One-step preparation of woven fabric-reinforced hydrogel composite. *Journal of Industrial Textiles*, (Epub ahead of print 19 May 2019), https://doi.org/10.1177/1528083719850832,1-16.

Koc, U., Eren, R., Aykut, And Y.2019b. Hydrogel Composite Yarn Prepared From Polyvinyl Alcohol/Cotton Hybrid Yarn. 17th National 3rd International the Recent Progress Symposium on Textile Technology and Chemistry, 20-22 November, Bursa, Turkey.

Koc, U., Eren, R., Aykut, Y. 2020a. Yarn-reinforced hydrogel composite produced from woven fabrics by simultaneous dissolution and cross-linking. *Polym&Polym Compos.*, https://doi.org/10.1177/0967391120903648, (Epub ahead of print 24 February 2020), 1-10.

Koc, U., Aykut, Y., Eren, R. 2020b. Natural fibers woven fabric reinforced hydrogel composites for enhanced mechanical properties. *Journal of Industrial Textiles*, https://doi.org/https://doi.org/10.1177/1528083720944485, (Epub ahead of print 24 July 2020), 1-18.

Koniuszewska, A. G., Kaczmar, J. W. 2016. Application of Polymer Based Composite Materials in Transportation. Progress in Rubber, Plastics and Recycling Technology, 32(1):1–24.

Koski, A., Yim, K., Shivkumar, S. 2004. Effect of molecular weight on fibrous PVA produced by electrospinning. *Mater Lett*, 58: 493–497.

Kumar, A., & Han, S. S. 2017. PVA-based hydrogels for tissue engineering: A review. *International Journal of Polymeric Materials and Polymeric Biomaterials*, 66(4):159–182.

Lin, F., Lu, X., Wang, Z., Lu, Q., Lin, G., Huang, B., Lu, B. 2019. In situ polymerization approach to cellulose–polyacrylamide interpenetrating network hydrogel with high strength and pH-responsive properties. *Cellulose*, 26(3): 1825–1839.

Liu, C., Lei, F., Li, P., Jiang, J., & Wang, K. 2020. Borax crosslinked fenugreek galactomannan hydrogel as potential water-retaining agent in agriculture. *Carbohydrate Polymers*, 236:116100.

Lee, S. Y., Kim, Z. H., Oh, H. Y., Choi, Y., Park, H., Jung, D., Lee, J. K. 2016. Fabric-hydrogel composite membranes for culturing microalgae in semipermeable membrane-based photobioreactors. *Journal of Polymer Science, Part A: Polymer Chemistry*, 54(1): 108–114.

Lee, H., Yamaguchi, K., Nagaishi, T., Murai, M., Kim, M., Wei, K., Kim, I. S. 2017. Enhancement of mechanical properties of polymeric nanofibers by controlling crystallization behavior using a simple freezing/thawing process. *RSC Advances*, 7(69): 43994–44000.

Lee, D. G., Suh, N. P. 2006. Axiomatic Design and Fabrication of Composite Structures: Applications in Robots, Machine Tools, and Automobiles. Oxford University Press, USA, 732 pp.

Lee, C.Y., Wahit, M.U., Othman, N. 2015. Thermal and flexural properties of regenerated cellulose (RC)/poly (3- hydroxybutyrate) (PHB) biocomposites, *Jurnal Teknologi*, 75(11):107-112.

Li, Q., Liu, C., Wen, J., Wu, Y., Shan, Y., Liao, J. 2017. The design, mechanism and biomedical application of self-healing hydrogels. *Chinese Chemical Letters*, 28(9):1857–1874.

Lim, M., Kwon, H., Kim, D., Seo, J., Han, H., Khan, S. B. 2015. Highly-enhanced water resistant and oxygen barrier properties of cross-linked poly (vinyl alcohol) hybrid films for packaging applications. *Progress in Organic Coatings*, 85:68-75.

Lin, S., Cao, C., Wang, Q., Gonzalez, M., Dolbow, J. E., Zhao, X. 2014. Design of stiff, tough and stretchy hydrogel composites via nanoscale hybrid crosslinking and macroscale fiber reinforcement. *Soft Matter*, 10(38): 7519–7527.

Liu, Y., Hsu, S. H. 2018. Synthesis and biomedical applications of self-healing hydrogels. *Frontiers in Chemistry*, 6:1–10.

Liu, Y., Vrana, N. E., Cahill, P. A., McGuinness, G. B. 2009. Physically crosslinked composite hydrogels of PVA with natural macromolecules: Structure, mechanical properties, and endothelial cell compatibility. *Journal of Biomedical Materials Research - Part B Applied Biomaterials*, 90 B (2):492–502.

Lu, B., Lin, F., Jiang, X., Cheng, J., Lu, Q., Song, J., Huang, B. 2017. One-Pot Assembly of Microfibrillated Cellulose Reinforced PVA-Borax Hydrogels with Self-Healing and pH-Responsive Properties. *ACS Sustainable Chemistry and Engineering*, 5(1):948–956.

Ma, S., Rong, M., Lin, P., Bao, M., Xie, J., Wang, X.,Liu, W. 2018. Fabrication of 3D Tubular Hydrogel Materials through On-Site Surface Free Radical Polymerization. *Chemistry of Materials*, 30(19): 6756–6768.

Ma, R.Y., Xiong, D.S. 2008. Synthesis and properties of physically crosslinked poly (vinyl alcohol) hydrogels. *Journal of China University of Mining and Technology*, 18(2):271–274.

Mallakpour, S., & Rashidimoghadam, S. 2020. Preparation, characterization, and in vitro bioactivity study of glutaraldehyde crosslinked chitosan/poly(vinyl alcohol)/ascorbic acid-MWCNTs bionanocomposites. *International Journal of Biological Macromolecules*, 144:389–402.

Ma, P.C., Siddiqui, N.A., Marom, G., Kim, J. K.2010. Dispersion and functionalization of carbon nanotubes for polymer-based nanocomposites: A review. *Composites Part A: Applied Science and Manufacturing*, 41(10):1345–1367.

Mantha, S., Pillai, S., Khayambashi, P., Upadhyay, A., Zhang, Y., Tao, O.,Tran, S. D. 2019. Smart hydrogels in tissue engineering and regenerative medicine. *Materials*, 12(20):3323.

Mansur, H. S., Sadahira, C. M., Souza, A. N., & Mansur, A. A. P. 2008. FTIR spectroscopy characterization of poly (vinyl alcohol) hydrogel with different hydrolysis degree and chemically crosslinked with glutaraldehyde. *Materials Science and Engineering C*, 28(4):539–548.

Martins, I. M., Matos, M., Costa, R., Lopes-da-Silva, F., Pascoal, A., Estevinho, L. M., Choupina, A. B. 2014. Transglutaminases: Recent achievements and new sources. *Applied Microbiology and Biotechnology*, 98(16):6957–6964.

Martin, N., Youssef, G. 2018. Dynamic properties of hydrogels and fiber-reinforced hydrogels. *Journal of the Mechanical Behavior of Biomedical Materials*, 85: 194–200.

Maitra, J., Shukla, V. K. 2014. Cross-linking in Hydrogels - A Review. *American Journal of Polymer Science*, 4(2):25–31.

Marks, R., Robinson, A.T.C. 1976. Principles of weaving. The Textile Institute, Manchester, UK, 256 pp.

Masoud, F., Sapuan, S. M., Mohd Ariffin, M. K. A., Nukman, Y., Bayraktar, E. 2020. Cutting processes of natural fiber-reinforced polymer composites. *Polymers*, 12(6):15–17.

Mazzarotta, A.2017.Engineered Hydrogel-Based Materials for Oligonucleotide Detection *Ph.D. Thesis,* Universita' Degli Studi Di Napoli "Federico II", Industrial Products and Process Engineering, Italy.

Miyazaki, T., Takeda, Y., Akane, S., Itou, T., Hoshiko, A., En, K. 2010. Role of boric acid for a poly (vinyl alcohol) film as a cross-linking agent: Melting behaviors of the films with boric acid. *Polymer*, 51(23):5539–5549.

Miracle, D.B.,Donaldson, S.L. 2002. Volume 21 Composites. ASM International, Ohio, USA,1201 pp.

Misnon, M. I., Islam, M. M., Epaarachchi, J. A., Lau, K. tak. 2014. Potentiality of utilizing natural textile materials for engineering composites applications. *Materials and Design*, 59:359–368.

Morton, W.E., Hearle, J.W.S. 2008. Physical Properties of Textile Fibres.Woodhead Publishing,Cambridge,UK,796 pp.

Mondal, S., Das, S., Nandi, A. K. 2020. A review on recent advances in polymer and peptide hydrogels. *Soft Matter*, 16(6):1404–1454.

Musgrave, C.S.A., Fang, F. 2019. Contact lens materials: A materials science perspective. *Materials*, 12(2):1–35.

Mohamed, M.G. 2018. Superabsorbent:Hydrogels,Editors:Haider,S.,Haider,A.,Intech Open Limited ,London,UK,pp:46-66.

Nawaz, A., Hümmelgen, I. A. 2019. Poly (vinyl alcohol) gate dielectric in organic field-effect transistors. *Journal of Materials Science: Materials in Electronics*, 30(6):5299–5326.

No, Y. J., Tarafder, S., Reischl, B., Ramaswamy, Y., Dunstan, C., Friedrich, O., Zreiqat, H. 2020. High-Strength Fiber-Reinforced Composite Hydrogel Scaffolds as Biosynthetic Tendon Graft Material. *ACS Biomaterials Science and Engineering*, 6(4): 1887–1898.

Nezhad-Mokhtari, P., Ghorbani, M., Roshangar, L., Soleimani Rad, J.2019. Chemical gelling of hydrogels-based biological macromolecules for tissue engineering: Photo- and enzymatic-crosslinking methods. *International Journal of Biological Macromolecules*, 139: 760–772.

Nikolić, M.,Stjepanovič, Z., Lesjak, F. Štritof, A. 2003. Compact spinning for improved quality of ring-spun yarns. *Fibres and Textiles in Eastern Europe*, 11(4):30–35.

Pandit, A. H., Mazumdar, N., Imtiyaz, K., Rizvi, M. M. A., & Ahmad, S. 2019. Periodate-Modified Gum Arabic Cross-linked PVA Hydrogels: A Promising Approach toward Photoprotection and Sustained Delivery of Folic Acid. *ACS Omega*, 4(14): 16026–16036.

Parhi, R. 2017. Cross-linked hydrogel for pharmaceutical applications: A review. *Advanced Pharmaceutical Bulletin*, 7(4):515–530.

Peng, N., Wang, Y., Ye, Q., Liang, L., An, Y., Li, Q., Chang, C. 2016. Biocompatible cellulose-based superabsorbent hydrogels with antimicrobial activity. *Carbohydrate Polymers*, 137:59–64.

Products, I. 2017. Engineered Hydrogel-Based Materials for Oligonucleotide Detection.*Ph.D* Thesis, Universita' Degli Studi Di Napoli "Federico II".Italy.

Priyanka, P., Dixit, A., Mali, H. S. 2017. High-Strength Hybrid Textile Composites with Carbon, Kevlar, and E-Glass Fibers for Impact-Resistant Structures. A Review. *Mechanics of Composite Materials*, 53(5):685–704.

Quanjin, M., Rejab, M. R. M., Kaige, J., Idris, M. S., Harith, M. N. 2018. Filament winding technique, experiment and simulation analysis on tubular structure. *IOP Conference Series: Materials Science and Engineering*, 342:012029.

Quanjin, M., Rejab, M.R. M., Zhang, B., Kumar, N. M. 2019. Filament Winding Technique: SWOT Analysis and Applied Favorable Factors. *SCIREA Journal of Mechanical Engineering*, 3:1.

Rajak, D. K., Pagar, D. D., Kumar, R., & Pruncu, C. I. 2019. Recent progress of reinforcement materials: A comprehensive overview of composite materials. *Journal of Materials Research and Technology*, 8(6):6354–6374.

Richbourg, N. R., & Peppas, N. A. 2020. The swollen polymer network hypothesis: Quantitative models of hydrogel swelling, stiffness, and solute transport. *Progress in Polymer Science*, 105 :101243.

Ricciardi, R., Auriemma, F., De Rosa, C., Lauprêtre, F. 2004. X-ray Diffraction Analysis of Poly (vinyl alcohol) Hydrogels, Obtained by Freezing and Thawing Techniques. *Macromolecules*, 37(5):1921–1927.

Reis, E. F., Campos, F. S., Lage, A. P., Leite, R. C., Heneine, L. G., Vasconcelos, W. L., Mansur, H. S. 2006. Synthesis and characterization of poly (vinyl alcohol) hydrogels and hybrids for rMPB70 protein adsorption. *Materials Research*, 9(2): 185–191. https://doi.org/10.1590/s1516-14392006000200014.

Rudra, R., Kumar, V., Kundu, P. P. 2015. Acid catalysed cross-linking of poly vinyl alcohol (PVA) by glutaraldehyde: effect of crosslink density on the characteristics of PVA membranes used in single chambered microbial fuel cells. *RSC Advances*, *5*(101): 83436–83447.

Samadi, N., Sabzi, M., Babaahmadi, M. 2018. Self-healing and tough hydrogels with physically cross-linked triple networks based on Agar/PVA/Graphene. *International Journal of Biological Macromolecules*, 107:2291–2297.

Saçak, M.2014. Polimer Teknolojisi.Ankara Üniversitesi, Fen Fakültesi Kimya Bölümü, Ankara, 461 s.

Satoh, K. 2014. Encyclopedia of Polymeric Nanomaterials. *Encyclopedia of Polymeric Nanomaterials*, 2–7. https://doi.org/10.1007/978-3-642-36199-9.

Sezgin, H.2018. Investigation and enhancement of the mechanical properties of the fabric reinforced hybrid composites. *Ph.D*. Thesis, Department of Textile Engineering, Istanbul Technical University, Istanbul.

Sheffield, C., Meyers, K., Johnson, E., Rajachar, R. 2018. Application of Composite Hydrogels to Control Physical Properties in Tissue Engineering and Regenerative Medicine. *Gels*, 4(2): 51.

Shi, Q., Liu, H., Tang, D., Li, Y., Li, X. J., Xu, F. 2019. Bioactuators based on stimulus-responsive hydrogels and their emerging biomedical applications. *NPG Asia Materials*, 11(1):64.

Spoljaric, S., Salminen, A., Luong, N. D., Seppälä, J. 2014. Stable, self-healing hydrogels from nanofibrillated cellulose, poly (vinyl alcohol) and borax via reversible crosslinking. *European Polymer Journal*, 56(1):105–117.

Sonker, A. K., Tiwari, N., Nagarale, R. K., Verma, V. 2016. Synergistic effect of cellulose nanowhiskers reinforcement and dicarboxylic acids crosslinking towards polyvinyl alcohol properties. *Journal of Polymer Science, Part A: Polymer Chemistry*, 54(16):2515–2525.

Sonker, A.K., Rathore, K., Nagarale, R., & Verma, V. 2018. Crosslinking of Polyvinyl Alcohol (PVA) and Effect of Crosslinker Shape (Aliphatic and Aromatic) Thereof. *Journal of Polymers and the Environment,* 26(5):1782-1794.

Steinmann, W., Saelhoff, AK. 2016. Essential properties of fibres for composite applications: Fibrous and Textile Materials for Composite Applications, Editors: Zimniewska, M., Wladyka-Przybylak, M., Springer, Singapore, pp: 39-73.

Thakur, S., Thakur, V. K., Arotiba, O. A. 2018. History, Classification, Properties and Application of Hydrogels: An Overview: Hydrogels, Gels Horizons: From Science to Smart Materials, Editor(s): Thakur, V.K., Thakur, M.K., Springer ,Singapore, pp:29-50.

Talebian, S., Mehrali, M., Taebnia, N., Pennisi, C. P., Kadumudi, F. B., Foroughi, J., Dolatshahi-Pirouz, A. 2019. Self-Healing Hydrogels: The Next Paradigm Shift in Tissue Engineering? *Advanced Science*, 6(16):1801664.

Taleb, M. F. A., El-Mohdy, H. L. A., El-Rehim, H. A. A. 2009. Radiation preparation of PVA/CMC copolymers and their application in removal of dyes. *Journal of Hazardous Materials*, 168 (1):68–75.

Taylor, D. L., in het Panhuis, M. 2016. Self-Healing Hydrogels. *Advanced Materials*, *28*(41):9060–9093.

Toxqui-López, S., Olivares-Pérez, A., Marroquín-Ramírez, J., & Fuentes-Tapia, I. 2018. Effect of degree of hydrolysis of polyvinyl alcohol on the diffraction efficiency from the gratings recorded in polyvinyl alcohol with ferric chloride films (p. 37). SPIE-OPTO Conference, 19 February, 2018, San Francisco, California, USA.

Thakur, S., Thakur, V. K., Arotiba, O. A. 2018. History, Classification, Properties and Application of Hydrogels: An Overview: Hydrogels, Gels Horizons: From Science to Smart Materials, Editors: Thakur, V.K., Thakur, M.K., Springer ,Singapore, pp:32-34.

Thakur, S., Thakur, V. K., Arotiba, O. A. 2018. History, Classification, Properties and Application of Hydrogels: An Overview: Hydrogels, Gels Horizons: From Science to Smart Materials, Editors: Thakur, V.K., Thakur, M.K., Springer ,Singapore, pp:65-67.

Varaprasad, K., Raghavendra, G. M., Jayaramudu, T., Yallapu, M. M., Sadiku, R. 2017. A mini review on hydrogels classification and recent developments in miscellaneous applications. *Materials Science and Engineering C*, 79:958–971.

Vasile, C., Pamfil, D., Stoleru, E., Baican, M. 2020. New developments in medical applications of hybrid hydrogels containing natural polymers. *Molecules*, 25:1539.

Venkateswaran, R., Babu, S., Kumar, S.S., Pillai, M.A., Sharma, P.V. 1990. Thermal decomposition of viscose rayon in the presence of inorganic additives. A kinetic study. *Journal of Applied Polymer Science*, 41(11-12):2783–2811.

Wang, T., Xu, X., Ren, Y., Qin, S., Sui, X., Wang, L. 2014. Kinetics of thermal degradation of viscose fiber and fire retardant viscose fiber. *Journal of Engineered Fibers and Fabrics*, 9(2):38–46.

Wang, Y., Chen, L. 2011. Impacts of nanowhisker on formation kinetics and properties of all-cellulose composite gels. *Carbohydr. Polym.*, 83(4):1937-1946.

Yang, X., Kim, J. C.,Jin Seo, H. 2012. Hydrogel of β-cyclodextrin-Grafted Polyethyleneimine: PH-Sensitive Release. *Journal of Dispersion Science and Technology*, 33(8): 1233–1239.

Yang, H., Yan, R. , Chen, H. , Lee, D.H., Zheng, C . 2007.Characteristics of hemicellulose, cellulose and lignin pyrolysis. *Fuel*,86 (12–13):1781–1788.

Yokoyama,Y.,Yusa, S. I. 2013. Water-soluble complexes formed from hydrogen bonding interactions between a poly(ethylene glycol)-containing triblock copolymer and poly(methacrylic acid). *Polymer Journal*, 45(9): 985–992.

Zin, M. H., Razzi, M. F., Othman, S., Liew, K., Abdan, K., Mazlan, N. 2016. A review on the fabrication method of bio-sourced hybrid composites for aerospace and automotive applications. *IOP Conference Series: Materials Science and Engineering*, 152(1):012041.

Zhang, K., Feng, W., Jin, C. 2020. Protocol efficiently measuring the swelling rate of hydrogels. *MethodsX*, 7:100779.

Zhang, R., Wu, Y., Lin, P., Jia, Z., Zhang, Y., Liu, F., Zhou, F. 2020. Extremely Tough Hydrogels with Cotton Fibers Reinforced. Advanced Engineering Materials, 2000508:1–6.

Zhang, S., Nie, Y., Tao, H., Li, Z. 2018. Hydrogel-Based Strategies for Stem Cell Therapy: Hydrogels Recent Advances, Editors: Thakur, S., Thakur, V. K., Arotiba, O.A., Springer ,Singapore, pp:87-112.

Zhao, X. 2014. Multi-scale multi-mechanism design of tough hydrogels: Building dissipation into stretchy networks. *Soft Matter*, 10(5): 672–687.

Name Surname	: Ümit KOÇ
Foreign Languages	: English

Education Status
    High School   : Malatya Anatolian High School, Turkey-2004
    Bachelor's   : Gaziantep University, Turkey-2012
    Master's   : Süleyman Demirel University-2015

Work Experience   : Bursa Uludağ University Department of Textile Engineering YÖK 100/2000 Scholarship (2017-..)

Contact (e-mail)   : kocumit44@gmail.com

Publications from the thesis studies:

Koc, U., Eren, R., Aykut, Y., 2019. High Strength Hydrogel Composite Prepared From Polyvinyl Alcohol/Cotton Woven Fabric. Proceedings of the 19th World Textile Conference on Textiles Autex-2019, 11-15 June, Ghent, Belgium.

Koc, U., Eren, R., Aykut, Y.2019. Hydrogel Composite Yarn Prepared From Polyvinyl Alcohol/Cotton Hybrid Yarn. 17th National 3rd International the Recent Progress Symposium on Textile Technology and Chemistry, 20-22 November, Bursa, Turkey.

Others:

Bulgurcuoğlu, E., Bostancı A., Koc,U., Eren, R., Aykut Y.2020. PVA ve PVP Ultra İnce Lif kaplı Yün/PVA kumaşlardan hidrojel kompozitlerin üretimi ve zamanla su kaybı tayini.6th.International Fiber and Polymer Research Symposium, 24-25 January, Bursa, Turkey.

Aykut, Y., Aydın, S., Koc, U. 2017. Electrospun nanofiber assisted hydrogel thin film on shaped surfaces. The Fiber Society 2017 Spring Conference Next Generation Fibers for Smart Products, 17-19 May, Aachen, Germany.